

Structural Analysis of Polyurethane Bonded Aggregate on Block Revetments

Master Thesis

M.C. Kruis

Technische Universiteit Delft



STRUCTURAL ANALYSIS OF POLYURETHANE BONDED AGGREGATE ON BLOCK REVTMENTS

MASTER THESIS

by

M.C. Kruis

in partial fulfillment of the requirements for the degree of

Master of Science
in Civil Engineering

at the Delft University of Technology,

Author:	M.C. Kruis	Delft University of Technology
Chairman:	prof. dr. ir. S.N. Jonkman	Delft University of Technology
Committee:	ir. H.J. Verhagen	Delft University of Technology
	ir. M.E.C. van de Ven	Delft University of Technology
	ir. E. Bijlsma	ARCADIS

PREFACE

This report is written in the context of my master thesis, which is part of the Master curriculum Hydraulic Engineering at Delft University of Technology. The purpose is to solve an actual and recent civil engineering problem independently and at a sufficient academic level based on knowledge, understanding and skills acquired in the preceding educational years. In my thesis I am studying the structural behaviour of a refurbishment material -Elastocoast- used to reinforce an existing pitched stone dike revetment. The focus will be on acquiring more insight into the mechanical behaviour, the effect of bonding between a pitching and cover layer and comparing this system with conventional refurbishment techniques.

I would like to express sincere gratitude to all of the members of my graduation committee for their support during this study, prof.dr.ir. S.N. Jonkman, ir. H.J. Verhagen, ir. M.F.C. van de Ven (Delft University of Technology) and ir. E. Bijlsma (ARCADIS). Also I would like to thank ARCADIS for the opportunity to do an internship at the ARCADIS Hoofddorp office.

*Marc Kruis
Hoofddorp, July 2014*

LIST OF SYMBOLS

Roman		
A	Area	[m ²]
b	Width	[m]
d	Thickness	[m]
E	Young's modulus	[Pa]
EA	Longitudinal stiffness	[N/m]
EI	Bending stiffness	[Nm ²]
E_s	Young's modulus soil	[Pa]
g	Gravitational acceleration	[m/s ²]
H_s	Significant wave height	[m]
I	Moment of inertia	[m ⁴]
i	Hydraulic gradient of water level	[-]
k	Permeability	[m/s]
k_s	Soil stiffness	[N/m ³]
L_0	Deep water wave length	[m]
l	Revetment length	[m]
M	Moment	[Nm]
N	Normal force	[N]
p	Pressure	[Pa]
q	Distributed load	[N/m]
q_0	Constant distributed load	[N/m]
q_t	Flow velocity top layer	[m/s]
q_x	Flow velocity filter layer in x-direction	[m/s]
q_y	Flow velocity filter layer in y-direction	[m/s]
q_α	Wave impact parameter	[-]
s	Wave steepness	[-]
T_p	Wave peak period	[s]
v	Deflection	[m]
W	Section Modulus	[m ³]
Z	Wave run down distance	[m]
z	Reference distance	[m]

Greek		
α	Structure slope angle	[rad]
β	Angle of the wave front	[rad]
γ	Weight density	[N/m ³]
Δ	Difference	[-]
δ	Angle of friction	[deg]
ϵ	Strain	[-]
κ	Curvature	[m ⁻¹]
λ	Leakage length	[m]
μ	Soil's Poisson ratio	[-]
ξ	Iribarren number	[-]
ρ	Mass density	[kg/m ³]
σ	Stress	[Pa]
φ	Angle of internal friction	[deg]
Φ	Hydraulic head	[m]
Φ_b	Hydraulic head due to wave height	[m]
ϕ	Beam angle	[rad]
ψ	Coefficient of friction	[-]

Commonly used indices

c	Concrete
f	Filter layer
G	Dead weight
h	Homogeneous
j	Joint
M	Moment
N	Normal force
p	Particular
pba	PBA layer
R	Resultant
t	Top layer
w	Water
max	Maximum
min	Minimum

Abbreviations

EB	Euler Bernoulli
CG	Centre of Gravity
NAP	Normaal Amsterdams Peil
NC	Normal Force Centre
OSA	Open Stone Asphalt
PU	Polyurethane
PBA	Polyurethane Bonded Aggregate
SWL	Still Water Level
VTV	Voorschrift Toetsen op Veiligheid

Trademarks

Abaqus is a registered trademark of Abaqus Inc.

Elastocoast is a registered trademark of BASF

Excel is a registered trademark of Microsoft

Maple is a registered trademark of Maplesoft

SUMMARY

For centuries dikes in the Netherlands have been protected against wave attack by revetments constructed of pitched blocks. Due to new insights into the behaviour of pitched blocks and increased hydraulic boundary conditions, a significant part of those dikes does not meet the current prescribed standards and safety norms anymore. As a result, large parts have to be reinforced in the coming years. The main failure mechanism of a placed block revetment is uplifting due to water overpressures. This happens when the upward pressures, caused by a hydraulic head difference over the revetment, exceed the dead weight of the structure. The concrete elements are lifted up and the waves subsequently induce erosion of the dike body. Therefore, the renovation of these revetments is currently done by adding more weight to the structure by covering the block revetment with large rocks, or even completely replacing the elements by bigger concrete blocks. In view of the large renovation areas, replacing the concrete elements is a time consuming process and will require considerable financial efforts. Therefore, innovative refurbishment techniques are desired and researched. A relatively new type of revetment is the polyurethane bonded aggregate (PBA) which consists of aggregate glued by the adhesive polyurethane (PU) and is currently marketed under the brand name Elastocoast. This study focuses on the use of PBA in strengthening pitched stone revetments.

In this report an effort is made to describe the mechanical behaviour of refurbished block revetments under wave loading. A PBA refurbishment layer adds coherence to the revetment and will prevent the blocks from uplifting. Another notable advantage is its high permeability. The studied design criterium in this research is the structure's flexural strength. If the hydraulic loads are increased, structural failure of the refurbished revetment will eventually occur when the bending stresses due to the external loads cannot be withstood by the PBA.

Besides considering the current design methods, also a more refined approach is adopted. Firstly, an analytical model was elaborated to gain a first general insight into the structural behaviour of a composite PBA/block revetment. In the analytical model, the interaction and stress distribution between the revetment and subsoil were modelled as an elastically supported beam (Winkler model). The analysis of beams on elastic foundations is widespread in civil engineering. Subsequently the structure was modelled with a finite element package. This finite element analysis helped to predict the structural behaviour of the composite revetment. It is assumed that the FEM model enables the most accurate modelling of the real situation. The main reason is that the Winkler model allows for tension forces in the subsoil which do not occur in reality. The analytical and FEM results were compared and discussed. With these models it was investigated which measures could be taken to improve the structural behaviour of the composite system. This study shows that the Winkler model greatly influences the bending stresses in the uplift region. On the other hand, it showed that when the upward displacements tend to zero or even become completely negative the Winkler model shows similarity with the FEM results.

An important input for the structural calculations were the load schematizations. Two load models were adopted in this research: the static and Wolsink load model. The static load model assumes a completely impermeable revetment. This is in contrast to the Wolsink load model, which assumes a certain permeability.

Although this research is based on multiple assumptions, it is possible to formulate some qualitative statements that resulted from this study.

1. The findings suggest that a rigid connection between the PBA layer and the existing block revetment is most effective in reducing the bending stresses in the PBA layer.
2. The results of this study support furthermore the idea that the composite PBA/block revetment could be schematized as an Euler Bernoulli bending beam.
3. The findings also indicate that the current design method is conservative. In this design method it is assumed that only the PBA cover layer contributes to the flexural strength of the structure. The results

of this thesis indicate that this design approach is conservative and therefore resulting in thick PBA layers.

4. Lastly, two conventional refurbishment techniques (Open Stone Asphalt (OSA) and hydraulic asphalt concrete) were compared with the PBA. Calculations were performed what the most effective approach would be. On the one hand, an impermeable cover layer constructed by asphalt concrete resulting in higher water pressures but increasing its dead weight (asphalt concrete), or on the other hand, applying a permeable refurbishment layer (PBA and OSA) which is less heavy but resulting in lower water overpressures. The results suggest that it is more effective to use a less heavier but more permeable material as a refurbishment than the other way around. It must be noted that this greatly depends of its permeability. If its leakage length is increased by clogging or when applying the refurbished material, it results in a significant increase of the maximum bending stresses. In this case the refurbishment techniques with asphalt concrete becomes more effective since it is heavier and therefore more effective in reducing the upward water pressures.

CONTENTS

List of Symbols	v
Summary	ix
1 Introduction	1
1.1 Problem description	1
1.2 Problem definition	3
1.3 Research Questions	4
1.4 Report Structure	4
2 Pitched Stone Revetments	7
2.1 Introduction	7
2.2 Properties	7
2.3 Element Types	8
2.3.1 Stability of Pitched Stone Revetments	9
2.4 Existing Reinforcement Methods	11
2.4.1 Replacement	11
2.4.2 Rotating	12
2.4.3 Riprap Refurbishment	12
2.4.4 Grouted Riprap Refurbishment	13
2.4.5 Asphalt Refurbishment	13
3 Polyurethane Bonded Aggregate	15
3.1 Introduction	15
3.2 PBA Components	15
3.2.1 Aggregate	15
3.2.2 Polyurethane Adhesive	15
3.3 Production Process and Preparation	15
3.3.1 Processing Notes	17
3.4 PBA Properties	18
3.4.1 High Porosity	18
3.4.2 Environmental Effects	18
3.4.3 Structural Properties	18
3.4.4 Erosion Resistance	21
3.5 Uneven Settlements	21
3.6 Layer Thickness	21
3.6.1 Minimum Functional Layer Thickness	21
3.6.2 Minimum Practically Achievable Layer Thickness	21
3.6.3 Minimum Required Cross Section	21
4 Loads Analysis	23
4.1 Waddenzee dike	23
4.2 Assumptions	24
4.3 Static Load Method	24
4.3.1 Water Pressure	24
4.4 Wolsink Method	27
4.4.1 Leakage Length	29
4.4.2 Situation 1 (Infinite Length)	29
4.4.3 Situation 2 (Finite Length)	31

4.5	Dead Load	33
4.6	Final Load Situations	34
4.6.1	Static Model	34
4.6.2	Wolsink Model	35
4.7	Conclusions.	38
5	Structural Analysis	39
5.1	Assumptions	39
5.2	Design Criteria	40
5.3	Structural Model	40
5.3.1	Theory	41
5.4	Supports	43
5.5	Soil and Foundation Characteristics	44
5.6	Young's Modulus	45
5.7	Stresses	45
5.7.1	Homogeneous Cross Section.	45
5.7.2	Inhomogeneous Cross Section.	46
5.8	Normal Force Analysis	47
5.9	Results Static Model.	49
5.9.1	Displacements	49
5.9.2	Bending Stresses	49
5.10	Results Wolsink Load Model	50
5.10.1	Displacements	50
5.10.2	Bending Stresses	50
5.11	Conclusions.	51
6	Finite Element Method Analysis	53
6.1	FEM Research Approach	53
6.2	Verifying Analytical Calculations	54
6.3	Static Load Model.	54
6.3.1	Winkler versus Continuous Foundation	54
6.4	Wolsink Load Model	56
6.5	Bending Beam Schematization	57
6.6	Conclusions.	59
7	Sensitivity Analysis	61
7.1	Young's Modulus	61
7.2	Hydraulic Loads.	62
7.2.1	Static Load Model	62
7.2.2	Wolsink Model	65
7.3	Full Friction versus Full Slip.	66
7.4	Friction Between Elements	69
7.5	Soil Variables	69
7.6	Supports	70
7.7	Simply Supported Beam Model	71
7.8	Conclusions.	72
8	PBA and Asphalt	75
8.1	Hydraulic Asphalt Concrete	75
8.1.1	Mechanical Properties	75
8.1.2	Permeability	76
8.1.3	Wave Impact	76
8.2	OSA and PBA	76
8.2.1	Mechanical properties	76
8.2.2	Permeability	76

8.3	Structural Modelling	77
8.3.1	Load Model	78
8.3.2	Hydraulic Asphalt Concrete	79
8.3.3	PBA and OSA.	80
8.4	Wave Impact	85
8.5	Durability	86
8.6	Costs	86
8.7	Conclusions.	87
9	Conclusions and Recommendations	89
9.1	Recommendations and Reflection	91
A	Appendix	95
A.1	Loads Analysis	95
A.2	Structural Analysis	96
A.3	Finite Element Method Analysis	96
A.4	Sensitivity Analysis	96
A.5	PBA and Asphalt	96
	List of Figures	97
	List of Tables	101
	References	103

1

INTRODUCTION

1.1. PROBLEM DESCRIPTION

On the 28th of February 2014 the Minister of Infrastructure and the Environment, Melanie Schultz van Haegen, revealed that 1302 km of the 3767 km primary flood defences are not sufficient any more to meet the established norms. Therefore, the water boards and Rijkswaterstaat are currently strengthening large parts of the Dutch dike system to satisfy these strict safety norms, i.e. 1:1250 (rivers), 1:4000 (coasts and deltas) and 1:10000 (Randstad) like shown in figure 1.1. This implies that dikes can withstand, after these improvements, more extreme water levels and severe storms. For instance, for Southern and Northern Holland the primary flood defences will have to withstand a design water level that has a 0.01 percent (1:10000) chance of occurring in any given year. Since 1996 the Dutch flood defences have to be tested every six years and checked whether the structures meet the standards described by law (Waterwet). The required safety standards differ per area. The purpose of this law is to ensure safety against possible floods and provide a general and clear procedure for Rijkswaterstaat and the water boards to check their flood defences. A guideline (Ministerie van Verkeer en Waterstaat, 2007) is prescribed by the Ministry of Infrastructure & the Environment which can be used by the owners of flood defences (water boards and Rijkswaterstaat) to check whether the dikes and structures are sufficient. However, it appeared that a significant part of the Dutch primary flood defence system does not meet the minimum standards.

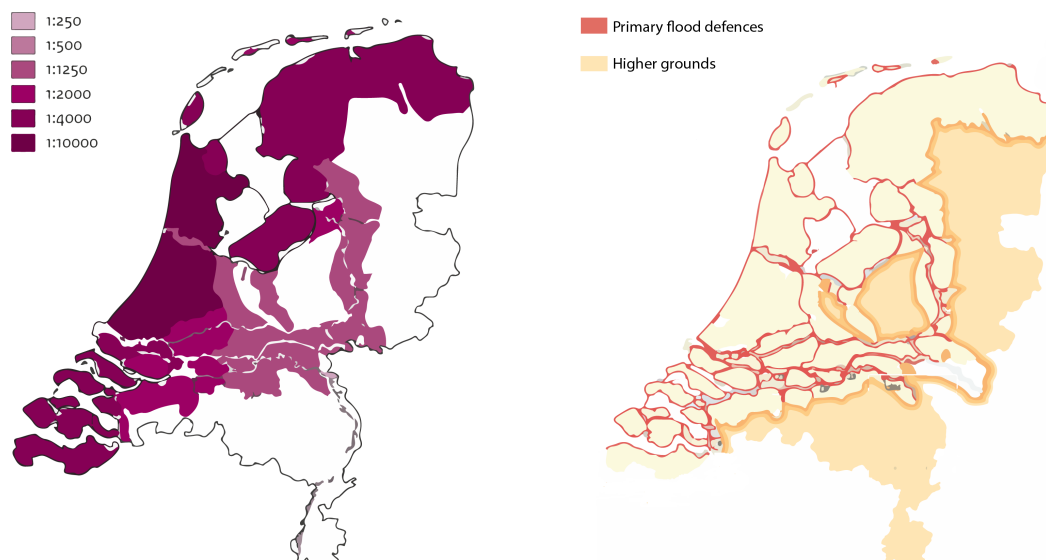


Figure 1.1: Left: Dutch safety norms of the primary flood defences according the "Waterwet", the required standards vary between 1:250 along river the Maas and 1:10000 for Southern and Northern Holland provinces. Right: the primary flood defences are indicated in red (Ministerie van Infrastructuur & Milieu, 2014)

As a consequence, large parts of the Dutch dikes, the mostly applied flood defences in the Netherlands, have to be reinforced in the coming years. Dikes can be breached by many failure mechanisms. The designer has to prove that the designed dike is able to meet the safety norms during the given lifetime of the structure. In general, one can distinct the failure mechanisms listed in the following enumeration and illustrated in figure 1.2.

- **Overflow and overtopping:** the height of the crest has to be sufficient to withstand the extreme water levels and wave heights. If a certain overtopping discharge is allowed, one has to check whether this discharge is not too high because the dike could fail. In case of a high discharge, the inner slope or the crest can erode which could result in failure of the dike. The overtopping discharge can also reduce its stability. If the overtopping discharge is too high, water will infiltrate in the top layer of the inner slope. This results in a saturated zone, i.e. a low effective soil stress and therefore a reduced resistance against sliding.
- **Piping:** stability problems through piping can occur when too many soil particles are transported by a strong seepage flow. Water seeps under the dike creating channels which undermine it.
- **Heave:** failure by heave occurs when upward seepage forces act against the weight of the soil, reducing the vertical stress to zero. Soil particles are lifted away by the vertical water flow and failure occurs.
- **Macro instability:** a sliding mechanism of large soil bodies. Sliding happens when there is no equilibrium of forces present any more. If the internal friction in the soil body of the dike decreases (when the water pressure increases), friction along the slip circle decreases and sliding will occur. It can happen on both sides of the dike, i.e. in the inner and outer slope.
- **Micro instability:** because water is seeping out of the slope, the grains are no longer stable and start to move out of the slope.
- **Liquefaction:** if water pressure increases in loosely packed soil layers, the internal friction between the grains will decrease. When the friction between the grains tends to zero, they loose their bearing capacity and sliding will occur.

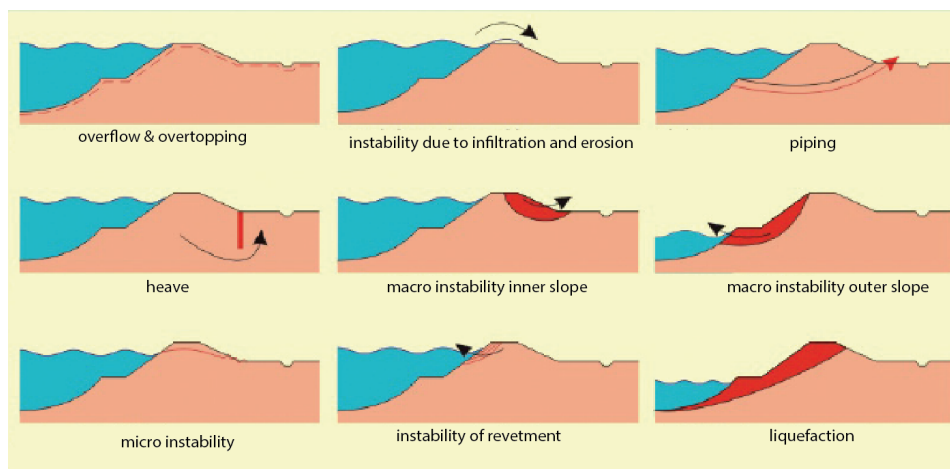


Figure 1.2: Failure mechanisms of a dike (Ministerie van Verkeer en Waterstaat, 2007)

- **Instability of the revetment protection:** the revetment on the seaward slope of the dike protects the dike body against erosion. The failure mechanism depends on the type of protections; the loads on these revetment types are the same, but completely different mechanisms determine the type of failure of the protection layer (Schiereck, 2012). The resistance of the protection is derived from friction, cohesion, weight of the units, friction between the units, interlocking and mechanical strength. As a result of the differences in strength properties, the critical loading conditions are also different. Maximum flow velocities will be governing for gravel/riprap, as they cause displacement of the material, while uplift pressures and impacts are of more importance for blocks and monolithic slabs as they tend to lift the protection.

In this thesis the focus will be on the last item of the previous enumeration, i.e. stability of the revetment protection. The most commonly used revetment in the Netherlands are pattern placed elements. For centuries the dikes have been protected by pitched blocks. More than 500 km of river, lake and sea dikes is protected by pitchings in the Netherlands (Dorst et al., 2012). A typical cross section of a dike consisting of pitched blocks is shown in figure 1.3. These block elements are mostly made of natural stone and concrete. The main fail-

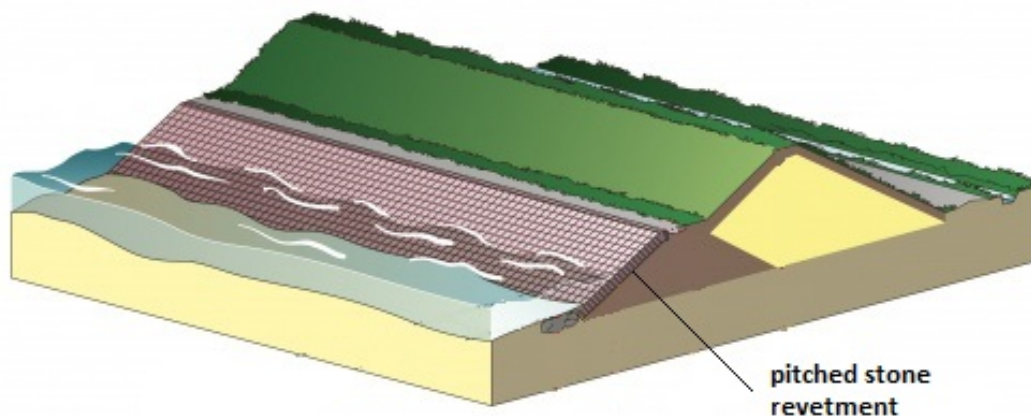


Figure 1.3: Cross section of a dike protected by a pitched stone revetment (Projectbureau Zeeweringen, 2010)

ure mechanism of a placed block revetment is uplifting due to water overpressures. This happens when the upward pressures, caused by an hydraulic head difference over the top layer, exceed the dead weight of the structure. Therefore, the renovation of these revetments is currently done by adding more weight to the structure by covering the block revetment with large rocks, or even completely replacing the elements by bigger concrete blocks. In view of the large renovation areas, replacing the concrete elements is a time consuming process and will require considerable financial efforts. A less time consuming possibility is constructing an asphalt refurbishment layer on top of the original block revetment. Although this approach results in extra coherence and dead weight, the revetment becomes (almost) completely impermeable resulting in higher water overpressures. Furthermore, asphalt is sensitive to repeatedly applied loads (fatigue). Therefore, innovative refurbishment techniques are desired and researched. One of these techniques is applying a thin PBA layer over the existing block revetment. PBA (polyurethane bonded aggregate), or called Elastocoast, is a relatively new type of revetment. The production process of a PBA revetment is easy and no specialized equipment is needed. Moreover, PBA has an high ecological potential. It can provide ecological benefits by acting as novel habitat for biological colonisation (Bijlsma, 2013). PBA is already successfully applied on dikes. However, there is still not much insight in the structural behaviour of a composite PBA/block revetment structure. Before one could apply PBA as refurbishment material, more research regarding its structural behaviour is desired.

1.2. PROBLEM DEFINITION

A significant part of the Dutch dikes does not meet the prescribed standards and safety norms. Also large parts of the dikes which are currently consisting of pitched stones have to be reinforced. In hydraulic engineering revetments are of great importance to protect hydraulic structures from eroding. A relatively new type of revetment is polyurethane bonded aggregate (PBA) which consists of aggregate glued by the adhesive polyurethane (PU) and is currently marketed under the brand name Elastocoast. This study focuses on the use of PBA in strengthening pitched stone revetments. A lot of research has been done regarding the behaviour of block revetments or PBA revetments applied individually. However, a revetment composed of PBA and concrete blocks has not been researched yet. The hypothesis is that adding a relatively thin layer of PBA on a pitched stone revetment effectively increases its resistance to wave loading and overpressures by mechanical interaction between the layers. At this moment it is unknown how the internal and external forces will be distributed within the structure.

1.3. RESEARCH QUESTIONS

The research questions provide a path through the research and are helpful to solve the problem definition and reach the research objectives. The main question is:

What are the characteristics of the structural behaviour of a composite PBA/block revetment in response to the governing hydraulic loads, i.e. what is the load distribution and which stresses and strains will occur within the cross-section?

To answer the main research question, three sub questions are formulated:

1. To what extent can the mechanical behaviour of the composite revetment be described in an analytical model and FEM model, and do the results of these models correspond?
2. Which type of bonding (full slip or full friction) between the two layers is most effective to withstand the hydraulic loads?
3. What are the main similarities and differences between a refurbishment constructed with asphalt and with PBA?

1.4. REPORT STRUCTURE

This research is related to the mechanical behaviour of a composite PBA/block revetment. In order to realize this structural analysis, first the structural behaviour and the failure mechanisms of a block revetment will be investigated. Secondly, an analytical model will be elaborated to gain a first general insight into the loading and structural behaviour of a composite PBA/block revetment. Subsequently the structure will be modelled with a finite element package. This finite element analysis should help to predict the structural behaviour of the composite revetment. The next step is to apply and compare the results. With the use of the FEM model, it will be investigated which measures could be taken to improve the behaviour and what the minimum required layer thickness should be. Furthermore it will be investigated which type of bonding (full slip or full friction) is most effective to withstand the hydraulic loads. Finally, the results of the FEM model will be compared with the behaviour of a conventional material (asphalt) as refurbishment layer on block revetments.

An overview of the nine chapters is shown in figure 1.4 and their relation with respect to the research questions. Every chapter ends with a brief conclusion of the most important findings and results of this specific chapter.

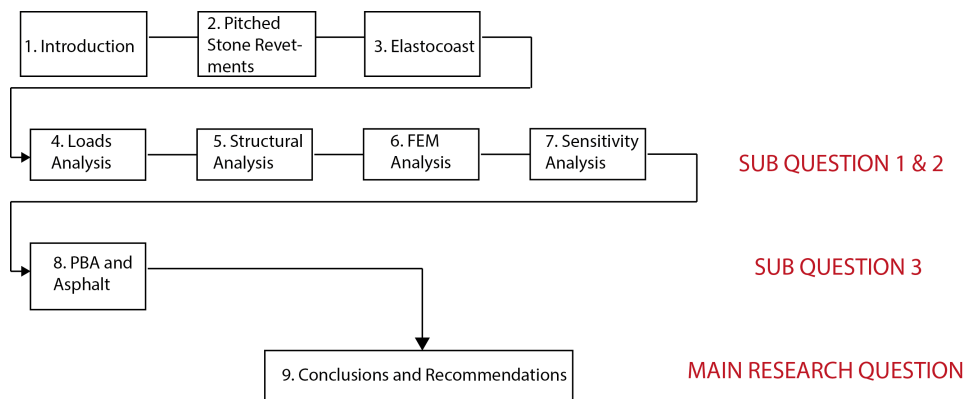


Figure 1.4: Overview of the chapters with respect to the research questions

1. Introduction:

This report starts with an introduction of the subject and the motivation of the topic being studied. Furthermore it provides the framework and indicates why it is necessary to conduct the study. Subsequently research questions are formulated to solve the problem definitions.

2. Pitched Stone Revetments:

The second chapter describes the main properties of a pitched stone revetment. To understand a composite PBA/block revetment it is important to get first an insight of the behaviour of an individual block

revetment before studying the composite system. In this chapter the different types of elements, the stability, the governing load situations and the failure mechanisms are discussed. This part contains furthermore an overview of the current dike reinforcement techniques used for pitched stone revetments.

3. Elastocoast:

The third chapter contains some general information about Elastocoast/PBA, mainly based on the PBA design manual. Firstly, the components of the PBA mixture are discussed followed by a brief description of the production process and the preparation procedure of the mixture. Secondly, different PBA properties are described, i.e. porosity, environmental effects and the structural properties. This chapter ends with a summary of some other important aspects which should be taken into account when applying PBA as revetment and specifically as refurbishment.

4. Loads Analysis:

The analysis of the loads is elaborating on the "Pitched Stone Revetments" chapter where the load mechanism and failure mechanism were discussed in general. In this subsequent chapter, two load models are described which have been used to calculate the hydraulic head differences over the revetment.

5. Structural Analysis:

The previous chapter is an important input for this chapter. The analytical model is described which have been used to calculate the maximum bending stresses in the outer fibres of the PBA layer. Calculations have been performed for the two load models described in the previous chapter.

6. FEM Analysis:

The next step in this research was modelling the problem with a finite element package. In this chapter, it is first explained how the FEM is used for this research, namely to reproduce the analytical model and add extra mechanisms that are too complex for an analytical approach. Subsequently the different models are explained, elaborated and compared.

7. Sensitivity Analysis:

In this part an evaluation of different parameters and input variables, which have been used in the loads, structural and FEM analysis, is done by performing sensitivity calculations. It is determined to what extent the different variables impact the outcomes under a given set of assumptions.

8. PBA and Asphalt:

It is interesting to compare two conventional refurbishment techniques (OSA and hydraulic engineering asphalt) with the new proposed technique (PBA). The pros and cons using PBA as refurbishment material in relation to the conventional method are discussed.

9. Conclusions and Recommendations:

Finally, this chapter reports the conclusions and recommendations that resulted from this study. It contains furthermore a scientific reflection of the results and the current design method.

It is important to distinguish the coherence between the chapters of this thesis. In the flowchart (figure 1.5) on the next page, the steps and the connection between the chapters are depicted.

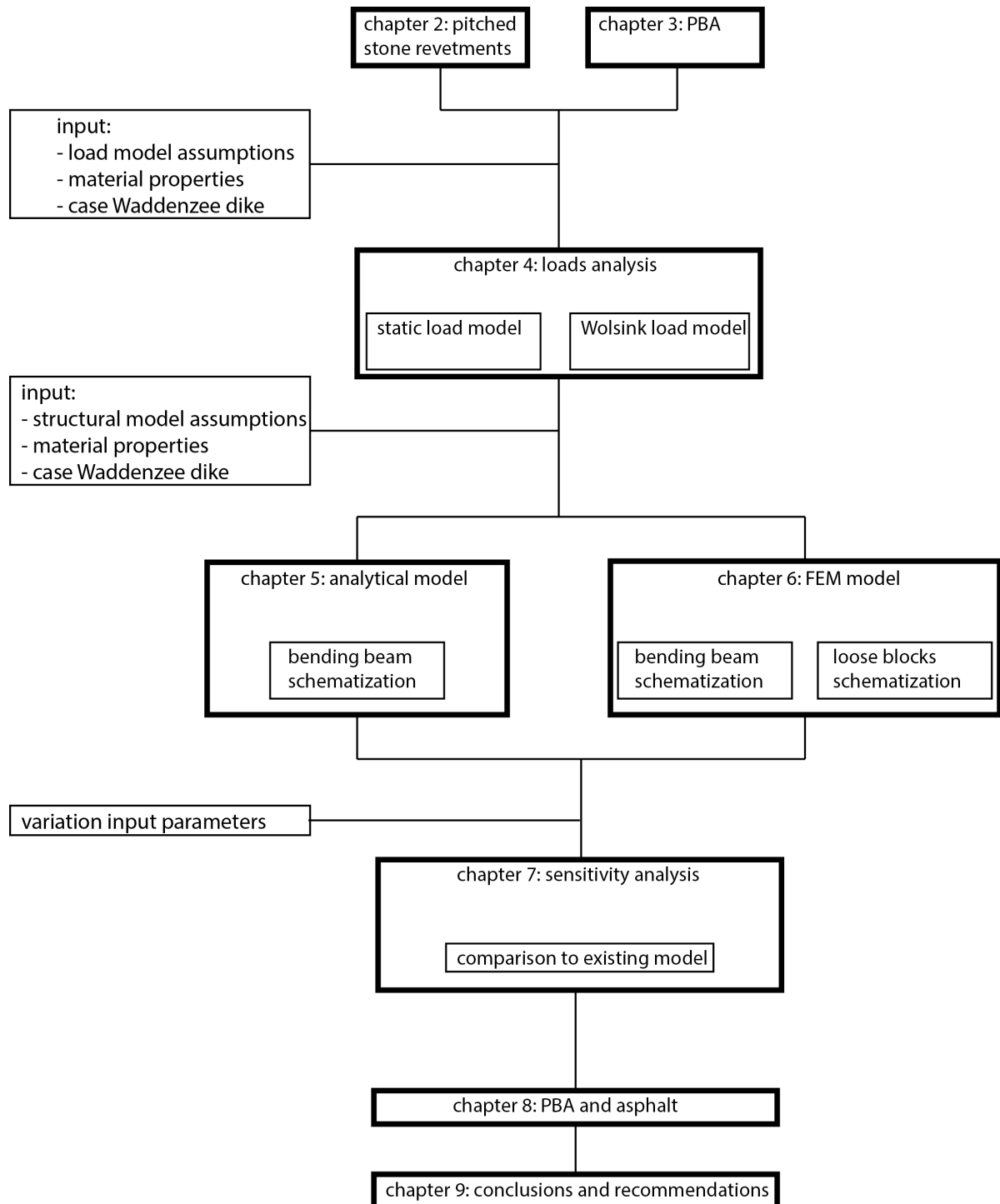


Figure 1.5: Flow chart of the different chapters

2

PITCHED STONE REVETMENTS

2.1. INTRODUCTION

Because the subject of this study is a PBA refurbishment applied on pitched stone revetments, firstly, the individual behaviour of pitched stone revetments is studied in detail. To study the structural behaviour of the composite PBA/block revetment, it is of importance to get more insight in the properties, failure mechanisms and structural behaviour of a pitched stone revetment without applying a refurbishment layer. The primary function of a revetment is to protect the dike body from erosion and therefore allow the dike to fulfil its function. In general three different types of revetments can be distinguished (Schierreck, 2012), the 3 categories are listed in table 2.1. Rocks (rip-rap) can be used to control erosion by armouring the dike. They dissipate

revetment type	properties
Loose rocks, rip-rap	open, permeable
Coherent	semi-permeable, pitched stone revetment
Impervious	asphalt, concrete, monolithic

Table 2.1: Revetment types with their characteristics (Schierreck, 2012)

the energy of storm waves and are highly porous if well designed and maintained. Loose rocks can be easily applied and cost less for maintenance.

Coherent revetments are pitched stone revetments. These placed blocks (or columns or other shapes) function well when applied as revetment, provided that the elements are placed with skill and care (Schierreck, 2012). The placed elements are mostly made of concrete. The coherence varies between the different types: blocks may be pitched, connected with cables or geotextile.

Impervious layers can be made out of concrete or asphalt. In contrast to the coherent revetments, the impervious revetment types form a whole instead of consisting of separate elements. Impervious means that there is no water or sand transport possible between the outer en the inner side, i.e. not permeable for water and sand tight. PBA is a combination of type 1 (Loose Rocks) and type 3 (monolithic). PBA acts like a plate structure (type 3) but is in contrast to concrete and asphalt permeable for water (and sand).

In the following sections the coherent revetment/block revetment type will be elaborated.

2.2. PROPERTIES

A block revetment is a protection of a shoreline with stony material, usually natural stone or concrete, with a thickness of only one layer of elements, and of which the elements are placed in a pattern, hence Dorst et al. (2012). When comparing block revetments with the other revetments listed in table 2.1, the difference is that the amount of material needed is significantly less than when using riprap. On the other hand, placing the concrete blocks is a time consuming process. The block is sometimes partially placed by hand to ensure maximum friction, therefore it involves very intensive labour, comparing with riprap. The main characteristics of this type of revetment can be summarised as follows:

- Usually single size blocks are used; sometimes gravel or sand is wedged between the blocks
- A block revetment has a relatively smooth surface
- The blocks are close jointed to minimise erosion of underlying soil. A loss of even one single element may trigger collapse by erosion of the underlying soil formation, therefore it requires frequent inspection

The transition between the blocks and the underlying soil is another variable (Schierreck, 2012). Main materials of a dike consist of sand and/or clay. The elements cannot be placed directly on the dike core otherwise the underlying material would be washed away through the joints. In figure 2.1 different possibilities are shown. First of all, the blocks can be placed with a geotextile on clay or sand. Geotextiles are permeable for water but sand tight and are made from natural or artificial fibres. This material is very useful to allow permeability and at the same time prevent the dike core from eroding. In the past the blocks were sometimes directly placed on clay. In section 2.3.1 it will be explained that a permeable top layer and an impermeable sublayer will lead to the most stable construction (small leakage length). This implies that if the blocks are placed directly on clay, one would obtain a very stable situation. However, such constructions are not stable in practice due to gully formation under the blocks (Schierreck, 2012). Another possibility is to construct a filter layer. Filter layers should hold the grains of the sub soil or core material of the dike and therefore prevent erosion.

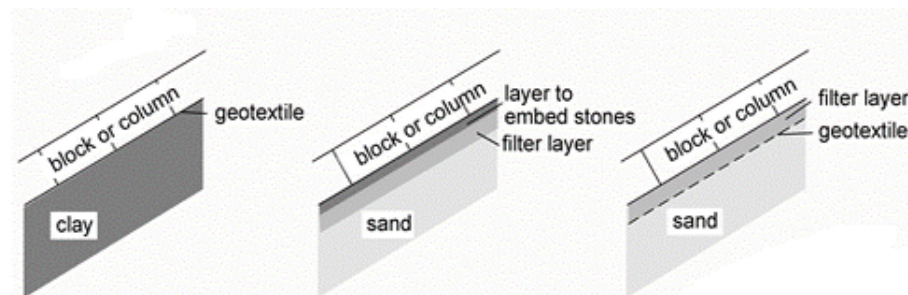


Figure 2.1: Block types and filters in revetments (Schierreck, 2012)

2.3. ELEMENT TYPES

There are several types of elements available. Usually if the element height is larger than its width, the elements are called columns. In contrast to blocks, where the surface diameter is larger than its height. To reduce labour costs, artificially shaped elements have been developed. The advantage of those elements is that they all have the same dimensions which results in an easier placement (e.g. by crane). The shape of the blocks is closely related to the permeability and therefore its stability. The blocks which have been developed in the recent years, are generally preferred since they have a column shape and a more open space between the elements. Several elements are shown in figure 2.2. To enhance the stability of the revetment, an

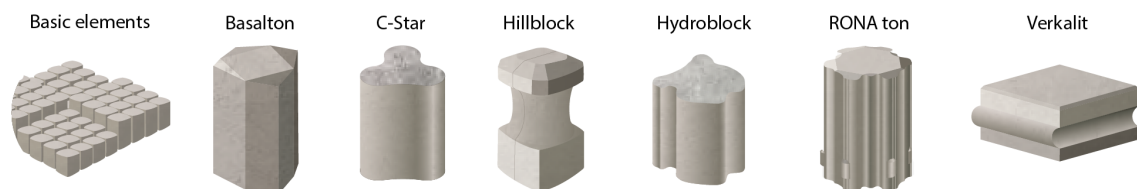


Figure 2.2: Impression of elements currently on the market, varying from (l) basic pitching stone elements ("checkerboard" placing) to alternative (less rectangular) shapes

additional interlocking mechanism can be used (Dorst et al., 2012). Interlocking increases the coherence of the entire structure and the blocks can therefore not simply be removed because one has to remove an entire section. Additional coherence can also be obtained by connecting the blocks with steel cables (e.g. Armorflex system). Although this results in a stable structure, it also results in less flexibility and maintenance/repairing is more difficult. An impression of the different mechanisms is shown in figure 2.3.

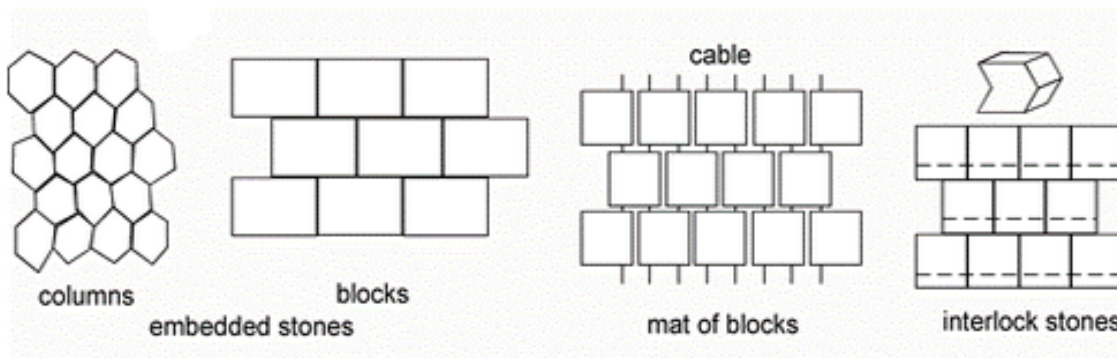


Figure 2.3: Placement of the blocks (Schierreck, 2012)

2.3.1. STABILITY OF PITCHED STONE REVETMENTS

Like stated in the introduction, dikes can be breached by many failure mechanisms. In this research the focus will be on failure due to instability of the pitched stone revetment protection. Before considering the stability of a pitched stone revetment, the loads have to be considered. Loads on a revetment can be divided into two groups: external loads and internal loads. One of the most important external loads is the impact load of the incoming waves. The waves carry a certain energy and this energy has to be (partly) restrained by the revetment to protect the dike body from erosion. On the other hand, there is an internal load because of the head difference between the ground water level within the dike body and the water level outside. This load is only of importance when applying not completely permeable revetments (if the layer is permeable (e.g. riprap) the water is able to move through the material and there is no pressure building up). The load distribution difference lies in the transfer function from the external to the internal load and from the internal load to the response of the structure (strength), hence Schierreck (2012). The load transfer can be illustrated by the leakage length parameter. The leakage length is the ratio between the permeability of the revetment (top layer) and the permeability of the filter layer, like shown in equation 2.1. One calculates the length which is needed for a water particle to flow through the filter layer which is equal as the time needed to flow through the top layer.

$$\Lambda = \sqrt{\frac{k_f d_f d_T}{k_T}} \quad (2.1)$$

Wherein:

Λ = leakage length parameter [m]

k_F = permeability of filter layer [m/s]

k_T = permeability of top layer [m/s]

d_F = thickness filter layer [m]

d_T = thickness top layer [m]

Therefore a high leakage length implies a relatively impermeable top layer compared with the filter layer which results in high pressure differences. Obviously, a low leakage length implies a very 'leaky' revetment which is preferable when reducing (water) overpressure difference. On the other hand, when considering equation 2.1, one could also solve this problem by making the filter layer less permeable. The leakage lengths of a rock, block and an asphalt revetment are respectively in the order of 0.1, 2.0 and 'infinitely high'. The leakage length should be considered in respect to the length in which the water level changes (Schierreck, 2012). This length is considered to be the length of the front of the wave (approximately 1-2 m for standard waves). An illustration of this theory is shown in figure 2.4. It can be concluded that a small leakage length is preferable, which implies that the top layer has to be more permeable than the filter/intermediate layer. For the pitched stone revetments the leakage length is in the order of the length in which the water level is varying ($\Lambda = L$).

In general, one can distinguish 3 failure mechanisms regarding block revetments (Ministerie van Verkeer en Waterstaat, 2007):

- Instability of the applied elements
- Sliding of the top layer/revetment

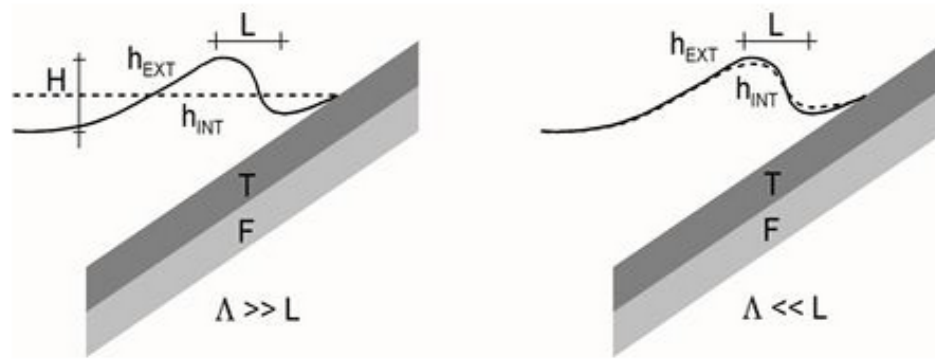


Figure 2.4: Influence Leakage Length (Schierreck, 2012)

- Transportation of soil particles/erosion from the underlying granular layers/filters

An overview of the failure mechanisms is shown in figure 2.5. Instability of the applied elements can be

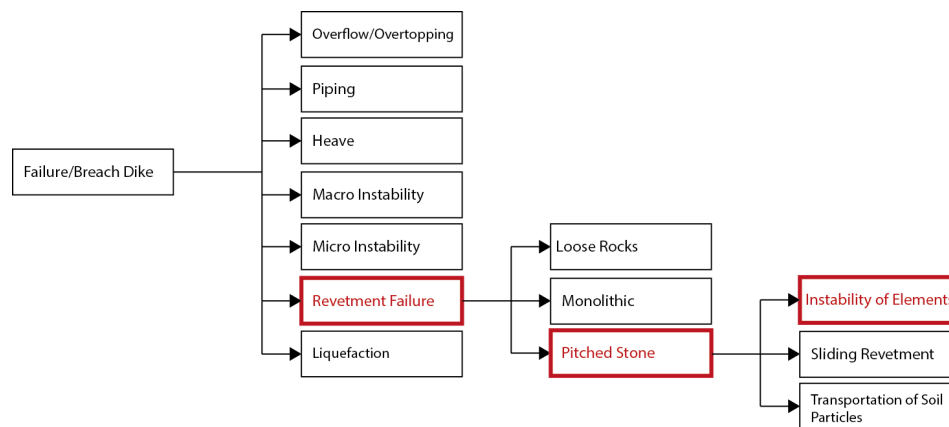


Figure 2.5: Overview Failure Mechanisms; the focus of this thesis will be on the subjects shown in the red boxes

seen as the governing failure mechanism of a pitched stone revetment (Ministerie van Verkeer en Waterstaat, 2007). This instability is caused by wave attack on the revetment. If a sufficient strong concrete class is used, the wave impact induced on the blocks is irrelevant. The governing failure mechanism is the uplifting force due to the head difference underneath the blocks. This is shown in figure 2.6. During maximum wave run-down the pressure is low in front of the wave, while under the blocks it is high due to the phreatic level within the dike core (Schierreck, 2012). There is no counter force to restrain the water (over)pressure from inside the core. As a consequence the water pressure tries to push the blocks out of the revetment. Due to this mechanism two types of failure can occur, i.e. piston type failure and the beam type failure (Schierreck, 2012). If one stone is pushed out due to the force underneath the stone the piston type failure will occur. A requirement for this failure mechanism is that the layer underneath the block revetment is permeable because water needs to be able to flow underneath the blocks. However, the block is trying to restrain this uplifting force with its dead weight, the friction force on both sides of the block and the fact that a certain inflow needs to occur like stated before.

The second mechanism is the beam type failure. This happens when a entire row of blocks is lifted out of the revetment. Due to the friction of the adjacent blocks it is possible that an entire row can be lifted out.

The head difference over the top/block layer can be calculated in several ways. In chapter 4 different methods are discussed. Considering the leakage length, one can conclude that the larger the leakage length is, the weaker the structure is, the more vulnerable the blocks are for uplifting. When the leakage length is small, i.e. a permeable structure, water is able to flow through the top layer and therefore the piezometric head difference is less. Besides the piston type failure, the beam type failure can occur when there is sufficient

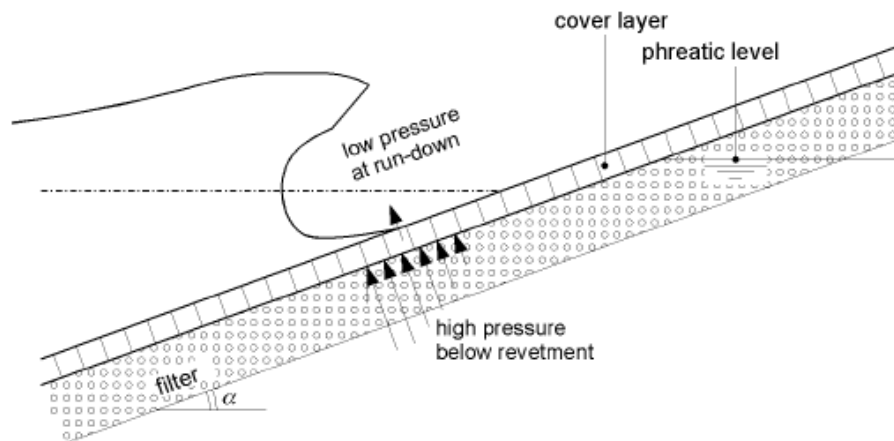


Figure 2.6: Loading mechanisms in block revetments (Burger, Klein Breteler, Banach, Bezuijen, & Pilarczyk, 1990)

friction present between the elements. During this failure mechanism a whole set of blocks is lifted up, like shown in figure 2.7. Figure 2.8 also shows failure of a pitched type revetment. In this case an entire mat of

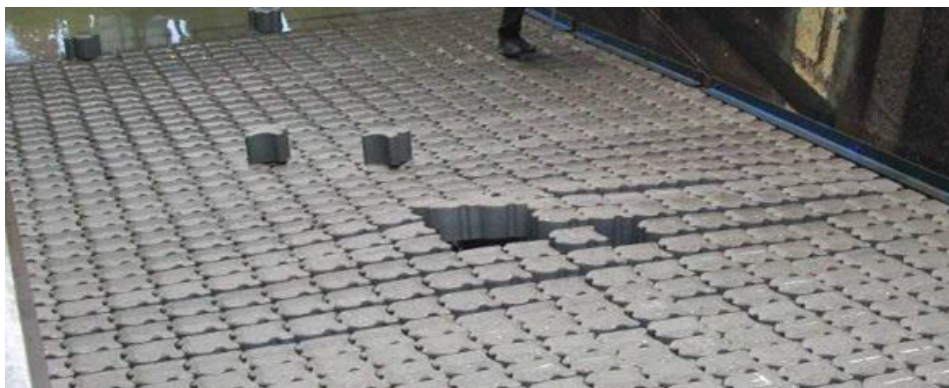


Figure 2.7: top: model beam type failure (photo: Verhagen)

blocks is lifted up and the revetment is not able to prevent the shore from eroding.

2.4. EXISTING REINFORCEMENT METHODS

Like stated in the introduction of this thesis, a significant part of the Dutch primary flood defence system does not meet the minimum standards and has to be reinforced in the coming years. Several strengthening techniques can be used to reinforce the existing pitched stone revetments. In the following section, the most commonly applied techniques are briefly discussed.

2.4.1. REPLACEMENT

One of the possibilities is replacing the current elements by bigger ones. By increasing the height of the blocks, the dead weight of the revetment per square meter increases and therefore its resistance against up-lifting. Like stated in section 2.3, lots of new element shapes have been developed in the recent years. Many manufacturers offer a wide range of elements that vary not only in thickness but also in their shape. Because the shape of the elements is closely related to the permeability of the structure, it also determines its stability. Furthermore, to reduce labour costs, artificially shaped blocks have been developed. The advantage of those elements is that they all have the same dimensions which results in an easier placement. However, placing new elements is still a time consuming process. One could also choose for interlocking blocks to create more friction between the elements. Besides a certain interlocking mechanism, the blocks can be linked together to form mattresses or mats. Usually the blocks are connected by steel cables through prefabricated holes in the elements.



Figure 2.8: Failure of interlocking blocks in New York (photo: Kruis)

2.4.2. ROTATING

To save money the existing concrete elements can also be reused in the new revetment. This method is often applied when the width of the original blocks is larger than its height. If the blocks are rotated and replaced again within the structure, a bigger (dead weight) density is realized. Obviously, for a part of the revetment still new elements have to be placed. In figure 2.9 an impression of this technique is shown.



Figure 2.9: The original elements are reused: by rotating the blocks, the dead weight per area increases ([Projectbureau Zeeweringen, 2010](#))

2.4.3. RIPRAP REFURBISHMENT

A relatively easy method to increase its dead weight, is by placing riprap on top of the current revetment (figure 2.10). The advantages of riprap are that it is highly durable and that these kinds of revetments are flexible. The main limitation of riprap revetments is that it is not suitable for steep slopes. Research regarding the stability of riprap has shown that a stable stone size is dependent on the velocity of the flow, the level of turbulence/flow conditions and the properties of the stone size (density).



Figure 2.10: Riprap refurbishment of an existing block revetment (photo: Hoogheemraadschap Hollands Noorderkwartier)

2.4.4. GROUTED RIPRAP REFURBISHMENT

In order to increase their stability and minimise the risk of loss of rocks during wave attacks, the riprap refurbishment is sometimes grouted with cement or bitumen. Comparing with loose riprap, grouting allows the use of a smaller rock size but the permeability of the revetment is significantly reduced (Escameia, 1998). When cement is used, there is also a reduction in flexibility and the revetment becomes less able to adjust to ground settlements. In case of riprap, bitumen is the material most commonly used. There are different degrees of grouting possible. The entire height can be grouted which results in a stiff structure. However, this results also in an impermeable layer and therefore increasing the loads. It is also possible to grout only a part of all the voids between the stones, and therefore allow some permeability.

2.4.5. ASPHALT REFURBISHMENT

Asphalt/bituminous revetments have been widely applied in the Netherlands. They can be divided into two main categories according to their porosity: permeable and impermeable (Escameia, 1998). Besides adding weight, it also adds coherence and stability to the original block revetment. Especially open stone asphalt (OSA) is often used in the Netherlands to protect the banks and dikes against erosion. An advantage of open stone asphalt is that the material is not impermeable like hydraulic asphalt concrete. The porosity is in the order of 20-25 % and it has a density of approximately 1900 kg/m^3 . The construction of OSA revetments is usually done in two stages: the preparation of the mastic and the mixing with the stones. The disadvantages are the fatigue sensitivity of the material and the 'unnatural' appearance of bitumen. Furthermore, when applied as refurbishment on existing pitched stone revetments, the permeability of the composite structure could be reduced. OSA can be placed with a crane with a slope profiling bucket, subsequently the material is profiled to the required thickness (Pilarczyk, 1998).

In the following chapters the reinforcement method with PBA is studied. In chapter 8 PBA is compared with these conventional techniques.

3

POLYURETHANE BONDED AGGREGATE

3.1. INTRODUCTION

This chapter contains some general information about polyurethane bonded aggregate (PBA), mainly based on the PBA design manual (Bijlsma, 2013). Firstly, the components of the PBA/Elastocoast mixture are discussed followed by a short description of the production process and the preparation procedure of the mixture. Secondly, different PBA properties are described, i.e. porosity, environmental effects and the structural properties. This chapter ends with a summary of some other important aspects which should be taken into account when applying PBA as a revetment.

3.2. PBA COMPONENTS

3.2.1. AGGREGATE

PBA consists of mineral aggregate bonded by a two component polyurethane adhesive (PU). In the PBA each individual rock is covered with a thin film of polyurethane. When the adhesive is cured, the rocks are bonded together only on their contact points and therefore creating a permeable structure hence Bijlsma (2013) in the PBA revetments design manual. For the granular material basically any grading class can be used and the material can be broken and/or rounded. However, in practice, the PBA revetment will be constructed from a narrow grade aggregate, with stone sizes varying from 8/11 mm to 40/60 mm. Table 3.1 shows two types of aggregate that have been used in PBA revetments.

Mineral aggregate	Used Grading	Density kg/m ³	Bulk density kg/m ³
Limestone	10/14 mm, 20/40 mm, 30/60 mm	2650-2700	1350-1450
Granite	16/36 mm, 40/60 mm, 50/60 mm	2600-2800	1600-1700

Table 3.1: Examples of materials and grading that have been used for PBA, (Bijlsma, 2013)

3.2.2. POLYURETHANE ADHESIVE

Polyurethane (PUR or PU) is already, before the application in the hydraulic engineering sector, applied in many other areas (e.g. automotive industry, consumer sector, building industry and the furniture and mattress sector (Isopa, 2009). It is a polymer composed of a chain of organic units joined by urethane links. The bonding system created by the polyurethane produces strong bonding forces between the aggregate material. The PU consists of two fluid chemical components: the A-component polyol and the B-component isocyanate (Bijlsma, 2013). The ratio of mixture A:B is approximately 2:1. Together these components create a strong adhesive. If the adhesive is cured, a durable solid of PU is created.

3.3. PRODUCTION PROCESS AND PREPARATION

The production process of a PBA revetment is relatively easy according to Bijlsma and Voortman (2009). First the PU adhesive is created with the the chemical components as stated in the previous section. Figure 3.1



Figure 3.1: Mixing of the components in situ: polyol and the isocyanate (photo: Bijlsma)

shows how this works in situ. Secondly, the bucket filled with PU is added in the mixing system and subsequently mixed with the aggregate which is inserted on top via a crane. The mixing of PU with the aggregate does not differ from the mixing of concrete. The process of mixing the PU and the granular aggregate takes approximately 3 minutes. For optimum strength it is required that each individual rock is completely covered with a thin film of polyurethane (Bijlsma, 2013). This is illustrated in figure 3.2.



Figure 3.2: The polyurethane and the aggregate are inserted and subsequently mixed (photo: Bijlsma)

Subsequently the mixture is then cast in-situ on the area of application where the adhesive cures into a durable solid. The curing process starts once the components come in contact with each other. Before this curing takes place, the unhardened mixture can be processed for approximately 20 minutes at a temperature of 23°C (see figure 3.3). During these 20 minutes the PU is sufficiently viscous to create connections between the contact point of the applied aggregate (Bijlsma, 2013). After 24 to 48 hours the PBA has reached its full

strength. This final bonding system creates an highly open and porous materials with an open pore volume of approximately 50%.



Figure 3.3: Before curing takes place, the unhardened mixture can be processed for approximately 20 minutes (photo: Bijlsma)

3.3.1. PROCESSING NOTES

The following requirements have to be taken into account for the construction of PBA revetments. Two main requirements are that the aggregate are dry and clean when the stones are mixed with the adhesive. Moisture remaining on the stones would otherwise lead to a reaction between the PU and water resulting in a weak bonding (figure 3.4). Also dust need to be avoided. Too many fine particles results in an increased amount of required polyurethane and therefore an increase in costs.



Figure 3.4: Example for a quality defect caused by residual moisture on the granular material during the mixing process (photo: IMS)

3.4. PBA PROPERTIES

The PU together with the aggregate creates an open, porous and monolithic structure. Due to this composition the PBA has many advantages in comparison to conventional revetments.

3.4.1. HIGH POROSITY

The incoming waves carry a certain amount of energy that has to be distributed at the interface of land and water. Energy that is not reflected or transmitted is absorbed on the dike slope and is always at the expense of the protection (Schierreck, 2012). The porous PBA structure efficiently absorbs (partly) the wave energy of incoming waves, resulting in a lower impact on the stones. The wave energy is distributed over a larger area and therefore diminishing local concentrations of surface pressure. A comparison with a conventional revetment is shown in figure 3.5. Furthermore the extent of the wave run-up, defined as the maximum water

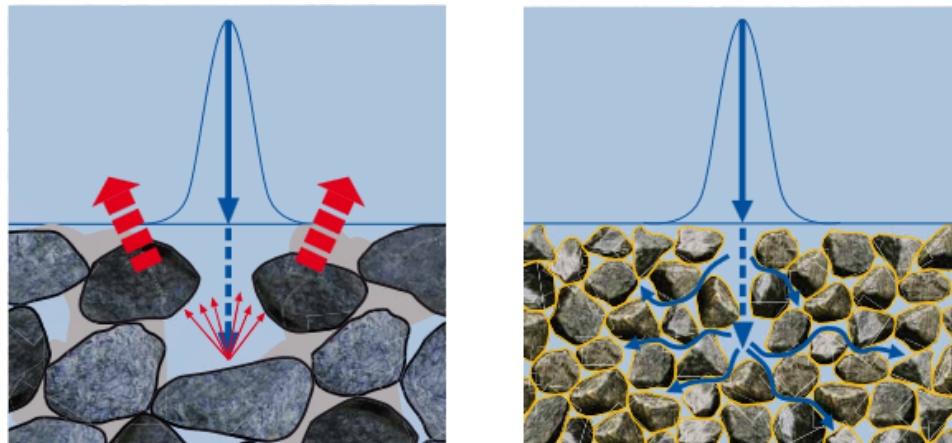


Figure 3.5: Wave energy dissipating when applying a conventional concrete revetment (left) and PBA (right) (BASF, 2010). Due to the open structure of PBA, the wave energy can be better absorbed.

level on a slope during a wave period, and the run-down, defined as the minimum water level on a slope, is significantly reduced due to the hydraulic roughness of PBA. The wave run-up can be reduced by 25 to 50% with a PBA revetment in comparison to an impermeable slope (Bijlsma, 2013).

3.4.2. ENVIRONMENTAL EFFECTS

Obviously, every hydraulic structure is subject to the weather when applied outdoor. The climate circumstances affect the structure constantly. To study these effects, the weathering of the material has to be studied. The main factors of weathering are solar radiation, temperature and water (moisture). From visual assessments and laboratory research it can be concluded that PU proves to be able to create a durable bonding of mineral aggregate in a marine environment hence Bijlsma (2013). Besides the weathering properties of PBA it has also an high ecological potential. Biological studies by the University of Amsterdam have shown that PBA revetments are colonized by the flora and fauna of the local region within just a few weeks (BASF, 2010). Unlike impervious revetments, PBA provide habitats for the animal and plant world. As a consequence PBA blends better into the local coastal landscape, like shown in figure 3.6. However, the permeability could be affected due to the presence of flora and fauna.

3.4.3. STRUCTURAL PROPERTIES

The structural properties are determined by a number of aspects. These aspects are shown in table 3.2.

MECHANICAL PROPERTIES

Before analysing the mechanical properties one has to conclude that these properties are linked to the grading class of the aggregate. Bijlsma (2013) concludes that the designer has to make a trade off between hydraulic properties, mechanical properties and costs. This dependency is explained as follows:

- use of high quality aggregate (i.e. basalt, granite) increases the bulk weight as well as the strength of the revetment



Figure 3.6: PBA ensures rapid new growth of algae and provides habitats (photo: Bijlsma)

aspect	property
density	dead weight of the PBA revetment
permeability	hydraulic conductivity
hydraulic roughness	wave run-up and run-down
minimum layer thickness	practical and functional limits
strength	flexural, compressive and tensile strength
stiffness	bending stiffness, deformation

Table 3.2: Structural Properties

- addition of finer fractions, a wide gradation or combinations of narrow gradations will increase strength but also the amount of PU needed
- a higher grading class increase hydraulic roughness and wave energy dissipation

Therefore it can be concluded that the choice of the grading class determines the mechanical properties. Furthermore the bonding material plays an important role.

The mechanical properties of PBA are described by [Gu \(2007\)](#) and [Bijlsma \(2013\)](#). Three important mechanical properties are:

1. stiffness
2. flexural strength
3. fatigue

STIFFNESS

Stiffness is of importance when deformation induces 'collapse' of the structure or structural element. It shows to what extent it resists deformation in response to an applied force. The Young's modulus is a measure of the stiffness of a material. Measurements at the Dutch KOAC/NPC company showed that PBA creeps much less than asphalt at the relevant lower temperatures. This implies that the revetment does not show time dependent (plastic or viscous) behaviour and can be assumed to behave elastic when applied as a revetment ([Bijlsma, 2013](#)). Figure 3.7 shows the stiffness of PBA related to the temperature. These results are based on 3-point and 4-point bending tests. Generally, the temperature of the revetment can be assumed to follow that of the (sea) water temperature. In a moderate climate the PBA stiffness can therefore be assumed at $E = 3000$ MPa ([Bijlsma, 2013](#)) for preliminary designs. This value is also used in this study. However, given the variation of stiffness shown in figure 3.7 it is advised to determine the design value, specific to the chosen mixture and conditions.

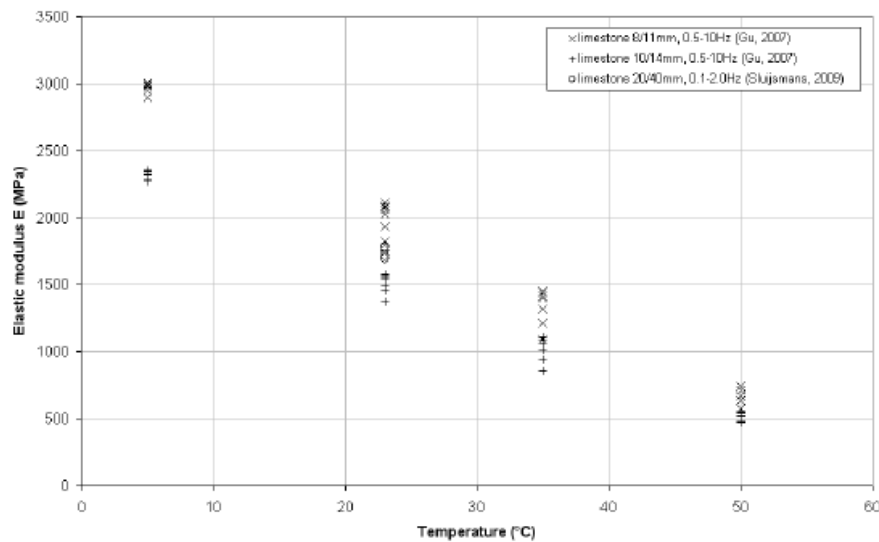


Figure 3.7: PBA measurements related to temperature (Bijlsma, 2013)

FLEXURAL STRENGTH

External loads will cause bending stresses in the PBA material. The flexural strength is a measure for the maximum bending stress that the material can restrain. The flexural strength strongly depends on the grain size (grading class) and the grain size distribution, but also on the type and quality of the aggregate hence Bijlsma (2013). Different tests were performed and the results are shown in figure 3.8.

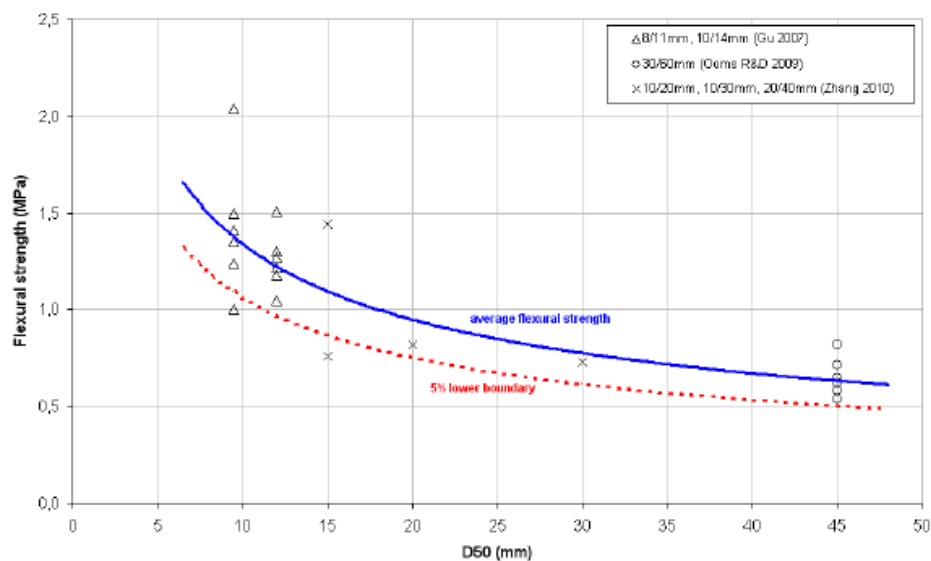


Figure 3.8: Flexural strength of PBA related to stone size (Bijlsma, 2013)

FATIGUE

Fatigue occurs when a material is subjected to repeated loading and unloading. It is structural damage that occurs when a material is subjected to cycling loading. Fatigue might be a problem when the subsoil is not sufficiently stiff, the material bends under wave impacts and the PBA is sensitive to fatigue (Verhagen, 2009). However, various bending tests have shown that PBA is not very susceptible to fatigue. Calculations (Gu, 2007) show that even with very pessimistic material properties elastomeric layers will not fail because of fatigue. The main reason is the open structure of the polyurethane bonded material (Verhagen, 2009).

3.4.4. EROSION RESISTANCE

Erosion occurs everywhere in nature where the bed consists of fine sediment (Schiereck, 2012). The most important current loads over sloping revetments are the result of wave run-up and wave run-down. The PBA revetment is well capable of withstanding high current velocities (Bijlsma, 2013). Because of the strong bonding between the individual rocks, the resistance to erosive forces is very high. Experiments show that PBA is able to restrain high currents without almost no damage. The strength of the bonding is therefore not affected. This high resistance is also confirmed in a wave overtopping test done in a simulator in Kattendijke. The results were performed by Infram B.V. (Infram B.V., 2008) and concluded that the PBA revetment was able to withstand a discharge of 125 l/m/s.

3.5. UNEVEN SETTLEMENTS

In cases where strong settlement behaviour of the dike body is expected after construction of the revetment, the effect of imposed deformation by uneven settlement must be taken into account in the design of the PBA layer (Bijlsma, 2013). Uneven settlement leads to an increase of internal stresses. Since the behaviour of PBA is elastic (see section 3.4.3) it will not be redistributed over time. The plate revetment is relatively stiff and is not able to adapt to these settlements. The extra internal stresses must therefore be taken into account when designing the PBA cover layer.

3.6. LAYER THICKNESS

In general PBA revetments are applied with a thickness of 0.10 m varying to 0.50 m (Bijlsma, 2013). The layer thickness is the largest of the following enumeration:

1. minimum functional layer thickness
2. minimum practically achievable layer thickness
3. minimum required cross section

3.6.1. MINIMUM FUNCTIONAL LAYER THICKNESS

A minimum layer thickness of approximately two times the median nominal diameter of the aggregate, is required to ensure complete coverage of the application area. This rule is commonly applied for dumped rock revetments.

3.6.2. MINIMUM PRACTICALLY ACHIEVABLE LAYER THICKNESS

It is not always feasible to achieve very thin revetment layers due to the used construction equipment. From a practical point of view a minimum layer thickness of approximately 2.5-3.5 times the median nominal diameter is advised. Besides the accuracy of the equipment, these numbers are based on stone size and the shape of the underground (Bijlsma, 2013).

3.6.3. MINIMUM REQUIRED CROSS SECTION

Besides the above functional and practical limitations, the layer thickness has to be designed with a certain cross-sectional height to restrain the hydraulic loads. The loads are: wave impact, uneven settlements, currents, traffic loads, ice loads and uplifting.

4

LOADS ANALYSIS

In this chapter an analysis of the different loads is elaborated. The loads are an important input for both the analytical and the FEM model. First of all, a practical case is discussed which is used for calculation purposes and to study the proposed theory. This part is followed by an overview of the governing loads. The governing load situation is assumed to occur during maximum wave run-down. During this situation, there will be an incoming wave that a moment later will cause wave impact. However, the pressure is very low in front of this wave, while under the blocks within the filter it is very high due to the phreatic level. This implies that during maximum wave down rush, there is no counter force to restrain the water pressure from inside the core which could result in uplifting of the blocks. Two loads models are described, i.e. the static load model and the Wolsink load model. The major difference between those models is whether the permeability of the revetment is taken into account and therefore considering a flow through the filter and top layer. Finally, the influence of a PBA refurbishment layer on the different models is discussed.

4.1. WADDENZEE DIKE

The theory explained in the following chapters is applied on a practical case in the Netherlands. To ensure its protection function, the water board recently decided to strengthen a dike at the Waddenzee. It appeared that the block revetment is not sufficient any more to withstand the future hydraulic loads. Currently it is studied whether a PBA refurbishment layer can be applied to strengthen the dike. Therefore, for calculation purposes, the proposed load and structural models are examined for this dike. A longitudinal cross section is shown in figure 4.1.

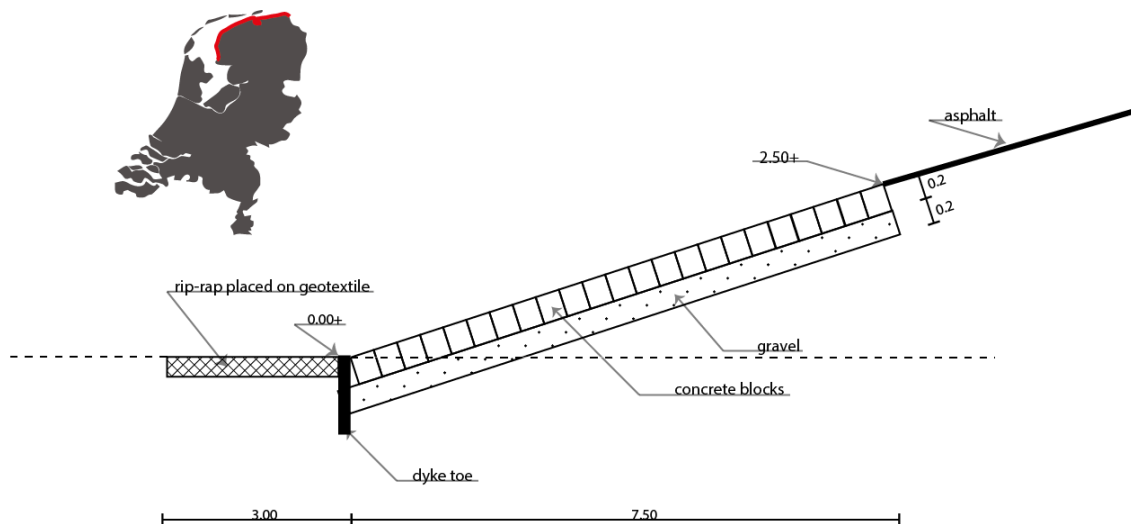


Figure 4.1: For calculation purposes the properties of a dike at the Waddenzee are used

The hydraulic data and properties for this situations are as follows:

Hydraulic Boundary Conditions	
significant wave height	0.96 m
wave peak period	6.67 s
still water level	NAP +2.5 m
water density	1025 kg/m ³
revetment length	7.5 m
block width	0.2 m
block height	0.2 m
filter thickness	0.2 m
PBA density	1400 kg/m ³
concrete density	2400 kg/m ³
dike slope	1:3

Table 4.1: Governing data for the Waddenzee dike

4.2. ASSUMPTIONS

The general assumptions used to define the load models, are stated in the following enumeration:

- The linear wave theory is valid
- The significant wave height (H_s) is determined with the Rayleigh distribution
- The wave height at the toe is equal to the significant wave height
- Deep water wave theory is assumed
- It is assumed that a hydrostatic water pressure defined by the still water level exists behind the revetment in the filter layer
- The water level outside is at rest and in stable equilibrium which results in an hydrostatic water pressure
- The water pressure within the dike starts from the water table, capillary movement is neglected

4.3. STATIC LOAD METHOD

A relatively simple load situation described in the literature, is the static load method. It is assumed that the revetment is completely impermeable and that there is no flow of water between the top and bottom of the revetment. Reduction of the pressure due to leakage through the joints between the blocks is therefore neglected. The wave front is schematized as a vertical line. Due to the assumed impermeable revetment layer, the pressure difference can immediately be calculated by considering the freatic level within the dike core and the water level outside. The method is illustrated in figure 4.2.

4.3.1. WATER PRESSURE

An assumption of this model, is that the wave run-down is equal to a distance Z measured from the still water level to the slope of the dike (Vrijling et al., 2001). This length can be calculated with the following formula:

$$Z = 0.33 H_s \xi \quad (4.1)$$

Wherein:

Z = vertical distance between SWL and slope [m]

H_s = significant wave height [m]

ξ = Iribarren number [-]

The Iribarren number can be calculated with the following formulas:

$$\xi = \frac{\tan \alpha}{\sqrt{s}} \quad (4.2a)$$

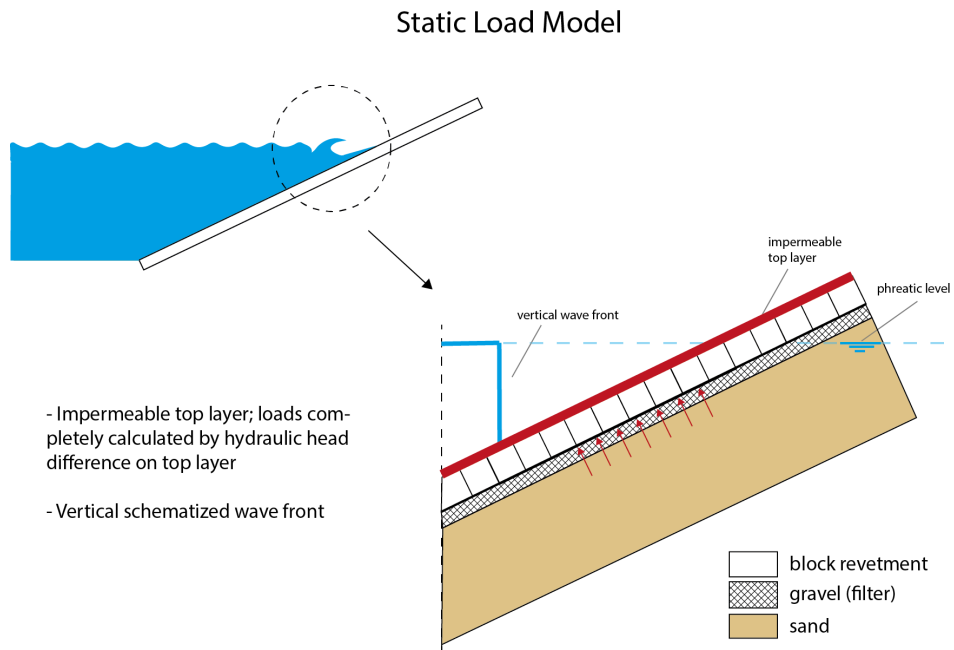


Figure 4.2: Static Load Model

The s variable is called the wave steepness and can be calculated with:

$$s = \frac{2\pi H_s}{g T_p^2} \quad (4.2b)$$

Wherein:

g = gravitational acceleration [m/s²]

T_p = wave peak period [s]

The maximum pressure difference can be determined by considering the piezometric level or hydraulic head. This is a specific measurement of liquid pressure above a datum/reference level. The piezometric head is defined as:

$$\Phi = z + \frac{p}{\rho_w g} \quad (4.3)$$

Wherein:

Φ = piezometric head [m]

z = height difference [m]

p = pressure [Pa]

ρ_w = water density [kg/m³]

Subsequently the hydraulic head has to be translated into a distributed load. This can be done by multiplying the hydraulic head difference between the top and filter layer with the specific weight of water.

$$q_R = \Delta\Phi \cdot \gamma_w \quad (4.4)$$

Wherein:

q_R = distributed load [N/m]

$\Delta\Phi$ = head difference [m]

γ_w = specific weight of water [N/m³]

When considering figure 4.3 the equation for the hydraulic head of the filter layer and top layer can be determined. The hydraulic heads, by considering the axis system and the reference level $z = 0$ in figure 4.3, are as

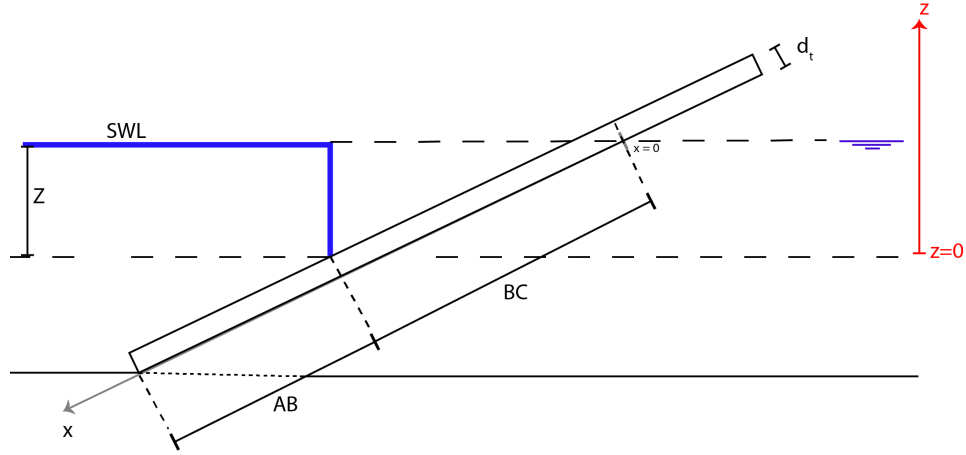


Figure 4.3: Static Load Situation

follows:

$$\Phi_{BC}^f = Z \text{ for } 0 < x < BC \quad (4.5a)$$

$$\Phi_{BC}^t = Z - \sin \alpha x \text{ for } 0 < x < BC \quad (4.5b)$$

$$\Phi_{AB}^f = Z \text{ for } BC < x < AB+BC \quad (4.5c)$$

$$\Phi_{AB}^t = Z \text{ for } BC < x < AB+BC \quad (4.5d)$$

The maximum head difference occurs at $x = \frac{Z}{\sin \alpha} + \frac{d_t}{\tan \alpha}$ ($x = BC$). The static load situation is calculated with the use of Maple software for the Waddenzee dike. The plots are shown in figure 4.4. In figure 4.5 the two lines

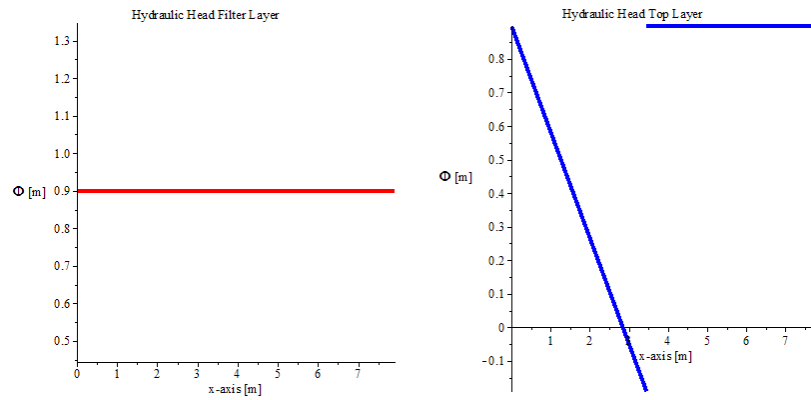


Figure 4.4: Hydraulic heads: blue = hydraulic head top layer, red = hydraulic head in the filter

are subtracted from each other which results in the pressure difference dependent of the x-coordinate. It can be concluded that the maximum head difference is equal to 1.09 meter. This value can also be obtained by adding the relatively height difference between the filter and top layer Δz (with respect to the reference level) and the Z value. This implies:

$$\Delta \Phi_{max} = Z + \Delta z = Z + d_t \cos \alpha \quad (4.6)$$

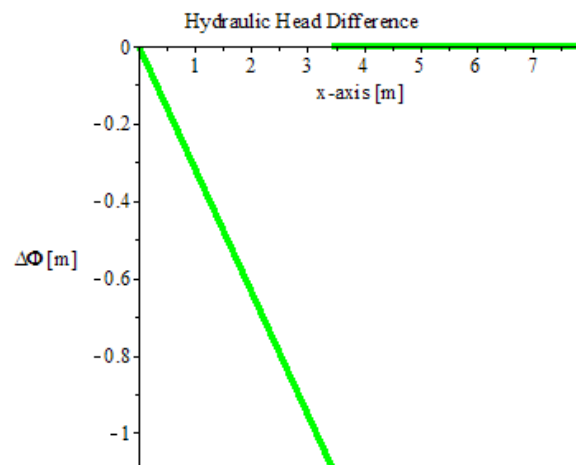


Figure 4.5: Hydraulic head difference between top and filter layer

4.4. WOLSINK METHOD

In the 'static load model' the revetment is assumed to be impermeable. Therefore the leakage length is considered to be very large. However, if a more leaky revetment is applied, i.e. rip-rap or a block revetment, there will occur a water flow in the filter layer and through the top layer. Due to the presence of a gradient in the filter, the maximum hydraulic load will be lower. The head difference ($\Delta\Phi$) in the filter can be calculated by using Wolsink's differential equation (Klein Breteler, 1991). The wave front is schematized as a linear front in his method. This model is illustrated in figure 4.6. The assumptions for this model are as follows (Burger et

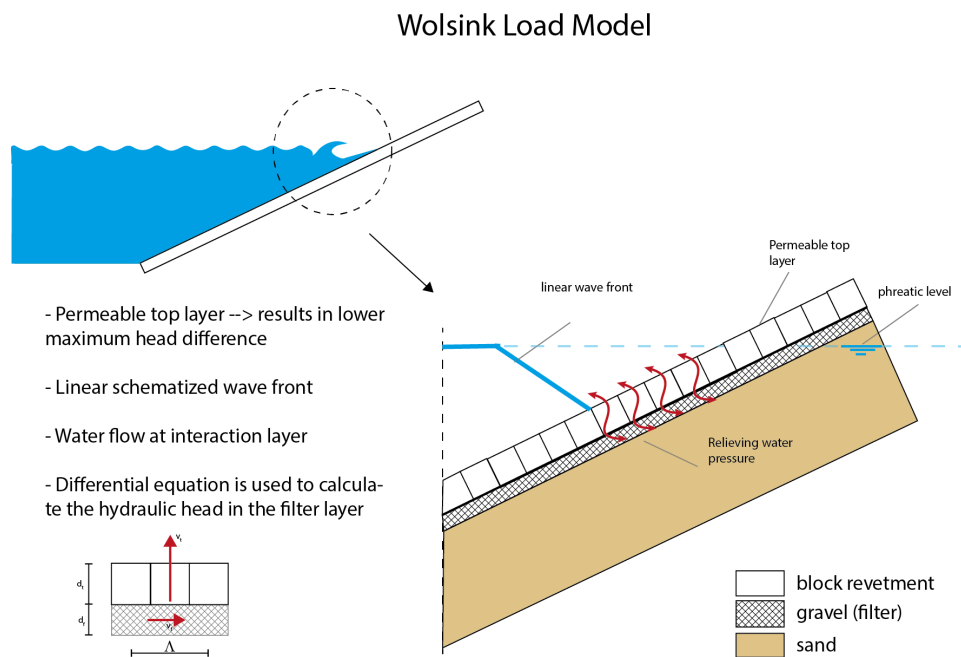


Figure 4.6: Wolsink Load Model

al., 1990):

- The flow in the filter layer can be considered to be one-dimensional
- The permeability of the top layer (k_t), which is concentrated in the joints between the blocks, is assumed to be homogeneous
- The blocks of the top layer do not move

- the phreatic level is fixed during a wave cycle
- The external time-dependent wave load can be schematized as a static situation that can be described by two parameters, i.e. Φ_b and β (see equations 4.10 and figure 4.9)

The differential equation can be determined by considering an infinitely small element, shown in figure 4.7. The derivation of the Wolsink equation is as follows (Burger et al., 1990).

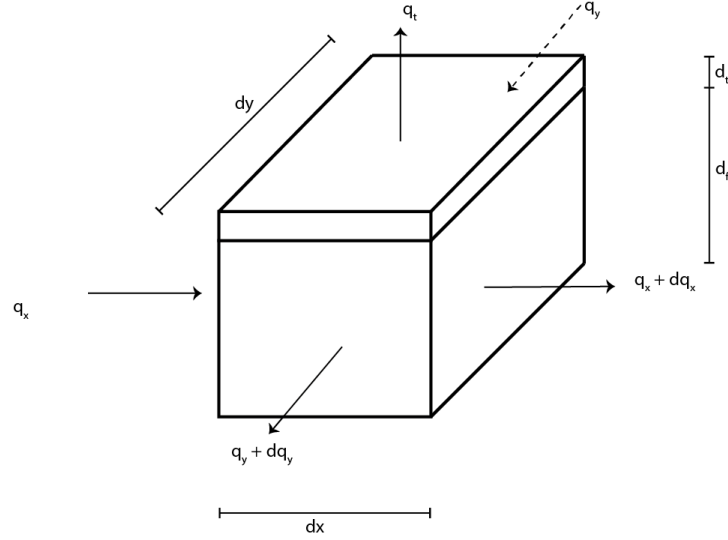


Figure 4.7: Small Element for Derivation Wolsink Differential Equation

Based on continuity, follows:

$$d_t \Delta q_y \Delta x + d_t \Delta q_x \Delta y + \Delta x q_t \Delta y = 0 \quad (4.7a)$$

$$d_t \frac{\delta q_y}{\delta y} + d_t \frac{\delta q_x}{\delta x} + q_t = 0 \quad (4.7b)$$

Subsequently by considering Darcy's law, the following discharge expressions can be derived.

$$q_t = k_t i_t = k_t \frac{\Phi_t - \Phi_f}{d_f} \quad (4.7c)$$

$$q_y = k_f \frac{\delta \Phi_f}{\delta y} \quad (4.7d)$$

$$q_x = k_f \frac{\delta \Phi_f}{\delta x} \quad (4.7e)$$

Substituting these expressions in the continuity equation, results in Wolsink's differential equation:

$$\frac{\delta^2 \Phi_f}{\delta y^2} + \frac{\delta^2 \Phi_f}{\delta x^2} + \frac{k_t}{d_t d_f k_f} (\Phi_t - \Phi_f) = 0 \quad (4.7f)$$

If the third dimension is neglected, this equation can be written as:

$$\Phi_f - \Phi_t = \Lambda^2 \frac{d^2 \Phi_f}{dx^2} \quad (4.7g)$$

Wherein:

q_x = flow velocity in x-direction [m/s]

q_y = flow velocity in y-direction [m/s]

q_t = flow velocity through top layer [m/s]

d_f = filter layer thickness [m]

d_t = block layer thickness [m]
 Λ = leakage length [m]
 k_t = permeability top layer [m/s]
 k_f = permeability filter layer [m/s]

4.4.1. LEAKAGE LENGTH

The leakage length used for the calculations performed in the following chapters, is based on the Waddenzee dike case. The filter layer has a thickness of 0.2 meter and consists of gravel. Gravel is assumed to have a porosity of 0.05 m/s. For the top layer a permeability of 0.001 m/s is assumed. The corresponding leakage length is therefore:

$$\Lambda = \sqrt{\frac{d_f d_t k_f}{k_t}} = \sqrt{\frac{0.2 \cdot 0.2 \cdot 0.05}{0.001}} \approx 1.5 \text{ m} \quad (4.8)$$

4.4.2. SITUATION 1 (INFINITE LENGTH)

If an infinitely large slope and a linear wave front is considered, equation 4.7g can be solved, the situation is shown in figure 4.8. Four solution domains are distinguished, i.e. Φ_1 , Φ_2 , Φ_3 and Φ_4 . The general solution is

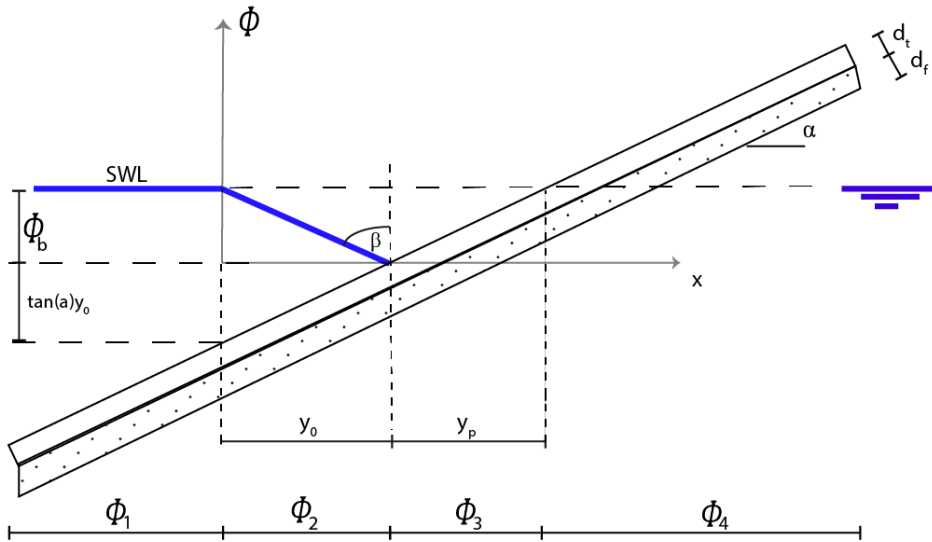


Figure 4.8: Situation Wolsink Load Model

shown in equation 4.9.

$$\Phi_f - \Phi_t = C_1 e^{(x/\Lambda)} + C_2 e^{-(x/\Lambda)} \quad (4.9)$$

Applying this general solution to the 4 different domains with respect to the axis system and considering the x-axis as reference level, one obtains:

1. $\Phi_{f1} = A e^{(x/\Lambda)} + B e^{-(x/\Lambda)} + \Phi_b$ for $-\infty < x < 0$
2. $\Phi_{f2} = C e^{(x/\Lambda)} + D e^{-(x/\Lambda)} + \Phi_b - \frac{\Phi_b}{\frac{\tan 0.5\pi - \beta}{\tan \alpha}} x$ for $0 < x < y_0$
3. $\Phi_{f3} = E e^{(x/\Lambda)} + F e^{-(x/\Lambda)} + x \tan \alpha - y_0 \tan \alpha$ for $y_0 < x < y_0 + y_p$
4. $\Phi_{f4} = G e^{(x/\Lambda)} + H e^{-(x/\Lambda)} + \Phi_b$ for $y_0 + y_p < x < +\infty$

The values for y_0 and y_p are respectively $y_0 = \frac{\Phi_b}{\tan 0.5\pi - \beta}$ and $y_p = \frac{\Phi_b}{\tan \alpha}$. Therefore, eight integration constants need to be solved. This can be done by applying 2 boundary conditions and 6 matching conditions. The boundary and matching conditions are listed in the following enumeration.

1. $x \rightarrow -\infty; \Phi_f = \Phi_b$ which leads to $B = 0$
2. $\Phi_{f1}(0) = \Phi_{f2}(0)$
3. $\frac{d\Phi_{f1}}{dx}(0) = \frac{d\Phi_{f2}}{dx}(0)$
4. $\Phi_{f2}(y_0) = \Phi_{f3}(y_0)$
5. $\frac{d\Phi_{f2}}{dx}(y_0) = \frac{d\Phi_{f3}}{dx}(y_0)$
6. $\Phi_{f3}(y_0 + y_p) = \Phi_{f4}(y_0 + y_p)$
7. $\frac{d\Phi_{f3}}{dx}(y_0 + y_p) = \frac{d\Phi_{f4}}{dx}(y_0 + y_p)$
8. $x \rightarrow \infty; \Phi_f = \Phi_b$ which leads to $G = 0$

Two remaining unknowns are the values for Φ_b and β . One of the assumptions of this model is that the time-dependent wave load can be schematized as a static situation that can be described by these two parameters. According to [Burger et al. \(1990\)](#) the wave front Φ_b and the wave steepness can be determined with equations 4.10. The definition sketch is shown in figure 4.9.

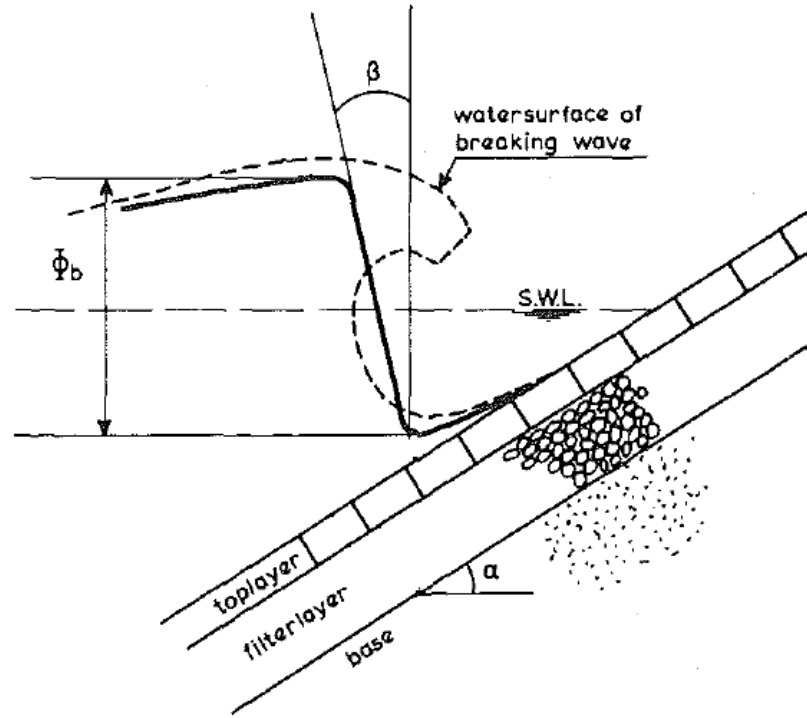


Figure 4.9: Definition sketch assumed wave front and steepness ([Burger et al., 1990](#))

$$\frac{\Phi_b}{H_s} = \max \left\{ 0.36 \cdot \sqrt{\frac{\tan \alpha}{H_s/L_0}}, 2.2 \right\} \quad (4.10a)$$

$$\tan \beta = \frac{0.17}{\sqrt{H_s/L_0}} \quad (4.10b)$$

$$L_0 = \frac{gT^2}{2\pi} \quad (4.10c)$$

If again the hydraulic boundary conditions of the Waddenzee dike are considered and the boundary/matching conditions are applied, the Wolsink equation can finally be solved with the help of Maple. The results are shown in figure 4.10.

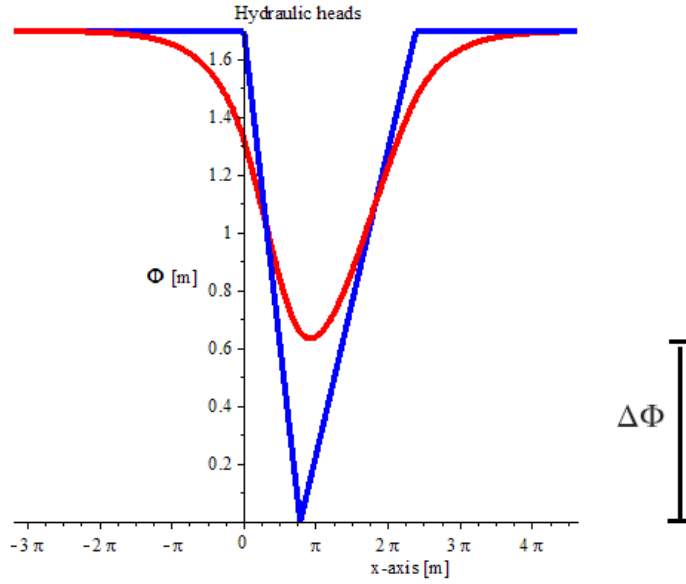


Figure 4.10: Results of solving Wolsink's DE for the Waddenzee dike; blue: hydraulic head top layer, red: hydraulic head in filter layer

From figure 4.11 it can be concluded that the head difference ($\Delta\Phi$) is less than the static model due to the water flow in the filter and top layer. The maximum head difference is equal to 0.66 m. The difference between the two models is significant, i.e. a difference of 0.43 meter. Because the permeability of the top and filter layer has been taken into account (via the leakage length) water can flow from inside to outside of the dike. This results in a lower head difference and therefore a lower water pressure against the revetment. In figure 4.11 the two lines are subtracted from each other which results in the pressure difference.

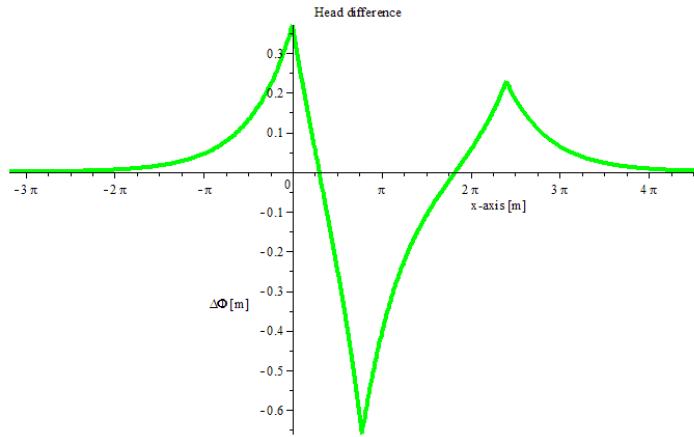


Figure 4.11: The resultant head difference, a minus height results in an upward water pressure

4.4.3. SITUATION 2 (FINITE LENGTH)

However, in the previous calculations a infinitely large dike section is considered. In reality, the Waddenzee dike, has a finite length. This length results in different boundary and matching conditions. The new situation is shown in figure 4.12. Only the block layer and the filter layer (dotted pattern) are assumed to be permeable, the rest is assumed to be water tight. This implies that the Wolsink differential equation does not hold for these parts. In this case, 5 solution fields have to be elaborated, i.e. Φ_1 , Φ_2 , Φ_3 , Φ_4 and Φ_5 . Applying the general solution (equation 4.9) to the 5 different solution fields, one obtains:

1. $\Phi_{f1} = \Phi_b$ for $-\infty < x < 0$
2. $\Phi_{f2} = \Phi_b$ for $0 < x < y_3$

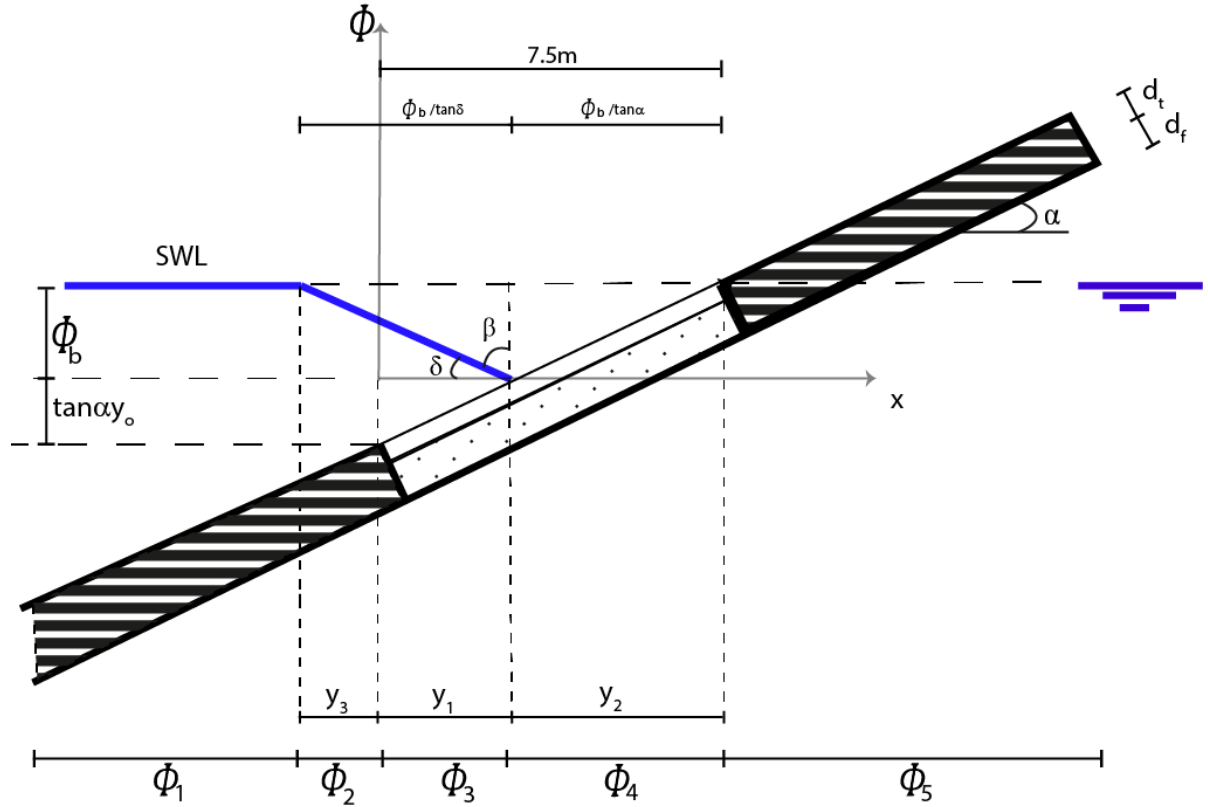


Figure 4.12: Situation Wolsink Load Model of Waddenzee dike; layers with a black line pattern are assumed to be impermeable

3. $\Phi_{f3} = Ee^{(x/\Lambda)} + Fe^{-(x/\Lambda)} + \Phi_b - \frac{\Phi_b}{\frac{\Phi_b}{\tan \delta} - \frac{\Phi_b}{\tan \alpha}} x$ for $y_3 < x < y_3 + y_1$
4. $\Phi_{f4} = Ge^{(x/\Lambda)} + He^{-(x/\Lambda)} + x \tan \alpha - y_0 \tan \alpha$ for $y_3 + y_1 < x < y_3 + y_1 + y_2$
5. $\Phi_{f5} = \Phi_b$ for $y_3 + y_1 + y_2 < x < +\infty$

The values for y_1 , y_2 and y_3 are respectively $7.5 - \frac{\Phi_b}{\tan \alpha}$, $\frac{\Phi_b}{\tan \alpha}$ and $\frac{\Phi_b}{\tan \delta} + \frac{\Phi_b}{\tan \alpha} - 7.5$. Therefore, 4 integration constants need to be solved. This can be done by applying 2 boundary conditions and 2 matching conditions. The boundary and matching conditions are listed in the following enumeration.

1. $\Phi_{f2}(y_3) = \Phi_{f3}(y_3)$
2. $\Phi_{f3}(y_3 + y_1) = \Phi_{f4}(y_3 + y_1)$
3. $\frac{d\Phi_{f3}}{dx}(y_3 + y_1) = \frac{d\Phi_{f4}}{dx}(y_3 + y_1)$
4. $\Phi_{f4}(y_3 + y_1 + y_2) = \Phi_{f5}(y_3 + y_1 + y_2)$

The general solution can be obtained by solving these equations in Maple. The plot of the results are shown in figure 4.13. In figure 4.14 the two lines are subtracted from each other which results in the pressure difference depended of the x-coordinate. The maximum head difference ($\Delta\Phi$) is in this case equal to 0.74 m. This difference is a bit higher than the head difference for the infinite slope. However, the overall head difference is much lower in the Wolsink model with respect to the static model because the piezometric height curve in the filter layer 'follows' the curve of the piezometric height in the top layer, which is more beneficial regarding load reduction.

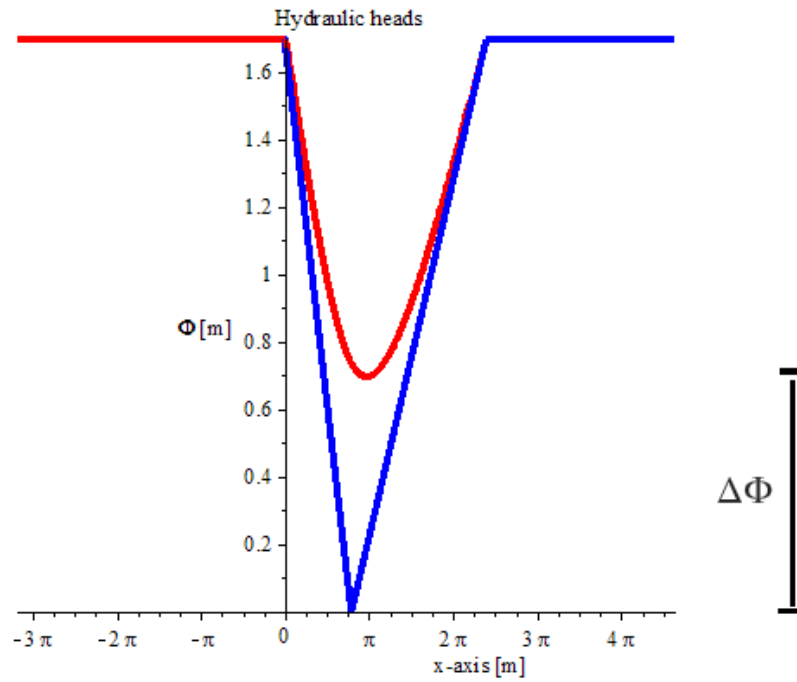


Figure 4.13: Maple results when applying the hydraulic parameters of the Waddenzee dike; blue is the hydraulic head of the top layer, red the hydraulic head in the filter layer

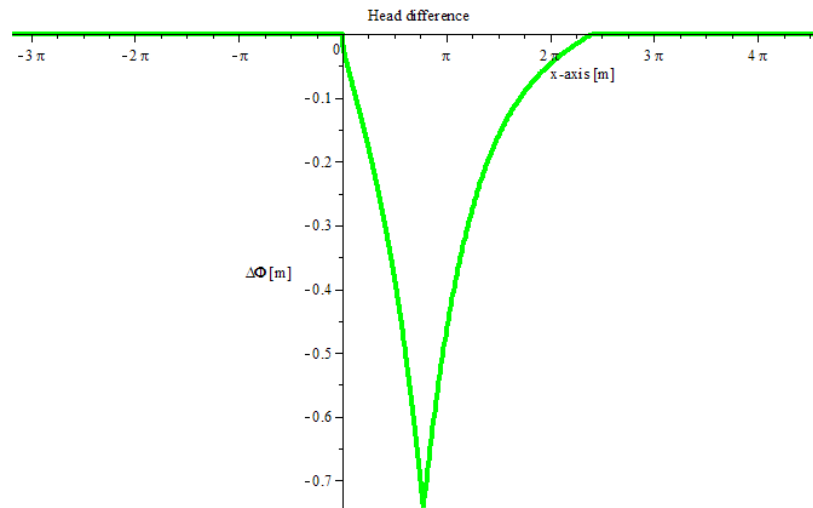


Figure 4.14: The resultant head difference (a minus height results in an upward water pressure)

4.5. DEAD LOAD

The resisting force is induced by the dead load of the revetment perpendicular to the slope. The gravity force will reduce the upward water pressure, elaborated in the previous chapter, and therefore increase the stability of the revetment. The dead load can be calculated with the following formula:

$$q_G = \rho_c g d_t \cos \alpha \quad (4.11)$$

Wherein:

q_G = distributed dead load [N/m]

ρ_c = density block revetment [kg/m³]

d_t = thickness top layer/block revetment [m]

The values used in this thesis are based on the Waddenzee dike, which can be found in chapter 4.1. If a refurbishment of PBA will be applied on top of the block layer, the dead load will increase.

$$q_G = \rho_c g d_t \cos \alpha + \rho_{pba} g d_{pba} \cos \alpha \quad (4.12)$$

Wherein:

ρ_{pba} = density PBA layer [kg/m³]

d_{pba} = thickness PBA layer [m]

These equations do not hold for the part of the revetment which is below water level. For this part the dead load is equal to:

$$q_G = (\rho_c - \rho_w) g d_t \cos \alpha \quad (4.13)$$

If a PBA refurbishment layer is applied, this equation changes into:

$$q_G = (\rho_c - \rho_w) g d_t \cos \alpha + (\rho_{pba} - \rho_w) g d_{pba} \cos \alpha \quad (4.14)$$

4.6. FINAL LOAD SITUATIONS

In the previous section the hydraulic heads and the dead load has been studied. The sum of the resultant water pressures and the dead load of the revetment perpendicular to the slope will be the input of the analytical calculations.

4.6.1. STATIC MODEL

Like stated in the literature study, three different areas can be distinguished when elaborating this model. In the first area (AB) the resultant load is equal to the under water dead load of the structure. In the second part (BC) there is no water pressure at the top layer, which results in a negative water pressure from the inner to the outer side over a certain length. In the third area (CD) there are no water pressures present, therefore the resultant load is equal to the dead load. The previous statements are explained in the following equations and in figure 4.15. For part AB holds:

$$q_R^{AB} = \Delta \Phi^{AB} \rho_w g + (\rho_c - \rho_w) g d_t \cos \alpha \quad (4.15a)$$

For part BC holds:

$$q_R^{BC} = \Delta \Phi^{BC} \rho_w g + \rho_c g d_t \cos \alpha \quad (4.15b)$$

And for part CD holds:

$$q_R^{CD} = \rho_c g d \cos \alpha \quad (4.15c)$$

All three areas are shown in figure 4.15.

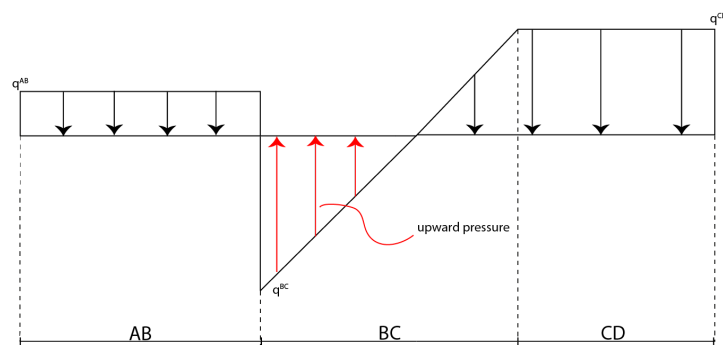


Figure 4.15: Resultant (distributed) loads on the revetment

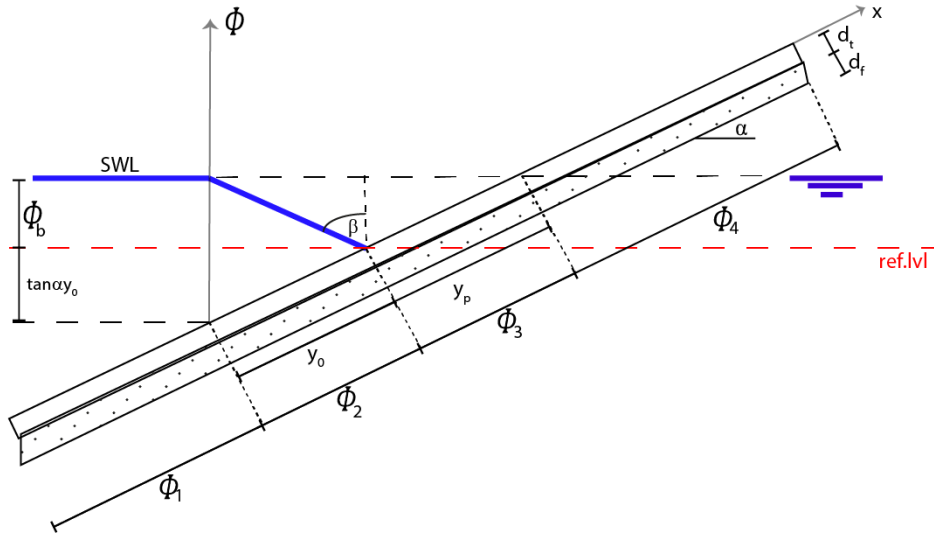


Figure 4.16: Wolsink load model: Infinite long slope, with the x-axis in the slope direction

4.6.2. WOLSINK MODEL

Eventually, the beam will be modelled as a beam on elastic foundation. For these calculation purposes, it is more handy to derive the solution of Wolsink's differential equation with a different x-axis. For these calculation, in contrast to the previous solutions which are a more handy input for the FEM calculation, the new x-axis will be chosen in the direction of the revetment, like shown in figure 4.16. The reference level for the piezometric levels is still the original x-axis. In contrast to the solution shown in the previous chapter with the x-axis perpendicular to the Φ axis (now called 'initial'), a few conditions will change.

- $y_0 = \frac{y_{0,initial}}{\cos \alpha} = \frac{\Phi_b}{\tan \alpha \cos \alpha}$
- $y_p = \frac{y_{p,initial}}{\cos \alpha} = \frac{\Phi_b}{\tan \alpha \cos \alpha}$

The general solutions of the 4 different fields are listed in the following enumeration.

- $\Phi_{f1} = Ae^{(x/\Lambda)} + Be^{-(x/\Lambda)} + \Phi_b$ for $-\infty < x < 0$
- $\Phi_{f2} = Ce^{(x/\Lambda)} + De^{-(x/\Lambda)} + \Phi_b - \frac{\cos \alpha}{\tan \beta} x$ for $0 < x < y_0$
- $\Phi_{f3} = Ee^{(x/\Lambda)} + Fe^{-(x/\Lambda)} + x \sin \alpha - y_0 \sin \alpha$ for $y_0 < x < y_0 + y_p$
- $\Phi_{f4} = Ge^{(x/\Lambda)} + He^{-(x/\Lambda)} + \Phi_b$ for $y_0 + y_p < x < +\infty$

The boundary conditions are similar as in the initial axis system. Solving these equations results in the following head differences over the revetment, illustrated in figure 4.17. The maximum head difference is equal to 0.64 meter. Multiplying these head differences ($\Delta\Phi$) with their specific weight (γ_w) and by adding the weight of the revetment perpendicular to the dike slope, the resultant load is obtained. It is assumed that for $-\infty < x < y_0$ the dead load below water level is applicable. The result is shown in figure 4.18. The shift in the green line between 0 and π can be explained due to the difference in dead load between below and above water level.

These calculations can also be done based on the Waddenzee case (finite revetment length). The situation with the new x-direction is shown in figure 4.19. The distances showed in figure 4.19 are equal to:

- $y_1 = \frac{y_{1,initial}}{\cos \alpha} = \frac{7.5}{\cos \alpha} - \frac{\Phi_b}{\tan \alpha \cdot \cos \alpha}$
- $y_2 = \frac{y_{2,initial}}{\cos \alpha} = \frac{\Phi_b}{\tan \alpha \cdot \cos \alpha}$
- $y_3 = \frac{y_{3,initial}}{\cos \alpha} = \frac{\Phi_b}{\tan \delta \cdot \cos \alpha} + \frac{\Phi_b}{\tan \alpha \cdot \cos \alpha} - \frac{7.5}{\cos \alpha}$

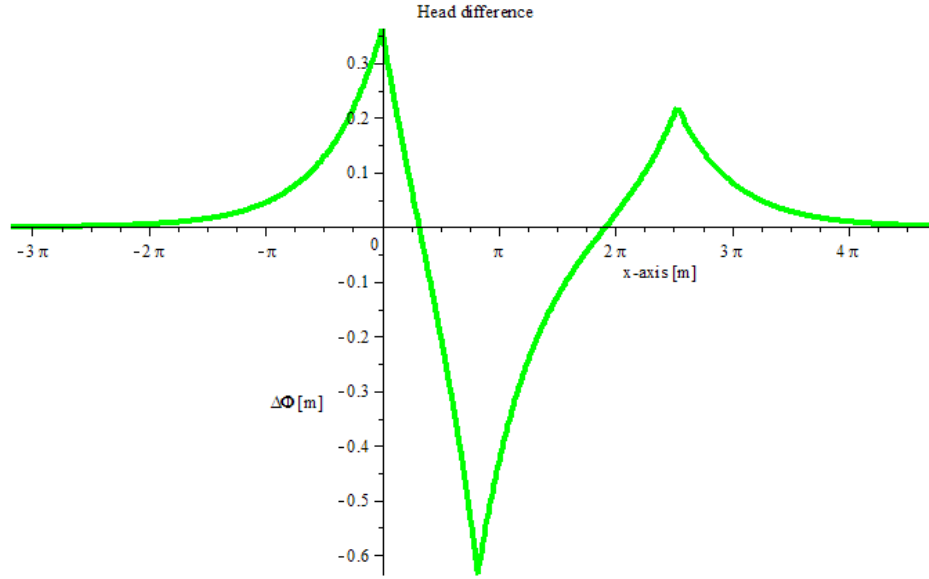


Figure 4.17: Head difference over the revetment with the x-axis in the slope direction

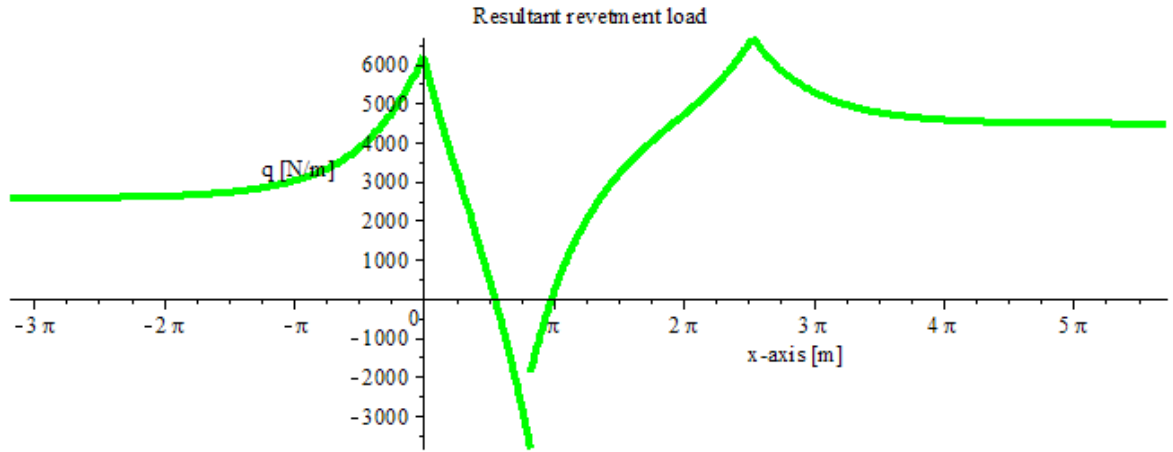


Figure 4.18: Resultant revetment load when using the Wolsink load model on an infinite slope

The general solutions of the 5 different fields are listed in the following enumeration.

1. $\Phi_{f1} = \Phi_b$ for $-\infty < x < 0$
2. $\Phi_{f2} = \Phi_b$ for $0 < x < y_3$
3. $\Phi_{f3} = Ee^{(x/\Lambda)} + Fe^{-(x/\Lambda)} + \Phi_b - \frac{\cos \alpha}{\tan \beta} x$ for $y_3 < x < y_3 + y_1$
4. $\Phi_{f4} = Ge^{(x/\Lambda)} + He^{-(x/\Lambda)} + x \sin \alpha - y_0 \sin \alpha$ for $y_3 + y_1 < x < y_3 + y_1 + y_2$
5. $\Phi_{f5} = \Phi_b$ for $y_3 + y_1 + y_2 < x < +\infty$

The boundary conditions are similar as in the initial axis system. Solving these equations results in the following head differences over the revetment. The maximum head difference is in this case equal to 0.70 meter. Just as in the previous model, by multiplying these head differences ($\Delta\Phi$) with their specific weight (γ_m) and by adding the weight of the revetment perpendicular to the dike slope, the resultant load can be obtained. It is assumed that for $-\infty < x < y_3 + y_1$ the dead load below water level is applicable. The result is shown in figure 4.21. The shift in the green line between 0 and π can be explained due to the difference in dead load between below and above water level.

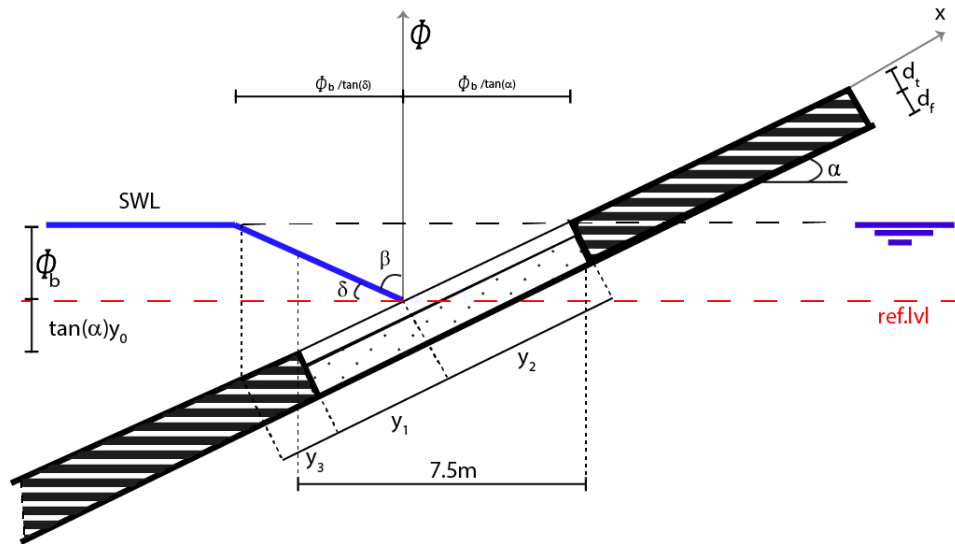


Figure 4.19: Wolsink load model: Waddenzee dike situation, with the x-axis in the slope direction

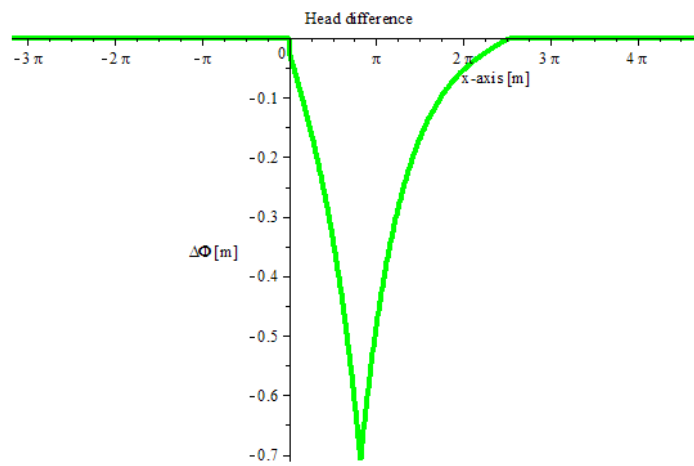


Figure 4.20: Head difference over the revetment with the x-axis in the slope direction for the Waddenzee case

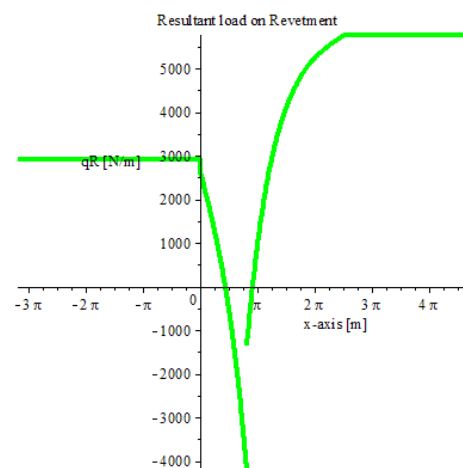


Figure 4.21: Resultant revetment load when using the Wolsink load model on an finite revetment for the Waddenzee case

4.7. CONCLUSIONS

In this chapter two load models were discussed. First of all, the static load model was discussed. Hereby it is assumed that the revetment is completely impermeable and that there is no flow of water between the top and bottom of the revetment. The wave front is schematized as a vertical line. As a consequence of its impermeability, the pressure difference can immediately be calculated by considering the water level outside and the phreatic level within the dike.

Subsequently, the Wolsink load model was elaborated. This model assumes a certain permeability of the revetment. By considering Wolsink's differential equation one can calculate the hydraulic head in the filter layer, given the hydraulic head at the top layer.

An important parameter of this differential equation is the leakage length. A low leakage length implies a permeable revetment. The more permeable the revetment, the lower the head difference over the revetment will be. As a results, a lower water pressure against the revetment will occur, and therefore it is less prone to uplifting and high bending stresses. An infinitely large value for the leakage length will result in the same pressure difference as the static load model.

For the assumed hydraulic boundary conditions at the Waddenzee dike the maximum head difference for the static and the Wolsink load model were respectively 1.09 m and 0.74. The difference is significant (0.35 m). Although these results are based on many assumptions, it can be concluded that a small leakage length is favourable for the stability of the blocks and that a higher permeability of the revetment leads to a more stable structure and that the resulting maximum hydraulic load difference is lower in the Wolsink load model than in the static load model.

5

STRUCTURAL ANALYSIS

In this chapter the (analytical) structural model is discussed. To perform an accurate analysis the model, geometry, support conditions, material properties and structural loads (previous chapter) have to be determined. With the structural analysis it is tried to compute a structure's deformations, internal forces, stresses and stability of a structure. First the assumptions and the theory of the structural model are discussed, subsequently the results for the static load model and the Wolsink load model are elaborated. In the flowchart of figure 5.1 an overview of the different steps is shown.

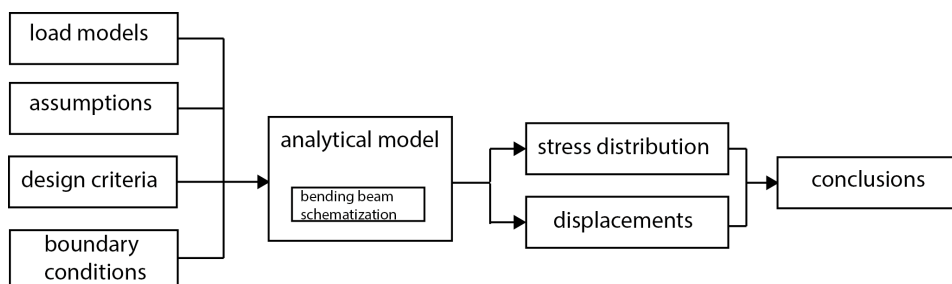


Figure 5.1: Flowchart Structural Analysis

5.1. ASSUMPTIONS

Dozens of parameters influence the structural behaviour of a composite PBA/block revetment. In order to solve this problem mathematically some assumptions have to be made. These assumptions are based on the literature study done in the beginning of this research and are listed in the following enumeration:

1. All the pitched block elements have the same dimensions and a general mass density
2. There is sufficient clamping and friction between the blocks
3. Due to the high permeability of the PBA layer, the permeability of the block revetment will be governing
4. The leakage length remains constant when varying the PBA layer thickness
5. The Euler-Bernoulli beam theory is valid: plane cross-sections remain planar and normal to the beam axis in a beam subjected to bending
6. The composite revetment acts as a bending beam
7. A 2D model and plane strain is assumed (i.e. a vertical/transversal cross-section of the dike is studied, the effects of the longitudinal direction are neglected)
8. Cross sectional rotations remain small

9. The fibres within the cross section show linear elastic behaviour (Hooke's law)
10. The foundation or soil can be replaced by a set of distributed linear elastic springs
11. Increase of internal stresses due to uneven settlements are neglected

5.2. DESIGN CRITERIA

A pitched stone revetment will fail when the concrete elements are lifted up out of the revetment and if the waves subsequently induce erosion of the dike body. A PBA refurbishment layer adds coherence to the block structure and will try to prevent the blocks from uplifting. When the PBA deforms during this prevention, bending stresses will occur in the PBA layer. The biggest bending stresses will occur in the outer fibres of the PBA layer. If the hydraulic loads are increased, structural failure of the revetment will eventually occur when the bending stresses due to the external loads cannot be withstood by the PBA. The external force induces a moment in the construction causing it to bend. This moment must be balanced by a moment induced by the internal stresses. These moments must be equal in order to counteract each other and maintain a state of equilibrium. Like all other materials, PBA is being limited in the maximum bending stress it can withstand. In chapter 3 it is explained that the flexural strength strongly depends on the grain size (grading class) but also on the type of aggregate. The flexural strength of PBA for different mixtures are based on test results and shown in figure 5.2 (Bijlsma, 2013). If a certain PBA mixture cannot resist the deformation, one could choose another mixture or one could apply a thicker PBA layer. The first method will result in a higher flexural strength when selecting a finer mixture like shown in figure 5.2. The other method, applying a thicker refurbishment layer, will not result in a higher flexural strength because the flexural strength is being limited by the type of mixture. When applying a thicker layer, the maximum stresses caused by the external loads will be reduced because its section modulus is increased. The maximum bending stresses which have to be restrained by the PBA is therefore decreased.

Mixture	Average flexural strength	Flexural strength for preliminary design
Limestone 8/11 mm	1.26 MPa	1.09 MPa
Limestone 10/14 mm	1.42 MPa	0.97 MPa
Limestone 20/40 mm	0.78 MPa	0.62 MPa
Limestone 30/60 mm	0.65 MPa	0.50 MPa

Figure 5.2: Design values of the flexural strength of PBA (Bijlsma, 2013)

5.3. STRUCTURAL MODEL

To model stress distribution and the interaction between the revetment and the subsoil, it is modelled as an elastically supported beam. The analysis of beams on elastic foundations is widespread in engineering. This approach is also used in several hydraulic engineering literature (e.g. Golfklap (Rijkswaterstaat, 2009)) to model the response of the revetment regarding the wave impact. Furthermore it is often used in the road and railway industry to model the behaviour of a road due to traffic loads. This model was originally proposed by Winkler, therefore the elastic foundation is also known as a "Winkler foundation". The Winkler foundation assumes that the deflection of the soil at a point is directly proportional to the stress applied at that point and independent of the surrounding soil behaviour. The Winkler foundation is based on the following three assumptions (Tsudik, 2013):

1. The load applied to the soil surface produces deflections of the soil only under the applied load and does not produce any deflections and stresses outside the loaded area
2. The soil can resist compression as well as tension stresses
3. The shape and size of the foundation do not affect the displacement of the soil

These assumptions are not always accurate because the mentioned assumptions represent a rough schematisation of the real soil behaviour. However, numerous experimental and theoretical investigations as shown by many scientists, proved that analysis based on Winkler foundation produces realistic results that are practically close enough to results obtained from soil testing and observations of settlements of real structures (Tsudik, 2013). In figure 5.3 the mechanical schematization is depicted.

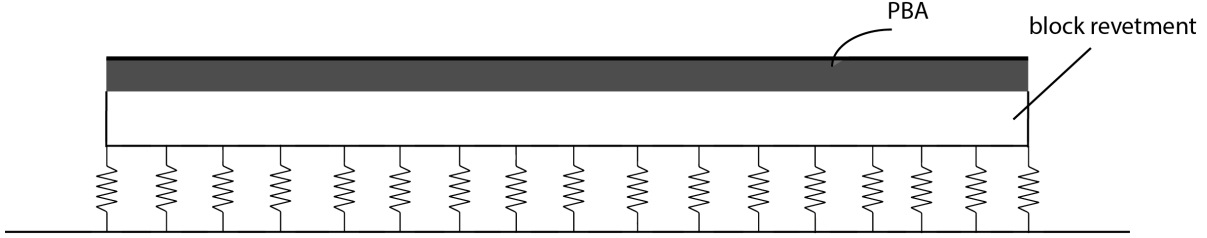


Figure 5.3: Non homogeneous elastically supported Euler Bernoulli bending beam

For this research the response is researched regarding the water pressure difference caused by the water level outside and the water table within the dike. The loads caused by these water pressure differences are discussed in chapter 4.

5.3.1. THEORY

The differential equation of the deflection of a Euler-Bernoulli Beam supported on an elastic foundation can be derived using figure 5.4 and considering the equilibrium (Simone, 2011). When considering the vertical

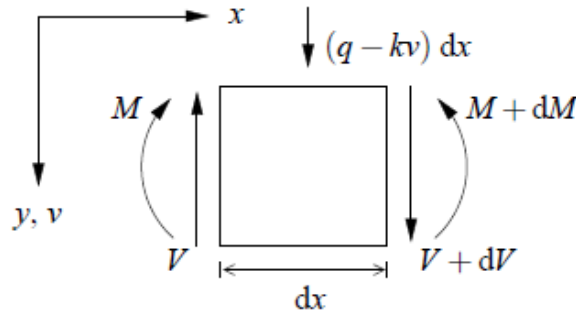


Figure 5.4: Equilibrium of an Euler Bernoulli beam element elastically supported (Simone, 2011)

equilibrium of the vertical forces, one can obtain equation 5.1a.

$$\frac{dV}{dx} - kv = -q \quad (5.1a)$$

By applying the properties of an Euler-Bernoulli beam (the kinematic and constitutive relations) and substituting them in the equilibrium equation, one can finally derive the differential equation (5.1d) for an EB-beam on an elastic foundation.

$$V = \frac{dM}{dx} \rightarrow \frac{dV}{dx} = \frac{d^2M}{dx^2} \quad (5.1b)$$

$$M = -EI \frac{d^2v}{dx^2} \rightarrow \frac{d^2M}{dx^2} = -EI \frac{d^4v}{dx^4} \quad (5.1c)$$

$$EI \frac{d^4v}{dx^4} + kv = q \quad (5.1d)$$

First the homogeneous solution of equation 5.1d will be derived. This can be done by substituting a possible general solution, i.e. $v = e^{mx}$ in the homogeneous equation. Substituting this general solution, the characteristic equation can be obtained:

$$m^4 + \frac{k}{EI} = 0 \quad (5.2)$$

Which has the roots:

$$m_1 = -m_3 = \lambda(1 + i) \text{ and } m_2 = -m_4 = \lambda(-1 + i) \quad (5.3)$$

The general solution of the differential equation becomes:

$$v = Ae^{\beta(1+i)x} + Be^{\beta(1-i)x} + Ce^{-\beta(1-i)x} + De^{-\beta(1+i)x} \quad (5.4a)$$

By applying the formulas of Euler:

$$e^{\beta ix} = \cos \beta x + i \sin \beta x \quad (5.4b)$$

$$e^{-\beta ix} = \cos \beta x - i \sin \beta x \quad (5.4c)$$

The final (homogeneous) solution becomes:

$$v_h = e^{\beta x} (C_1 \cos \beta x + C_2 \sin \beta x) + e^{-\beta x} (C_3 \cos \beta x + C_4 \sin \beta x) \quad (5.4d)$$

The next step is to find the particular solution of equation 5.1d. When considering the loads, like stated in chapter 4, three types of loads can be distinguished.

1. uniform (constant) q-load $\rightarrow q(x) = q_0$
2. linear q-load $\rightarrow q(x) = q_0 x$
3. exponential q-load $\rightarrow q(x) = q_0 e^{\gamma x}$

The linear q-load is applicable to the static load model, the exponential q-load is used in the Wolsink load model. Subsequently one has to derive the particular solutions for the non-homogeneous parts. This can be done by implementing a general solution in the differential equations. When implementing the general solution $v_{GS} = A$ the particular solution can be derived as follows:

$$EI \cdot 0 + kA = q_0 \rightarrow A = \frac{q_0}{k} \rightarrow v_p = \frac{q_0}{k} \quad (5.5a)$$

For the linear q-load ($v_{GS} = Ax$):

$$EI \cdot 0 + kAx = q_0 x \rightarrow A = \frac{q_0}{k} \rightarrow v_p = \frac{q_0}{k} x \quad (5.5b)$$

For the exponential q-load ($v_{GS} = Ae^{\gamma x}$):

$$EI \cdot \gamma^4 Ae^{\gamma x} + kAe^{\gamma x} = q_0 e^{\gamma x} \rightarrow A = \frac{q_0}{EI \cdot \gamma^4 + k} \rightarrow v_p = \frac{q_0}{EI \cdot \gamma^4 + k} e^{\gamma x} \quad (5.5c)$$

The final solution of equation 5.1d consists of the homogeneous and the particular part:

$$v_{tot} = v_h + v_p \quad (5.6)$$

By using Maple software, the differential equation 5.1d is solved. The load situations discussed in chapter 4 are implemented in Maple. The infinitesimal element which was used in the derivation of the beam on elastic foundation excluded the presence of discontinuities. Discontinuities in bending stiffness, distributed load or other variables, may be dealt by using matching conditions. In this case the bending stiffness is assumed to be constant (prismatic beam). However, the load is not continuous over the entire beam length. The differential equation has to be considered in each domain, separately, and the matching/boundary conditions have to be used to solve the unknown integration constants. If, for example, the load function is continuous in 3 domains, also 3 solution domains have to be defined, i.e. v_1 , v_2 and v_3 . This is the case when applying the static load model on the bending beam. This procedure results in 12 unknown integration constants. Because the differential equation -which describes the beam behaviour on elastic soil is of the fourth order- one has

to distinguish 4 boundary conditions and 8 matching conditions. With those 12 conditions, the 12 unknown constant can be solved. In the boundaries between the 3 fields, the compatibility equations hold. This implies that, if a (fictitious) boundary is assumed at $x = a$ between field 1 and field 2, there has to be compatibility between the displacement (v), angle (ϕ), moment (M) and shear force (V):

$$v_1(a) = v_2(a) \quad (5.7a)$$

$$\phi_1(a) = \phi_2(a) \quad (5.7b)$$

$$M_1(a) = M_2(a) \quad (5.7c)$$

$$V_1(a) = V_2(a) \quad (5.7d)$$

The same procedure holds for the Wolsink load model, however, more solution domains have to be considered and therefore more unknown integration constants have to be determined.

5.4. SUPPORTS

Structural systems transfer their loading through a support to the subsoil. In order to be able to analyse a structure, it is necessary to study the forces that can be transferred and resisted at its supports. The pitched stones at the Waddenzee dike are enclosed at the left side with a toe and at the right side with an asphalt revetment (see figure 5.5). The actual behaviour of a support can be quite complicated therefore assump-

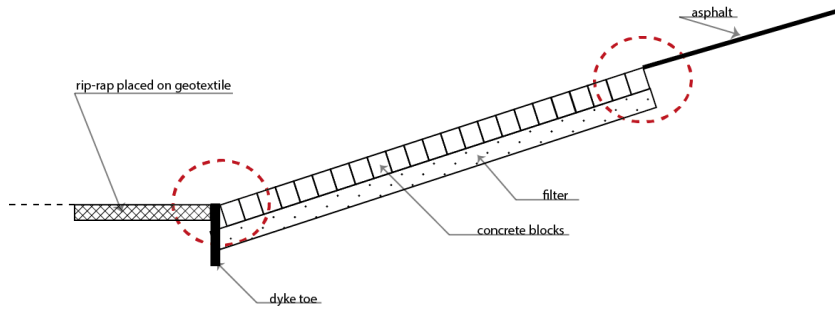


Figure 5.5: To perform calculations a representation of the boundary conditions is made. At the left side the revetment is bounded by a dike toe, at the right side the structure is bounded by a refurbishment of asphalt.

tions have to be made. In order to perform calculations these boundary conditions have to be translated into general support conditions. First of all the rigidity and flexibility of the connections/supports must be considered. Rigid, stiff or fixed connections are one extreme while hinged or pinned connections are the other limit. A stiff connection maintains the angle between the connected members, while a hinged connection allows a relative rotation. In general there are three support types (figure 5.6):

1. Fixed: fixed supports can resist vertical and horizontal forces as well as a moment. Since they restrain both rotation and translation, they are also known as rigid supports.
2. Roller: roller supports are free to rotate and translate along the surface on which the roller rests. The resulting force is always a single force that is perpendicular to the surface.
3. Pinned: A pinned support can resist both vertical and horizontal forces but not a moment. They will allow the structural member to rotate but not to translate in any direction. Many connections are assumed to be pinned connections even though they might resist a small amount of moment in reality. The representation of a pinned support includes both horizontal and vertical forces.

A roller support is not likely in this case. An assumption of a roller support is that as soon as a lateral load of any kind pushed on the structure it will roll away in response to the force. Since dike revetments are subjected to lateral loads this is not a good representation. It is likely that a certain rotation is possible at both ends because it is not fully clamped at both side. Therefore it is assumed that both ends of the dike revetment can be represented as pinned supports. They allow the structure a small rotation but not to translate in any direction.

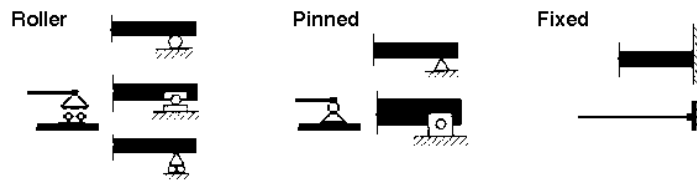


Figure 5.6: Three different support types

5.5. SOIL AND FOUNDATION CHARACTERISTICS

The foundation or soil is replaced by a set of distributed linear elastic springs. An important parameter of the Winkler model is the spring stiffness k as shown in the previous section. The determination of this stiffness, also known as the modulus of foundation, is a difficult problem. Numerous methods are used in practical applications, hence Tsudik (2013).

There is several literature available to determine this foundation modulus k . However, the order of magnitude does not vary that much in literature. The modulus greatly depends on the type of soil on which the beam rests. For this research a technical report of the US Department of Transportation (Eres Consultants, 1994) is used. A table which points out the range of k -values for various types of soils is shown in figure 5.7.

Major Division	Soil Group and Typical Description	CBR (percent)	Approximate Range of k -values kPa/mm (lb/in ² /in)
Gravel and gravelly soils	Well-graded grave and gravel-sand mixtures. Little or no fines.	80-100	136 — 190 (500 — 700)
	Well-graded gravel-sand-clay mixtures. Excellent binder.	80-100	109 — 190 (400 — 700)
	Poorly graded gravel and gravel-sand mixtures. Little or no fines.	30-60	81 — 136 (300 — 500)
	Gravel with fines, very silty gravel, clayey gravel, poorly graded gravel-sand-clay mixtures.	30-60	68 — 136 (250 — 500)
Sands and Sandy Soils	Well-graded sands and gravelly sands. Little or no fines.	25-60	68 — 156 (250 — 575)
	Well-graded sand-clay mixtures. Excellent binders.	25-60	68 — 156 (250 — 575)
	Poorly graded sand. Little or no fines.	15-25	54 — 156 (200 — 575)
	Sand with fines, very silty sand, clayey sands, poorly graded sand-clay mixtures.	10-25	48 — 88 (175 — 325)
Fine-grained soils with low to medium compressibility	Silts (inorganic) and very fine sands, rock flour, silty or clayey fine sands with slight plasticity.	5-25	41 — 81 (150 — 300)
	Clays (inorganic) of low to medium plasticity, sandy clays, silty clays, low plasticity clays.	5-15	34 — 61 (125 — 225)
	Organic silts and organic silt-clays of low plasticity.	3-10	27 — 48 (100 — 175)
Fine-grained soils with high compressibility	Micaceous or diatomaceous fine sandy and silty soils, elastic silts.	1-5	14 — 48 (50 — 175)
	Clays (inorganic) of high plasticity, fat clays	1-3	14 — 41 (50 — 150)
	Organic clays of medium to high plasticity.	1-3	14 — 34 (50 — 125)

Figure 5.7: Approximate range of CBR and k -values for soil groups of the soils classification as used by the Corps of Engineers (Eres Consultants, 1994)

From this table it is expected that the k -value for the Waddenzee dike is in the range of 68-156 kPa/mm (well graded sands and gravelly sands).

5.6. YOUNG'S MODULUS

An assumption of the proposed mechanical model is that the block revetment is behaving like a bending beam. In the previous section, it is stated that when no refurbishment layer is applied, the cross section is homogeneous. However, in reality, a block revetment does not consist only of one material and is therefore in principle not homogeneous (see figure 5.8). It is only assumed that the cross-section has one (constant)

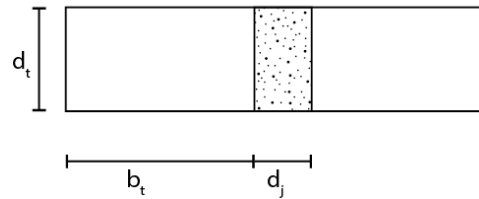


Figure 5.8: The block revetment is a sandwich beam consisting of concrete blocks and gap filling material

Young's modulus. To determine the stiffness modulus of a block revetment, Peters (2003) stated that the stiffness modulus is in the order of 10 percent of the mother material of the block revetment (concrete). This implies that according this theory, the modulus is in the order of:

$$E_{beam} = 0.1 \cdot 30000 = 3000 \text{ MPa} \quad (5.8)$$

The Young's modulus can also be calculated by considering the width and the height of the concrete blocks and gaps between the block. Frissen (1996) did research at TNO and proposed the following formula:

$$\frac{E_{beam}}{E_c} = \frac{1}{1 + \frac{d_j}{b_t} \frac{E_c}{E_j}} \quad (5.9)$$

Wherein:

E_{beam} = Young's modulus of the bending beam [Pa]

E_c = Young's modulus of the concrete blocks [Pa]

E_j = Young's modulus of the gap filling material [Pa]

d_j = thickness of the joints [m]

b_t = block width [m]

The following values are assumed (based on the Waddenzee dike case):

- $E_c = 30000 \text{ MPa}$ (concrete)
- $E_j = 50 \text{ MPa}$ (coarse sand)
- $d_j = 8.1 \text{ mm}$
- $b_t = 200 \text{ mm}$

Applying equation 5.9 results in an modulus of elasticity (E_{beam}) of 1360 MPa. The Young's modulus of PBA is discussed in the literature study and is equal to 3000 MPa.

5.7. STRESSES

By solving the differential equation which describes the behaviour of an Euler Bernoulli beam, the stresses and strains within the cross-section can be calculated when using the equilibrium, constitutive and kinematic relations. An important input are the cross-sectional properties of the beam. It is assumed that the fibres within the cross-section, behave according the linear elastic theory (Hooke's law).

5.7.1. HOMOGENEOUS CROSS SECTION

Within a homogeneous cross-section, the Young Modulus is constant.

NORMAL STRESSES

The total stress in a cross-section consist of the stresses due to the moment (bending stress) and the normal force. The sum of those two is the resultant stress. This is elaborated in the following formula:

$$\sigma_{tot} = \sigma^N + \sigma^M = \frac{N}{A} + \frac{Mz}{I_y} \quad (5.10)$$

Wherein:

A = cross sectional area [m^2]

z = distance between the fibre and centre of gravity [m]

I_y = moment of inertia [m^3]

If one is only interested in the (maximum) stress in the outer fibres, the bending stress can also be calculated by using the section modulus W :

$$\sigma^M = \frac{M}{W} \text{ with } W = \frac{1}{6}bd^2 \quad (5.11)$$

5.7.2. INHOMOGENEOUS CROSS SECTION

When a PBA layer is applied the cross section is not made out of one single material any more, it changes into an inhomogeneous cross-section. This implies that the Young's modulus varies over the cross-section $E(y, z)$. It is assumed that the connection between the materials is rigid. Therefore, Bernoulli's theory applies and the strain distribution is linear of depth.

NORMAL STRESSES

It is common to choose the origin of the coordinate system such that the static moments (S_y and S_z) become zero. Therefore the position of the y-z-coordinate system has to be chosen at the normal force centre (NC) of the cross section. For a homogeneous cross section this coincides with the centre of gravity. However, for inhomogeneous cross sections this no longer holds (Hartsuijker & Welleman, 2012). The position of the NC has to be calculated first by taking into account the different Young's modulus of the two materials (block layer and PBA layer), like illustrated in figure 5.9 and equation 5.12.

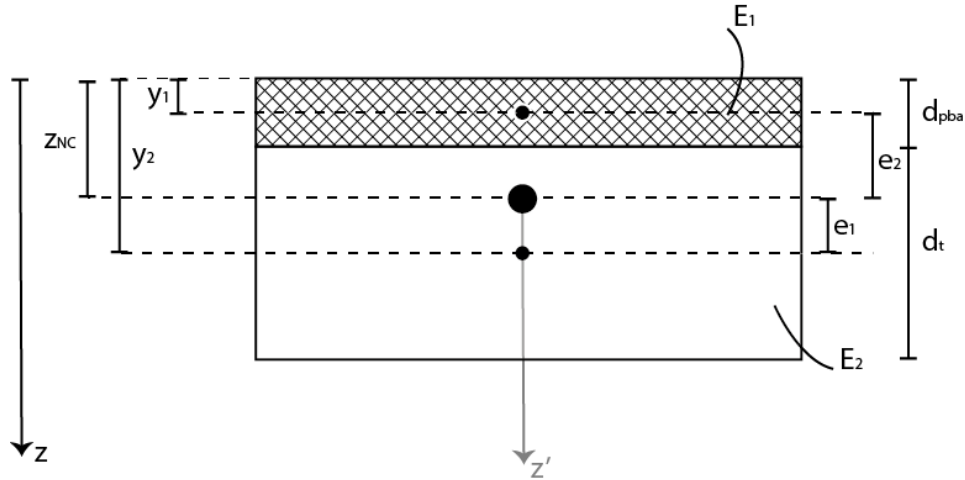


Figure 5.9: Determining the centre of gravity of an inhomogeneous cross section, taking into account the different MOE

$$z_{NC} = \frac{\sum E \cdot A \cdot e}{[E \cdot A]} = \frac{(E_1 \cdot A_1 \cdot y_1) + (E_2 \cdot A_2 \cdot y_2)}{(E_1 A_1 + E_2 A_2)} \quad (5.12)$$

In order to be able to determine the bending stresses, the effective bending stress needs to be determined according to:

$$[E \cdot I]_{eff} = \sum E \cdot I + \sum E \cdot A \cdot e^2 \quad (5.13)$$

The eccentricity e is the distance between the center line of the individual members and the centre of gravity.

$$[E \cdot I]_{eff} = \sum E \cdot I + \sum E \cdot A \cdot e^2 = (E_1 I_1 + E_2 I_2) + (E_1 A_1 e_1^2 + E_2 A_2 e_2^2) \quad (5.14)$$

If the bending moment is known, the curvature κ can be calculated by:

$$\kappa = \frac{M}{EI_{eff}} \quad (5.15)$$

With the curvature, the strains and subsequently the stresses can be calculated in every fibre over the cross-section by applying Hooke's law.

$$\varepsilon(z) = \kappa \cdot z \quad (5.16a)$$

$$\sigma(z) = E(z) \cdot \varepsilon(z) \quad (5.16b)$$

When analyzing the moments, the curvature (κ) from equation 5.15 can be calculated, via the curvature the strains and stresses can be determined with the help of Hooke's law. The stresses are calculated at 4 characteristic points in the cross section. These points are illustrated in figure 5.10 for a small element with a positive bending moment. Because the modulus of elasticity of PBA is higher than of the block revetment, the stresses will be higher for the same strain.

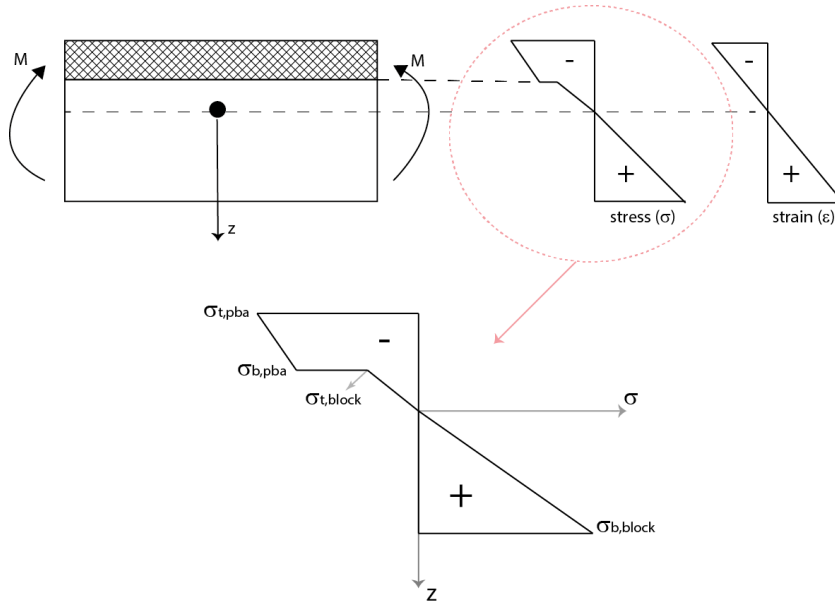


Figure 5.10: Illustration of the stress and strain distribution over the cross section

5.8. NORMAL FORCE ANALYSIS

On a slope, the force gravity of the revetment, can be resolved into two components: a component acting perpendicular to the slope and a component acting tangential to the slope. The component acting tangential to the slope causes a normal force in the revetment. The perpendicular component of gravity helps to hold the object in place on the slope. The shear strength at the interface between the object and the slope can be calculated by multiplying the perpendicular gravity component with a friction factor. The lower this shear force the higher the normal force than can be developed in the structure. Furthermore, if the dike slope is steep, the gravity tangential component is much greater than the shear strength, resulting in a higher normal force. A high normal force can also be obtained when the blocks are placed on a foundation without friction. Sliding down, and therefore inducing normal stresses within the revetment happens when:

$$F_{z,x} > F_{z,y} \cdot \psi \quad (5.17)$$

Wherein ψ is the coefficient of friction that can be determined by:

$$\psi = \tan \delta \quad (5.18)$$

Wherein δ is the angle of friction between the revetment and the soil. This value can be estimated by $\frac{2}{3}\varphi$ (Manual Hydraulic Structures (2011)). The variable φ is the internal friction angle of gravel/sand, which is approximately 30-35 degrees. Therefore equation 5.17 can be rewritten to:

$$F_z \sin \alpha > F_z \cos \alpha \tan \frac{2}{3}\varphi \quad (5.19a)$$

Therefore sliding down occurs when:

$$\alpha > \frac{2}{3}\varphi \quad (5.19b)$$

If for example the Waddenzee dike is considered, the dike slope is very flat and equation 5.19b will not be satisfied. Usually dike slopes are relatively flat and therefore the tangential gravity component will not be satisfied. However, if the friction between the soil and the revetment is reduced, the shear strength will be reduced and a normal force can develop in the structure. This happens over the dike length where there are upwards water pressures present. For the Waddenzee case, the developed normal force is calculated over the length where the water pressure is negative (upwards) for a refurbishment layer of 0.1 meter thickness. This results in figure 5.11. The next step is to transform the normal force in the normal stresses. For a non

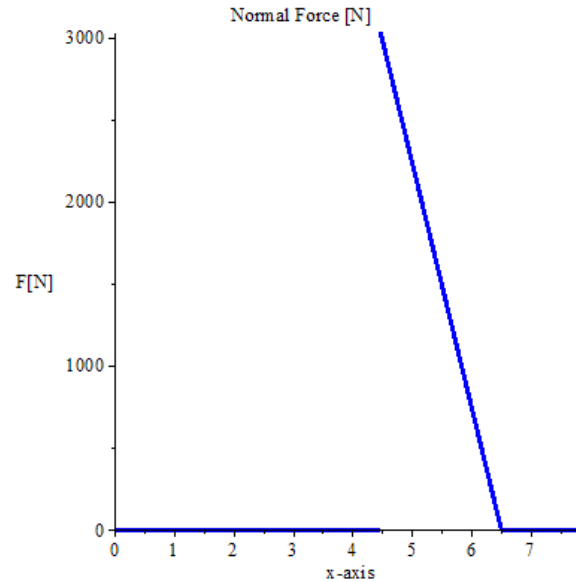


Figure 5.11: Normal force as a function of the beam length, a normal force can only be developed over the length where the waterpressure is negative

homogeneous cross section holds:

$$\sigma^N = \frac{N \cdot E_{pba}}{EA} \quad (5.20)$$

The maximum normal force in figure 5.11 is equal to 3000 N. This results in a compression stress of $\sigma_{pba}^N = -0.02$ MPa and $\sigma_{blok}^N = -0.009$ MPa. These stresses are negligible small and therefore the normal stresses will be neglected in this thesis. Despite of the small normal force in the revetment, the experience in practice is that there is still sufficient clamping present between the blocks in the revetment (Peters, 2003). This is induced by:

- Placing the blocks very tight within the revetment in practice
- Placing the blocks in a small camber which results in a better clamping mechanism due to future settlement of the revetment

- Application of gap filling material in the joints
- Settlement of the blocks due to the wave load. When a PBA refurbishment is applied on the block revetment, it also increases the coherence of the entire structure which results in beam like behaviour

5.9. RESULTS STATIC MODEL

In this section the results of the described analytical model will be discussed. For calculation purposes, the parameters from the reference case of the Waddenzee dike are used.

Three situations will be considered in this chapter: the current situation (no refurbishment layer), a PBA layer of 0.10 m and a PBA layer of 0.15 m. First the displacements are compared, followed by the moment distribution and bending stresses for the three situations. Furthermore a Young Modulus of 3000 MPa is used for the block revetment and a foundation modulus of 70 MPa/m is applied to model the subsoil.

5.9.1. DISPLACEMENTS

In figure 5.12 the displacement of the beam is shown for the three situations when assumed that the beam is simply supported on both ends. It can be concluded that, although it is very small, there is still an upward

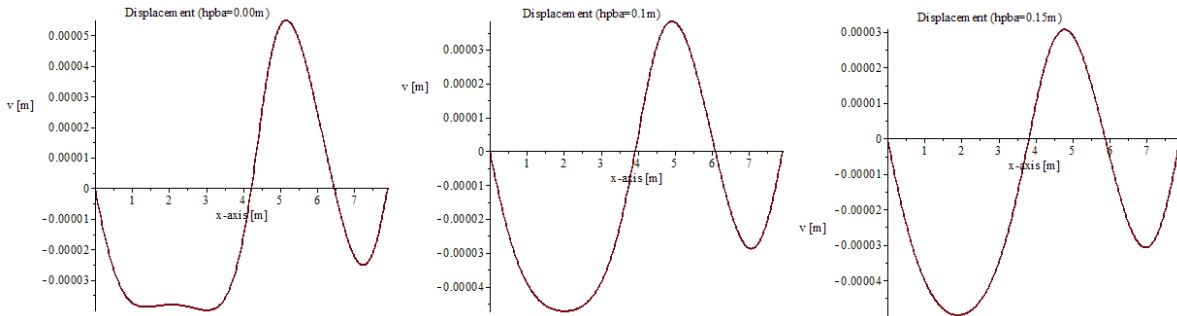


Figure 5.12: Displacements [m] of the revetment based on the static load model for the three situations

displacement. This is an important conclusion and will be elaborated in the next chapter.

5.9.2. BENDING STRESSES

The next step is to analyse the moments and the bending stresses. The 3 bending moment diagrams are shown in figure 5.13. The maximum positive and negative stresses with their corresponding distances are shown in table 5.1.

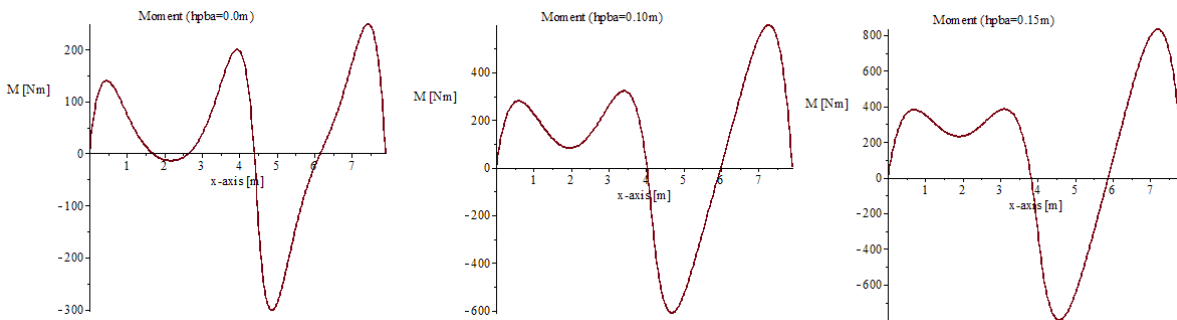


Figure 5.13: Moment (left) and Shear force (right) diagram of the block revetment

In table 5.2 the stresses are listed for different PBA layers.

thickness PBA [m]	positive Moment [Nm]	distance x [m]	negative Moment [Nm]	distance x [m]
0 (current situation)	250	7.45	300	4.85
0.1	600	7.25	610	4.70
0.15	830	7.2	800	4.60

Table 5.1: Governing positive and negative moments based on the static load model for the three situations

For positive M:				
thickness PBA [m]	$\sigma_{t,pba}$ [Pa]	$\sigma_{b,pba}$ [Pa]	$\sigma_{t,block}$ [Pa]	$\sigma_{b,block}$ [Pa]
0 (current situation)	0	0	-37250	37250
0.1	-39920	-13305	-13305	39920
0.15	-40780	-5825	-5825	40780

For negative M:				
thickness PBA [m]	$\sigma_{t,pba}$ [Pa]	$\sigma_{b,pba}$ [Pa]	$\sigma_{t,block}$ [Pa]	$\sigma_{b,block}$ [Pa]
0 (current situation)	0	0	45350	-45350
0.1	40700	13565	13565	-40700
0.15	39125	5590	5590	-39125

Table 5.2: Bending stresses over the cross section for different PBA layers

5.10. RESULTS WOLSINK LOAD MODEL

The same calculations can be performed while considering Wolsink's load model (applied on the Waddenzee dike situation). Like mentioned earlier, one has to distinguish more than 3 solution domains as used for the static model.

5.10.1. DISPLACEMENTS

The displacements are shown in figure 5.14.

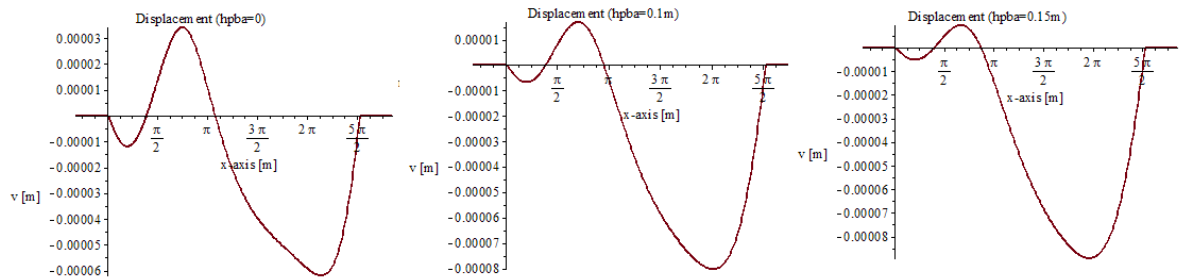


Figure 5.14: Displacements [m] of the revetment based on the Wolsink load model for the three situations

5.10.2. BENDING STRESSES

The 3 bending moment diagrams are depicted in figure 5.15. The maximum negative and positive moments are shown in table 5.3. The corresponding maximum positive and negative stresses are shown in table 5.4.

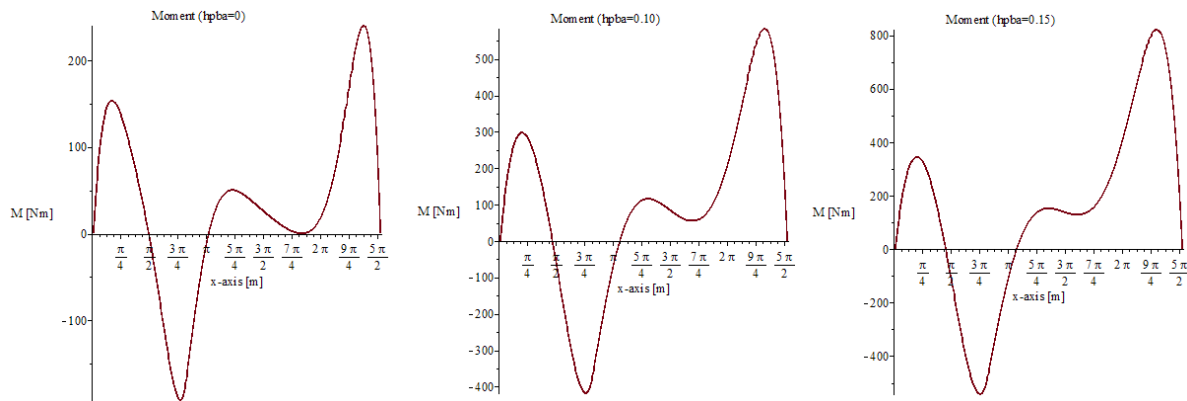


Figure 5.15: Moment diagrams for different PBA thicknesses based on the Wolsink load model

thickness PBA [m]	positive Moment [Nm]	distance x [m]	negative Moment [Nm]	distance x [m]
0 (current situation)	240	7.50	192	2.45
0.1	585	7.30	420	2.40
0.15	820	7.25	540	2.35

Table 5.3: Governing positive and negative moments based on the static load model for the three situations

5.11. CONCLUSIONS

In this section the analytical structural model is discussed. An assumption of the proposed mechanical model is that the block revetment is behaving like a (homogeneous) Euler Bernoulli bending beam. The block revetment and the PBA layer act therefore as a composite bending beam. As a consequence a (fictious) Young's modulus has to be assumed for the block revetment. If a structure is made up of multiple elements, the elements will "carry" load in proportion to their relative stiffness. The stiffer an element, the more load it will attract.

To model the stress distribution and the interaction between the revetment and the subsoil, it was modelled as an elastically supported beam. It assumed that the subsoil can be replaced by a set of distributed linear springs. The deflection of the soil at a point is directly proportional to the stress applied at that point and independent of the surrounding soil behaviour. The analysis of beams on elastic foundations is widespread in civil engineering.

Structural failure will eventually happen when the bending stresses due to the hydraulic loads cannot be withstood by the PBA. The results of this chapter indicate that the normal force in the revetment is negligible small. Calculations were furthermore performed for different values of the PBA thickness and for both

For positive M:				
thickness PBA [m]	$\sigma_{t,pba}$ [Pa]	$\sigma_{b,pba}$ [Pa]	$\sigma_{t,block}$ [Pa]	$\sigma_{b,block}$ [Pa]
0 (current situation)	0	0	-35990	35990
0.1	-38895	-12965	-12965	38895
0.15	-40235	-5750	-5750	40235
For negative M:				
thickness PBA [m]	$\sigma_{t,pba}$ [Pa]	$\sigma_{b,pba}$ [Pa]	$\sigma_{t,block}$ [Pa]	$\sigma_{b,block}$ [Pa]
0 (current situation)	0	0	28800	-28800
0.1	27850	9285	9285	-27850
0.15	26570	3795	3795	-26570

Table 5.4: Bending stresses over the cross section for different PBA layers

load models as input. Generally, the thicker the refurbishment layer, the better the upward displacement is reduced. The static load model resulted in higher bending stresses than the Wolsink load model. Due to the difference in wave front, the point of maximum deflection differs between the two load models. The highest stresses appear at the part of the beam where the maximum (upward) deflection occurs. The maximum bending stress for the static and Wolsink load model are respectively 40 kPa and 28 kPa when applying a PBA layer of 10 cm. Based on the design values of figure 5.2 these stresses can be withstood by the different mixtures. A thicker PBA layer results in lower bending stresses since it reduces the maximum upward deflection. The point where the maximum stress occurs, hardly changes when applying a thicker layer. However, the maximum stresses can overall easily be withstood by the PBA.

In the next chapter the results will be compared with a finite element analysis. An import aspect of this subsequent chapter, is to what extent the elastic foundation influences the stress distribution in the uplifting part of the bending beam.

6

FINITE ELEMENT METHOD ANALYSIS

The finite element method (FEM) is a numerical technique for finding solutions to boundary value problems. It involves the discretization of the structure into elements that are defined by nodes which describe the elements. The behaviour of each sub domain (element) is predicted by mathematical equations. The computer then adds up all the individual elements to predict the behaviour of the actual object. Using this method, it is possible to calculate the displacements, strains and stresses under internal and external loads. Several FEM software packages are available, for this research an Abaqus software package is used. Abaqus is a software suite for finite element analysis and computer-aided engineering. In this chapter, firstly it is explained how the FEM is used for this research. Subsequently the different models are briefly explained, elaborated and compared. Thirdly, the results are compared with an existing approach which is currently used for preliminary designs. In the flowchart of figure 5.1 an overview of the different steps is shown.

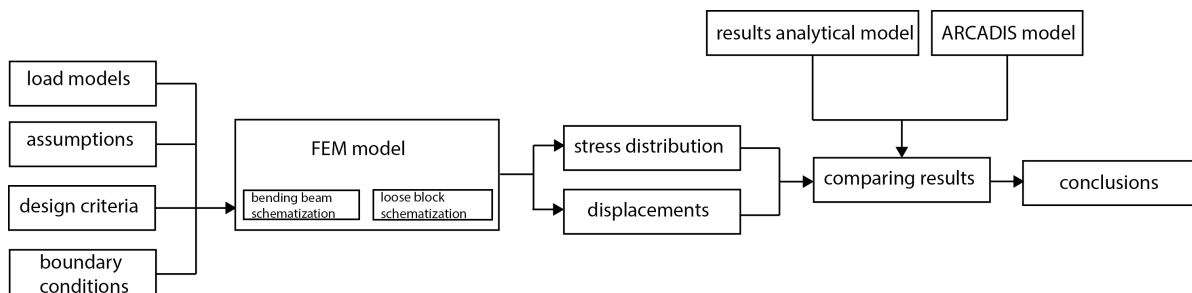


Figure 6.1: Flowchart FEM Analysis

6.1. FEM RESEARCH APPROACH

The first step is to check the analytical calculations. These analytical results, showed in chapter 5, are elaborated with the use of Maple. The Maple calculation sheets include a large number of equations. However, when the sheets are finished, it is a lot faster and more convenient to change a few input numbers (e.g. wave height, dike length etc.) than to make the same changes to an entire FEM model. This is a big advantage compared to FEM software, where every situation has to be created uniquely in the software, which is a time consuming process. It is important, because of the large number of equations in the Maple sheets, to check the Maple outcomes. Therefore two basic situations are also calculated with the help of Abaqus. If the results correspond, it can be concluded that the analytical (Maple) results are correct. The next step is to compare the results of the analytical model and the FEM models. Firstly, it is researched to what extent the elastic foundation of the analytical model reflects the soil behaviour. In reality, the foundation is continuous which results in a spreading of the load. This behaviour is not taken into account when using the Winkler foundation. The displacement of a certain point is directly dependent of the deflection of this specific point. This theory is illustrated in figure 6.2. The spring foundation just right of the cut, which is not loaded, does not support the loaded part beam.

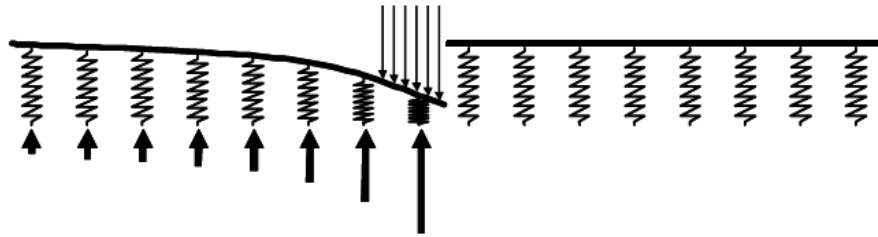


Figure 6.2: A beam resting on a Winkler foundation on which a part is loaded and unloaded. The arrows illustrate the amount of support; the bigger the deflection the higher the supporting force

Subsequently the block revetment, which is to this point only modelled as a bending beam, is now modelled as a structure consisting of individual concrete blocks to model the block revetment as realistic as possible. Between the different blocks a certain amount of friction is applied. A schematisation of the calculations done in this research are shown in figure 6.3.

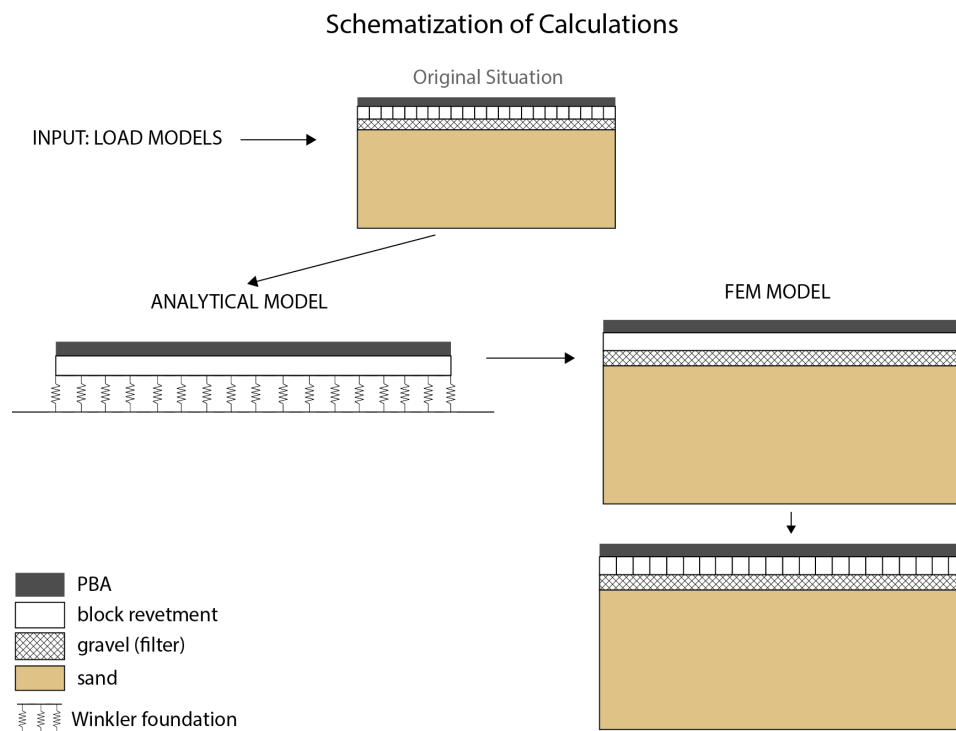


Figure 6.3: Schematization of the different calculations done in this research

6.2. VERIFYING ANALYTICAL CALCULATIONS

To verify the analytical calculations, two elastically supported beams are also modelled in Abaqus, i.e. a beam loaded by the static load model and a beam loaded by the Wolsink load model. As mesh size decreases, the FEM solutions will move toward the exact solutions. The results are shown in figure 6.4. With a sufficient fine mesh, it can be seen that the analytical and FEM solutions (almost) correspond. Therefore it can be concluded that there are no errors present in the Maple calculations.

6.3. STATIC LOAD MODEL

6.3.1. WINKLER VERSUS CONTINUOUS FOUNDATION

Like stated in the introduction, in fact, the external loads are spread in the subsoil. This is in contrast to the Winkler foundation where the deflection of the soil at a certain point of the beam is directly proportional to

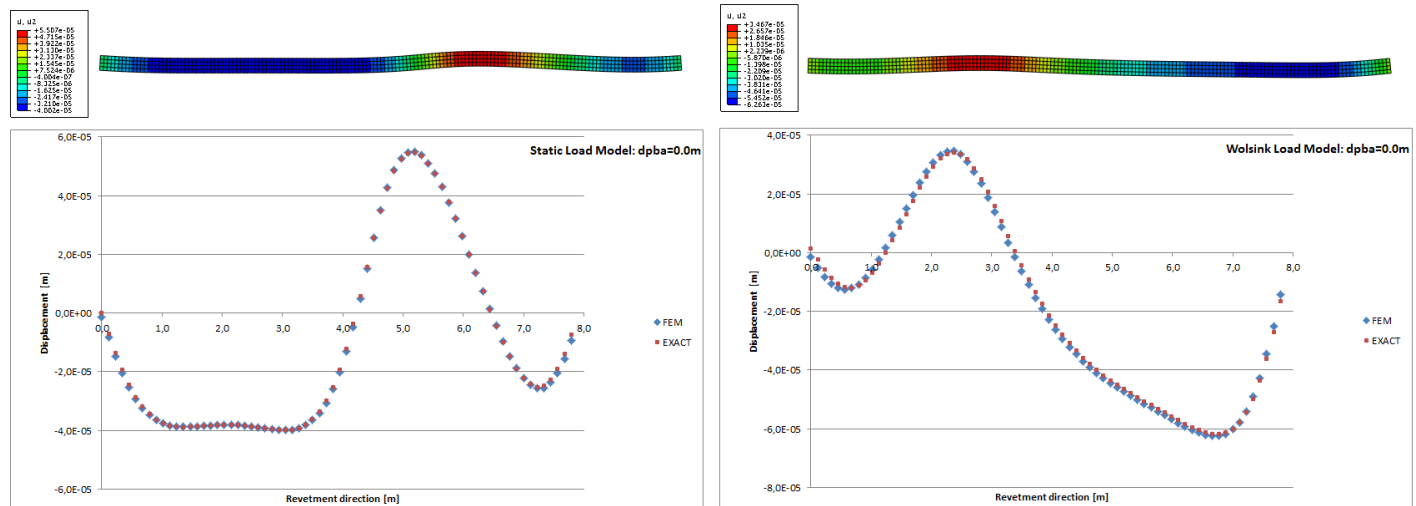


Figure 6.4: Displacements of the revetment when loaded with the two load models, calculated analytically and with FEM software. In this case there is no PBA refurbishment layer present. A fictitious stiffness is used for the block revetment like explained in chapter 5. Left: static load Model; right: Wolsink load model

the force applied at that point and independent of the surrounding soil behaviour. When modelling such a continuous foundation in FEM software, one has to enter a certain value of the soil's Youngs modulus. It is assumed that the dike consist of two soil layers, i.e. a gravel filter layer underneath the revetment and a sand core. According to Bowles (1997) the stiffness of sand and gravel varies between 50-150 MPa for loosely packed material and between 100-200 MPa for densely packed soil. In the following calculations it is assumed that the filter layer has a stiffness of 100 MPa and the sand dike core has a stiffness of 150 MPa. Calculations with other stiffness values are performed in the sensitivity analysis (chapter 7). Furthermore it has to be researched to what extent the uplifting and downlifting of the beam can be modelled with the proposed analytical model. First the two models are compared when applying the static load model. It is interesting to check the bending stresses in the top fibres of the PBA layer because the governing bending stresses will occur here like stated in chapter 5.2. The PBA refurbishment layer will deform during the uplifting of the concrete elements. This deformation induces bending stresses within the PBA layer. The highest bending stresses will occur in the most outer fibres of this PBA refurbishment layer. Structural failure will eventually happen when the bending stresses due to the external loads cannot be withstood by the PBA. The flexural strength strongly depends on the grain size, type of aggregate and the thickness of the layer (see section 3.4.3). Three FEM models are considered and elaborated, i.e. a pitched stone revetment with a PBA refurbishment of 10 cm, 20 cm and 30 cm. In figure 6.5 the bending stresses in the outer fibres of the PBA layer are shown for both models. The blue dotted line displays the results from the FEM calculations, the red dotted line illustrates the outcomes of the analytical model. Unfortunately, like shown in figure 6.5, the stresses in the top fibres of the PBA layer between the two approaches differ significantly. One of the assumptions (see chapter 5.3) of the Winkler foundation is that it can take, besides compression stresses, also tension stresses. This is in contrast to the FEM model, where a tensionless character of the subsoil is assumed. It is well known that soil does not resist any tension stresses. In reality the subsoil cannot take tension forces, i.e. the soil will withstand downward displacements but if the beam will be lifted up, the soil will not counter this upward displacement. Apparently, although these upward displacements are very small (in the order of 0-1 mm), it plays evidently an important role. Therefore it can be concluded that the Winkler foundation greatly influences the bending stresses in outer fibres of the part which is lifted up for this situation. It is interesting what will happen if the dead weight is increased by applying a thicker PBA layer on top of the revetment because adding weight will result in a lower uplift of the structure. The bending stresses in the outer fibres of the PBA layer are shown in figure 6.6. It can be noted that, when the uplift displacement is decreased, the analytical model will move toward the FEM results. Similarly, when applying even a thicker layer (30 cm PBA) the models almost correspond. This is shown in figure 6.7.

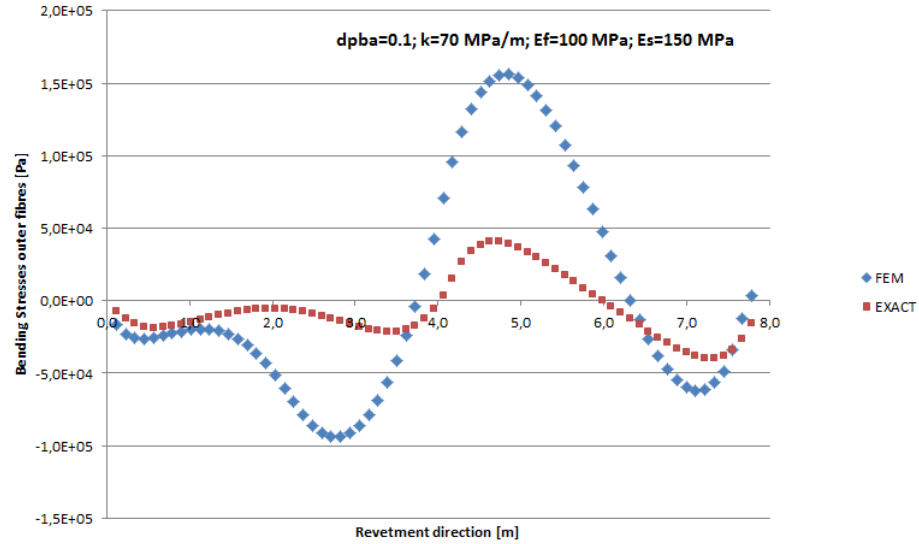


Figure 6.5: Bending stresses in the top fibres of the PBA refurbishment layer (10 cm) both for the analytical and FEM model (Waddenzee data is used)

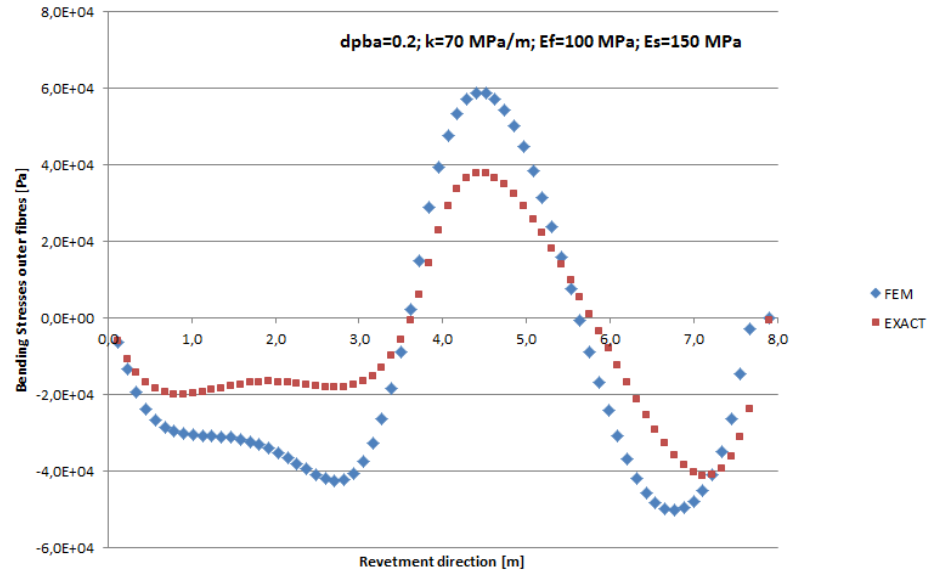


Figure 6.6: Bending stresses in the outer fibres of the PBA refurbishment layer (20 cm) both for the analytical and FEM model (Waddenzee data is used)

6.4. WOLSINK LOAD MODEL

The next step is to apply the Wolsink load model as input for the FEM analysis. The same soil stiffness values are used for these calculations, i.e. 100 MPa for the filter layer and 150 MPa for the sand dike core. In figure 6.8 the results are shown for a refurbishment PBA layer of 10 cm. The red dotted line displays the results of the analytical calculations, the blue line shows the outcomes of the FEM analysis. Similarly, one can conclude that the analytical model, although the upward displacements are very small, underestimates the bending stresses in comparison with the tensionless continuum foundation in the FEM model. If the upward displacements tend to almost completely zero, the analytical model will move toward the FEM results. This can be seen in figure 6.9. When the uplift displacements tend to zero or even become completely negative by adding more weight/increasing the height of the PBA layer, the models better corresponds. Like shown in figure 6.9, the part over which there is an upward distributed force present is not governing any more because the (upward) displacements are very small in this case. The governing bending stresses occur in another part of the beam.

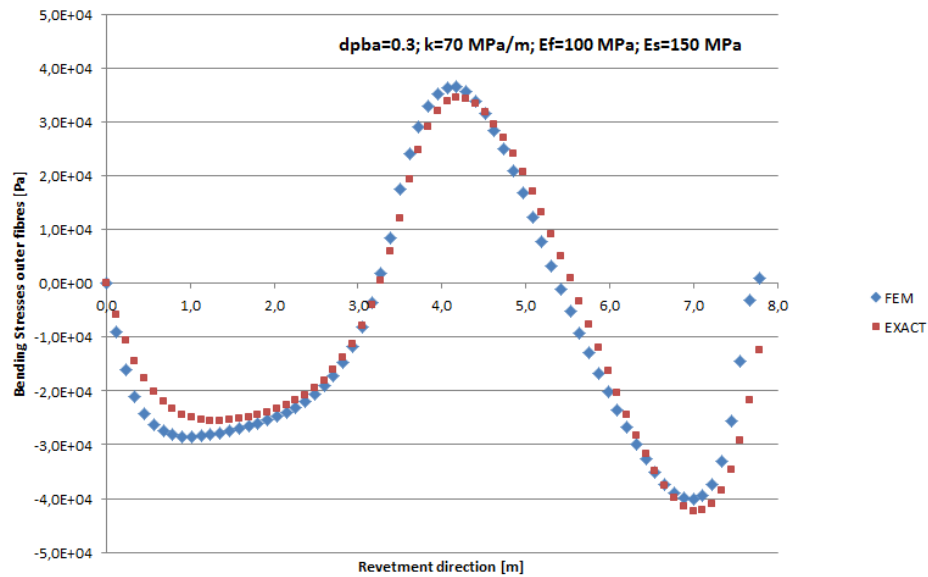


Figure 6.7: Bending stresses in the top fibres of the PBA refurbishment layer (30 cm) both for the analytical and FEM model

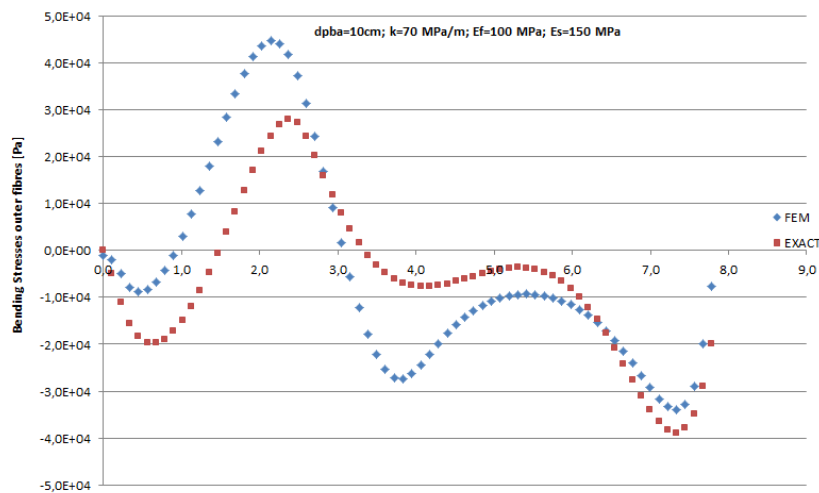


Figure 6.8: Bending stresses in the top fibres of the PBA layer (10 cm) both for the analytical and FEM model

6.5. BENDING BEAM SCHEMATIZATION

Previously, the PBA refurbishment and the block revetment were modelled as a composite bending beam to calculate the maximum bending stresses within the PBA layer. This assumption has to be checked with the help of Abaqus. First a block revetment (thus without PBA refurbishment) is modelled in Abaqus. Therefore the revetment is modelled in Abaqus consisting out of individual concrete blocks. A concrete Young's modulus of 30000 MPa is used for these blocks thus no fictitious Young's modulus of 3000 MPa any more for the entire block revetment. Furthermore a certain friction coefficient is applied between the blocks. To model a revetment consisting out of loose blocks as an Euler-Bernoulli bending beam is a rough schematization. It is assumed that the pitched stone revetment acts according to the linear elastic theory. This implies that plane cross-sections remain planar and normal to the beam axis in a beam subjected to loading. Furthermore, the strain distribution is linear over the cross-section. This also means that the top of the block revetment can withstand tension stresses. However, in fact, the revetment consists of blocks and joints of gap filling material (e.g. gravel). These joints cannot take any tension stresses. This can also be concluded from the FEM results, shown in figure 6.10. Due to the loading mechanism, the blocks will be lifted up and rotated. The larger the friction between the concrete blocks, the lower the upward displacement will be. A certain force will be developed in the compression zone (where the blocks are pushed together). If the hydraulic loads will be increased,

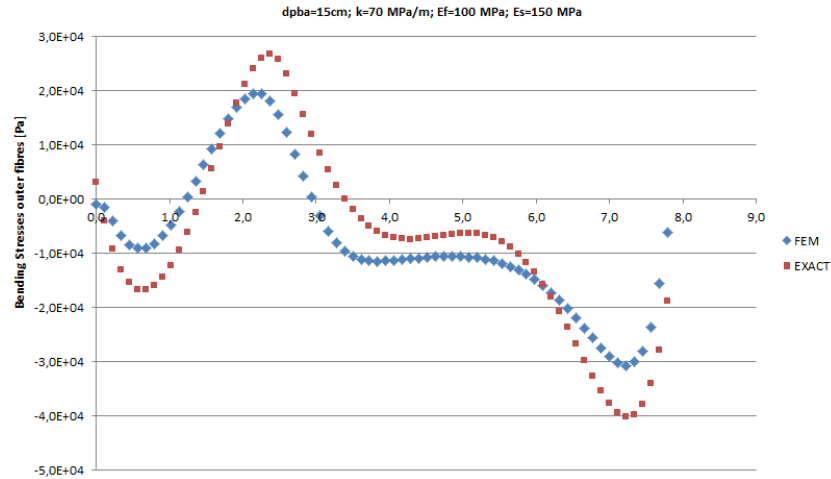


Figure 6.9: Bending stresses in the top fibres of the PBA layer (15 cm) both for the analytical and FEM model

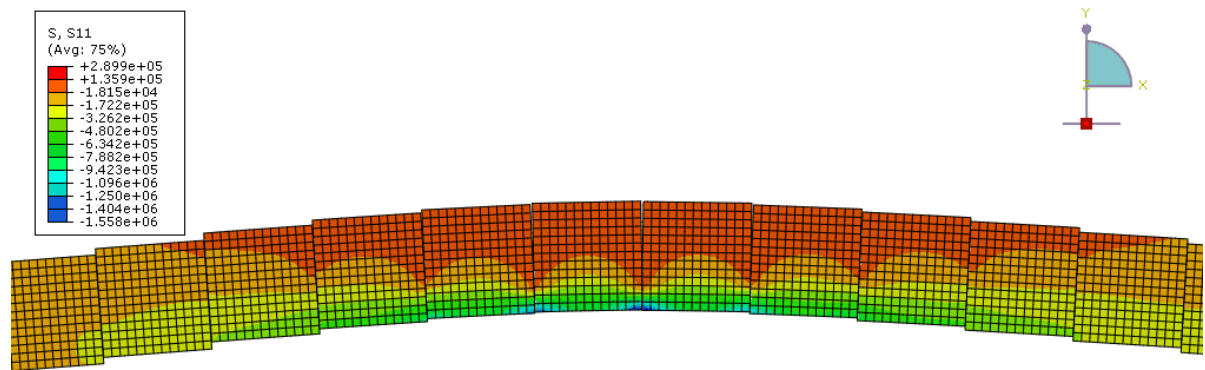


Figure 6.10: Pitched stone revetment (without refurbishment layer) modelled as individual concrete blocks, i.e. no bending beam schematisation. The blocks are lifted up and rotated. The hydraulic conditions of the Waddenzee are used.

the displacement and rotation will grow. If the displacement and rotation will increase, this (eccentric) compression force will become larger and therefore the structure is able to withstand the larger bending moments caused by the increased loads. The moment capacity of the revetment is equal to the developed compression force times its eccentricity. The structure will eventually fail when the compression strength of the concrete is reached or the upward displacement becomes too large. In figure 6.11 it can be seen that in the top region of the revetment, the blocks are moving away from each other. The tension stresses are very small in this region; the maximum tension stress in the governing cross section is equal to 0.073 MPa, the maximum compression stress is equal to 1.56 MPa. However, if the revetment would act as an Euler Bernoulli bending beam, the stresses in the top fibres and the bottom fibres would be equal (in case of pure bending). Therefore it can be concluded that modelling a block revetment as a bending beam is not an accurate schematisation of the real structural behaviour.

The question then arises whether this also holds for the situation when applying a PBA refurbishment on top of the block revetment since the PBA layer adds for example extra coherence to the structure. In figure 6.12 the bending stresses in the PBA top fibres are shown of the structure modelled as a bending beam and the structure modelled with individual concrete blocks. It can be concluded that the behaviour can be pretty accurately modelled as a bending beam in this case. In contrast to the concrete blocks, the PBA refurbishment is one single monolithic plate. Although the blocks do not displace in a smooth line relatively from each other, the PBA will (this also explains the scatter of the FEM results in figure 6.12). The results indicate that, when designing a PBA layer and therefore checking the maximum bending stresses while uplifting, the composite bending beam schematisation is a good approximation. Especially in the areas of interest (uplift region) the two approaches show similarity regarding the maximum bending stress in the PBA layer, which is governing

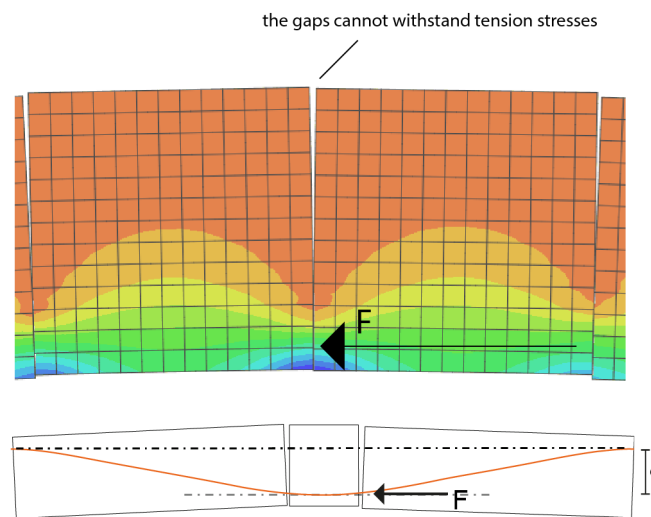


Figure 6.11: An eccentric (e) compressive force develops in the bottom of the concrete blocks. As a result the structure is able to withstand the bending moments caused by the external loads ($M = F \cdot e$)

when designing a PBA refurbishment. An impression of the FEM calculations are shown in figure 6.13.

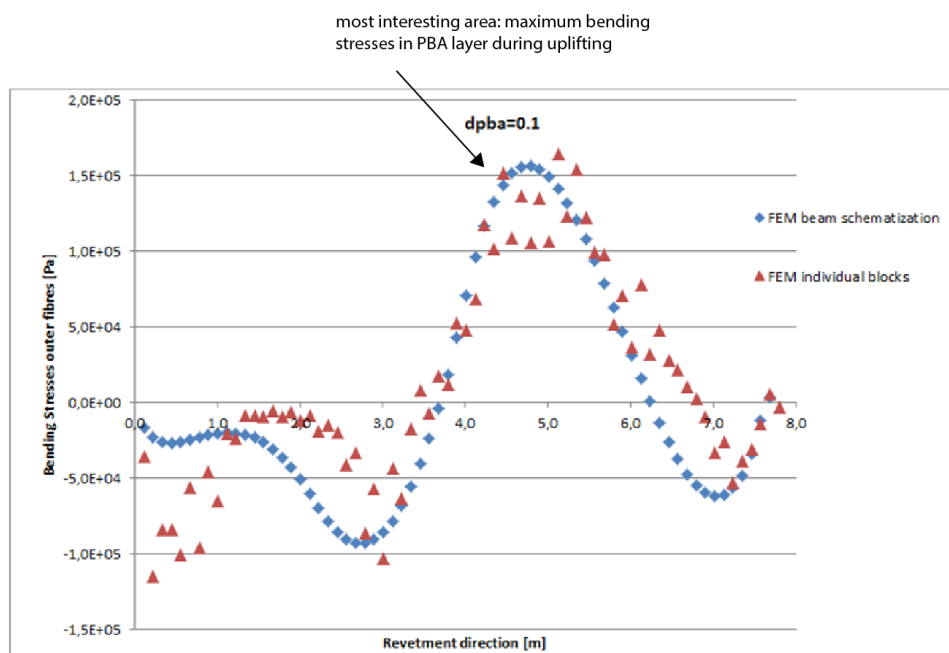


Figure 6.12: The block revetment/PBA structure modelled both as a bending beam (blue) and modelled as individual concrete blocks

6.6. CONCLUSIONS

In this part the results of the analytical model (previous chapter) and the FEM model were compared and discussed. In general, it is assumed that the FEM model is a better schematization of the real revetment behaviour than the analytical elastically supported beam. The main reason is that the Winkler foundation assumed tension forces in the subsoil which do not occur in reality since soil cannot resist tension stresses. Furthermore the load applied to the soil surface produces deflections of the soil not only under the applied load but also produces deflections and stresses outside the loaded area. This is in contrast to the elastic foundation approach. The findings show that the Winkler foundation greatly influences the bending stresses in the uplift region although these displacements are very small. On the other hand, it showed that when the upward displacements tend to zero or even become completely negative the proposed analytical model shows

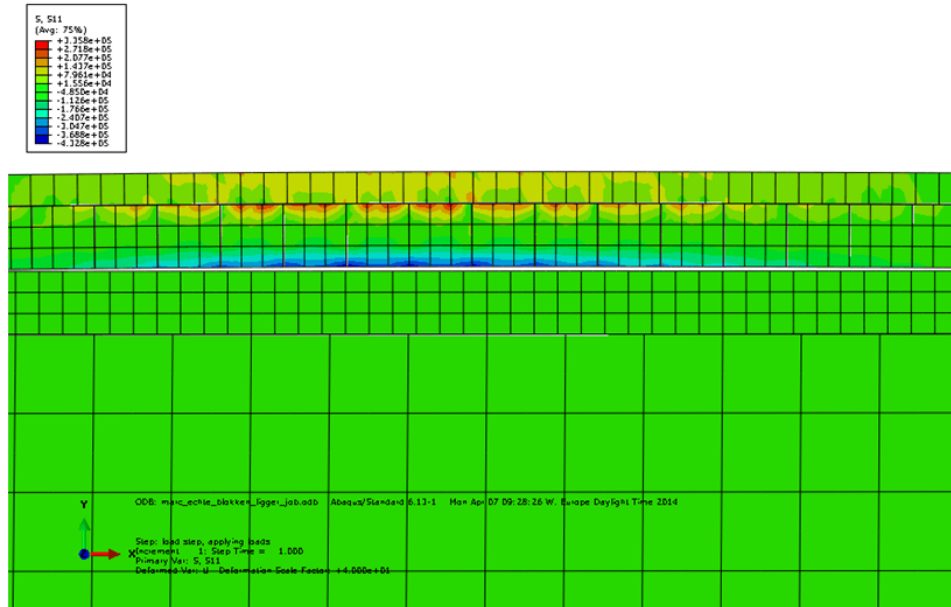


Figure 6.13: An impression of the FEM results of the block/PBA revetment modelled as individual concrete blocks (region of upward displacements)

similarity with the FEM results. An important aspect for both models (analytical and FEM) was the assumption that the PBA-block revetment act as an Euler Bernoulli bending beam. The results of this schematization showed good similarity with the results when modelling the block revetment as individual concrete elements. Especially in the (governing) part where the beam is lifted up. Therefore this assumption seems to be a suitable approach. An important reason is the extra coherence and monolithic behaviour induced by the PBA layer. In these calculations the PBA layer and the block revetment were fully (rigid) connected. In the next chapter the influence of the type of bonding between the two layers will be studied.

7

SENSITIVITY ANALYSIS

In this chapter a sensitivity analysis is done. In the previous chapters a lot of assumptions were made to perform the calculations regarding the structural behaviour of the composite PBA/pitched stone revetment. It is studied how the uncertainty of the most important input parameters in mathematical models (structural, load and FEM models) influence the outcomes. During each analysis, a particular variable is changed while the others are kept constant. It has to be noted that this sensitivity analysis is performed with the static load model. It is more convenient to study the sensitivity of the input variables when using this load model. However, the conclusions that are drawn from the analyses are independent of the load model and thus also hold when applying the Wolsink load model. Obviously, for the sensitivity analysis of the different hydraulic loads, both load models are studied. Also for these calculations, the situation at the Waddenzee is considered. Before performing additional calculations, firstly it is tried to estimate the influence of the different input parameters by using reasoning and general theories. Subsequently the hypotheses are checked by performing extra calculations. In the flowchart of figure 7.1 an overview of the different steps is shown.

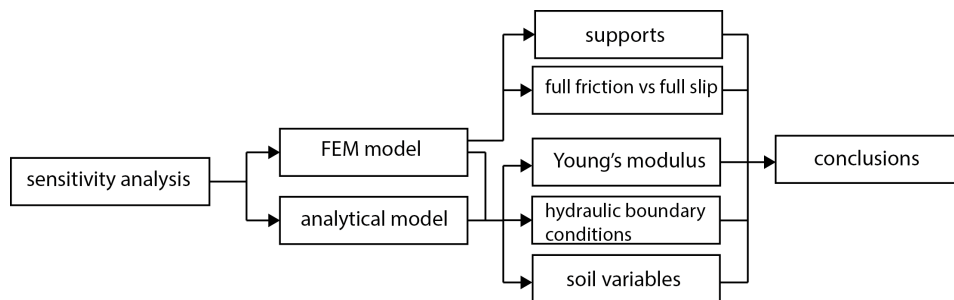


Figure 7.1: Flowchart Sensitivity Analysis

7.1. YOUNG'S MODULUS

The Young's modulus or elastic modulus is a measure for the stiffness and therefore greatly influences the stress distributions within the cross section. Lots of research is done regarding the stiffness of PBA. Because PBA act as a monolithic plate and can be seen as a more or less homogeneous material, the proposed stiffness of chapter 3 (3000 MPa) is pretty accurate. However, it is hard to predict the Young's Modulus of a pitched stone revetment because a block revetment is highly heterogeneous; it consists of concrete blocks and gap filling material. In the structural analysis chapter, two possible methods were explained. One method is based on the thickness of the joints and the stiffness of the gap filling material (usually sand or gravel) and the Young's modulus of the blocks (concrete). With a formula (Frissen, 1996) one can subsequently calculate the Young's Modulus of the block revetment. This resulted, for the Waddenzee dike, in a Young's Modulus of 1360 MPa. Based on his (more recent) research, Peters (2003) proposed another method to determine the Young's modulus of a pitched stone revetment. He concluded in his study that the stiffness of the block revetment is in the order of 10 percent of the mother material (concrete) when considering the gaps between the elements and the presence of the gap filling material. When using this theory, the Young's Modulus is in the

order of 3000 MPa. This value was subsequently used in the calculations performed in the previous chapters. However, it is interesting to investigate to what extent the stiffness of the pitched stone revetment influences the stress distribution in the PBA refurbishment. If a structure is made up of multiple elements, the elements will carry loads in proportion to their relative stiffness. The stiffer an element, the more load it will attract. The elements will carry loads in proportion to their stiffness. Therefore, it is expected that, if calculations are performed with a less stiffer block revetment (1360 MPa), the PBA will carry more load, resulting in higher bending stresses. On the other hand, the concrete elements will "attract" less load, resulting in lower bending stresses. This hypothesis is checked with additional calculations done in Abaqus. From figure 7.2 it can be

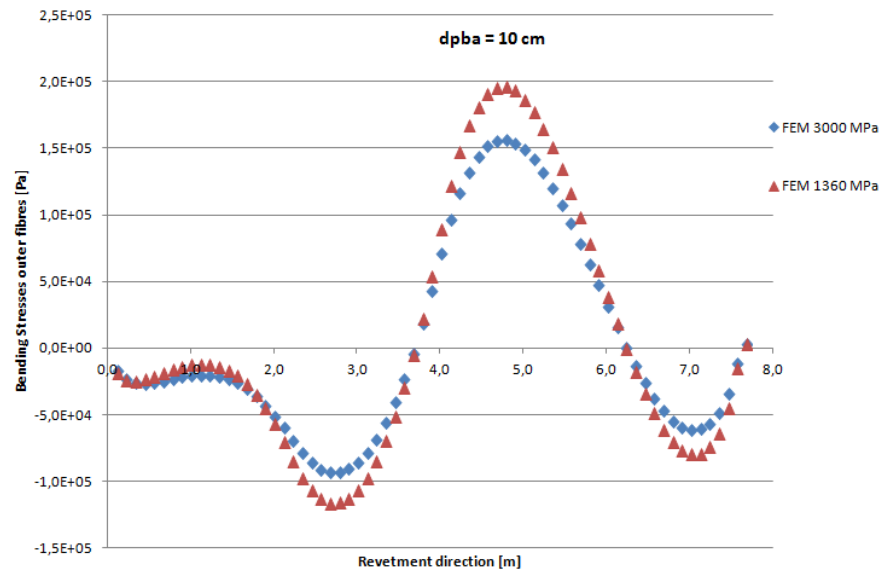


Figure 7.2: The blue line displays the original FEM results, i.e. the calculations performed with a block revetment (modelled as a bending beam) with a Young's modulus of 3000 MPa. The red line shows the results when applying a Young's modulus of 1360 MPa.

concluded that the hypothesis correct. The maximum occurring bending stresses increase in the outer fibres of the PBA refurbishment layer when using a lower stiffness for the block revetment.

When considering the previous chapters and thus applying a stiffness of 3000 MPa for the bending beam representation of the concrete block revetment, it resulted in a good approximation of the structural behaviour of the FEM model when using individual concrete elements (with $E_c = 30000$ MPa). Besides the similarity of results with the calculations performed with loose concrete blocks, this approach has more advantages. Firstly, it is very easy to estimate its stiffness just by taking 10 percent of the mother material (concrete). Secondly, by coincidence, PBA has a Young's modulus of 3000 MPa too, which is very convenient. As a result, one can make preliminary designs with a homogeneous cross-section which reduces the time needed for performing calculations significantly and makes the calculations less complex.

7.2. HYDRAULIC LOADS

The next step is to change the hydraulic loads. First the most important input variables of the static load model are studied, followed by the variables of the Wolsink load model. Reference is made to chapter 4 for further and more detailed explanations about the theory.

7.2.1. STATIC LOAD MODEL

Obviously, it is assumed that the bending stresses in the outer fibres of the PBA layer will increase when the hydraulic loads will grow. Increasing the wave height, will increase the upward loading and therefore the occurring bending stresses. Furthermore it is expected that when a thicker PBA layer is applied, the bending stresses will be reduced since its section modulus and dead weight will become higher.

PBA THICKNESS

With the help of Maple different load scenarios are calculated, shown in figure 7.3 for the static load model. The larger the thickness of the additional layer the bigger the load function in AB. Obviously, a thicker layer

results in bigger dead weight and therefore the function shifts in the positive y-direction. Furthermore, due to the dead weight increase, the upward pressure area reduces. This is illustrated in the graph with a shift of the linear line to the left. Moreover, there is a shift of the q -load in the positive y-direction. Similarly as in BC, the increase of dead weight results in a higher resultant distributed load.

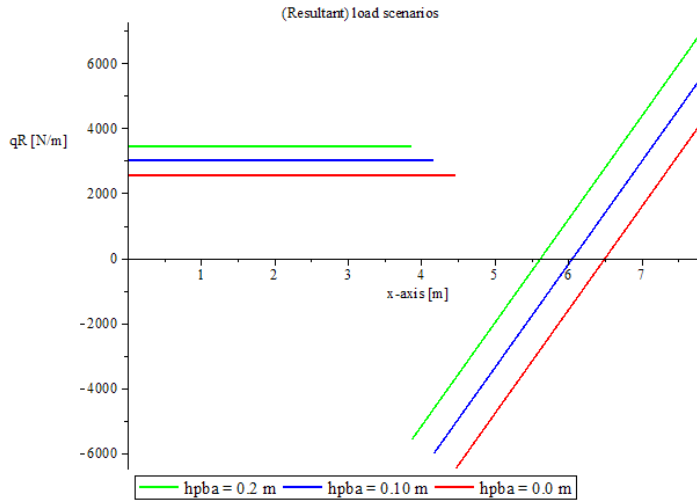


Figure 7.3: Different load scenarios (static load model) when applying a PBA layer of 0.2 m (green), 0.1 m (blue) and no layer (red)

WAVE HEIGHT AND WAVE PERIOD

Increasing wave height results in a higher vertical distance Z between SWL and slope (since $Z = 0.33H_s\xi$). The vertical drop between q_1 and q_2 , like shown in figure 7.4, is equal to $\rho_w g Z$. By increasing the wave height, and therefore Z , the difference between q_1 and q'_2 becomes larger with $\rho_w g \Delta Z$. The values of q_1 and q_3 are only dependent of the thickness and density of the PBA layer and the concrete blocks. Therefore these values will not differ by changing the hydraulic boundary conditions. Furthermore, the distance over which the distributed load becomes negative increases with Δx , see figure 7.4. The same holds for the wave period.

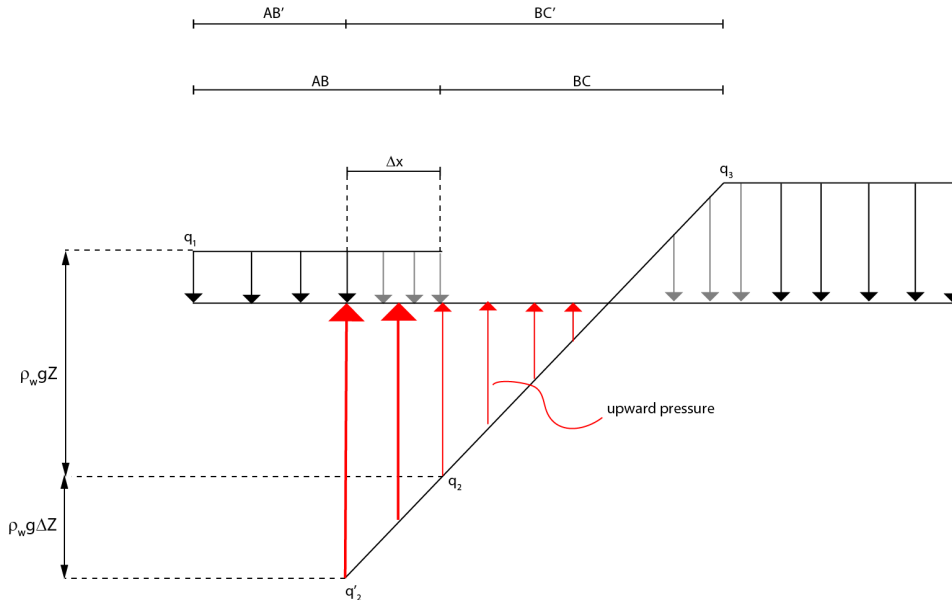


Figure 7.4: Increasing the wave height results in a different load diagram; q_2 is the initial situation, q'_2 is the adjusted situation

When the period is increased, the wave steepness decreases (if the wave height is kept constant) resulting in a higher Iribarren number.

IRIBARREN NUMBER

Also the Iribarren number is of importance. A higher Iribarren number results in a higher wave front. Therefore a steeper dike slope in combination with a more gentle wave, results in larger Iribarren numbers since the Iribarren number is given by $\xi = \frac{\tan \alpha}{\sqrt{s}}$.

BENDING STRESSES

Subsequently it is interesting to study to what extent the increase of the previously mentioned variables influences the design criteria, i.e. the bending stresses in the outer fibres of the PBA refurbishment layer. Figure 7.5 shows the bending stresses in the PBA layer when applying a wave height of 1.5 and 2.0 meter. It can be

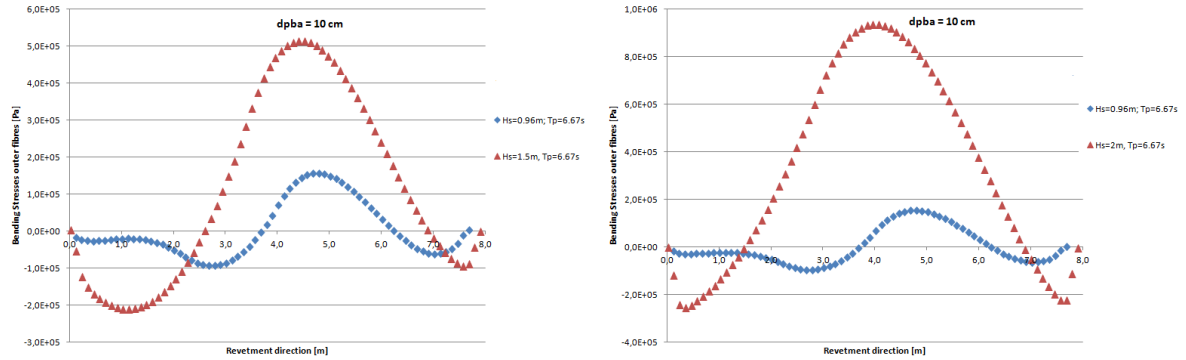


Figure 7.5: FEM results: bending stresses in the outer fibres of the PBA layer when loading with a significant wave height of 1.5 m (left) and 2.0 m (right)

seen that the stresses increase significantly. In general there are two possibilities to deal with this increase. First of all, one can choose a mixture which can withstand higher stresses. By taking a finer mixture the PBA is able to restrain higher bending moments. From figure 5.2 in chapter 5 it can be concluded that one has to apply a mixture of limestone 20/40 mm for a wave height of 1.5 m and a 10/14 mm class for a wave height of 2.0 m while a mixture of 30/60 mm was good enough for the original wave height of 0.96 m. Another possibility is applying a thicker PBA layer. A thicker layer will result in a higher section modulus and therefore lower bending stresses. In figure 7.6 the stresses are shown for a PBA thickness of 10 cm, 15 cm and 20 cm while loaded with a significant wave height of 1.5 m.

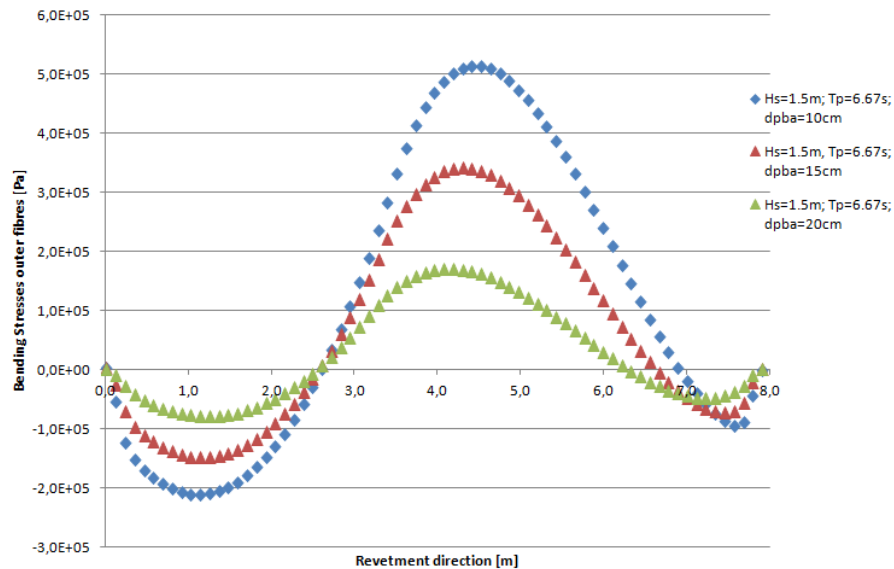


Figure 7.6: FEM results: bending stresses for varying PBA layer thickness, a wave height of 1.5 m is applied

7.2.2. WOLSINK MODEL

LEAKAGE LENGTH

When solving Wolsink's differential equation, the leakage length parameter (Λ) is of great importance. In chapter 4, it is described that the leakage length can be described with:

$$\Lambda^2 = \frac{k_f d_f d_t}{k_t} \quad (7.1)$$

Applying a PBA refurbishment layer will influence the leakage length as follows.

$$\Lambda_{pba}^2 = \frac{k_f d_f d_{pba}}{k_{pba}} \quad (7.2)$$

Since k_{pba} is very small due to its high permeability, this value will be negligible small.

$$k_{pba} \ll k_{block} \rightarrow \Lambda_{pba}^2 \ll \Lambda_{initial}^2 \quad (7.3)$$

Therefore it can be concluded that the contribution of the PBA layer to the initial leakage length is negligible small. On the other hand, due to the additional PBA layer, the dead weight of the structure increases and therefore its stability.

It is interesting to see the influence of the leakage length parameter. For a large leakage length ($\Lambda \rightarrow \infty$) the layer is assumed to be impermeable. This results in a horizontal piezometric level plot. The maximum head difference is therefore equal to Φ_b and there is no flow in the filter present. On the other hand, when a small leakage length is assumed ($\Lambda \rightarrow 0$), the layer is very 'leaky' and the piezometric level in the filter therefore completely follows the curve of the hydraulic level present at the top layer. As a result there is no head difference and therefore no pressure difference. These two situations are shown in figure 7.7. Therefore

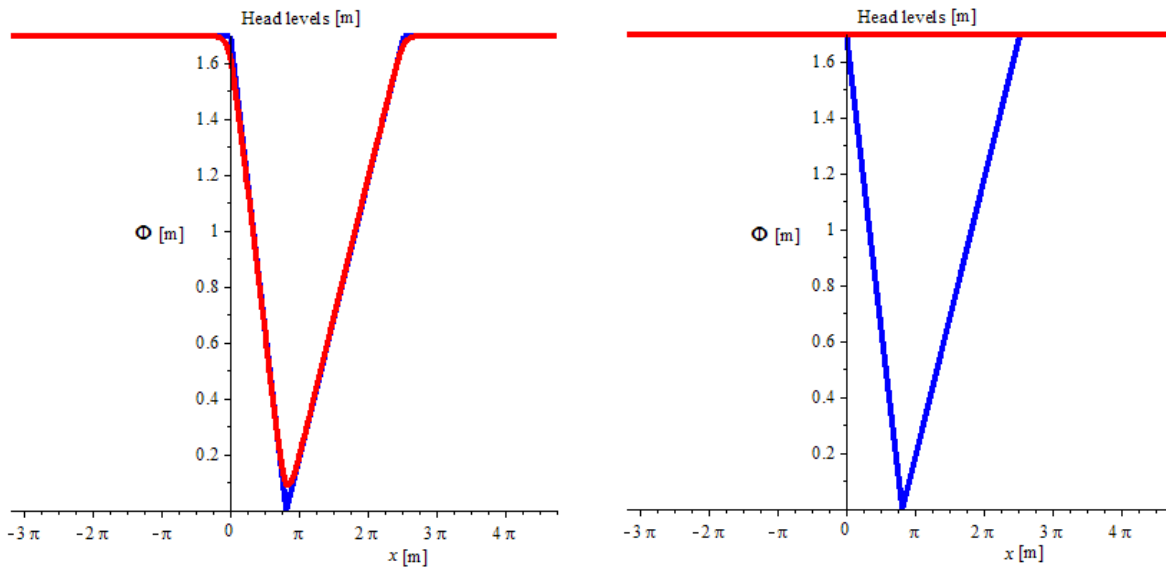


Figure 7.7: Piezometric levels in filter (red) and at top layer (blue); left: very large leakage length, right: very small leakage length

it is expected that the lower the leakage length the lower the hydraulic loads on the revetment. To study this hypothesis the following calculations are performed. In chapter 4 the leakage length has been calculated:

$$\Lambda = \sqrt{\frac{d_f d_t k_f}{k_t}} = \sqrt{\frac{0.2 \cdot 0.2 \cdot 0.05}{0.001}} \approx 1.5 \text{ m} \quad (7.4)$$

If it is supposed that due to clogging the permeability of the block revetment is reduced with a factor 10, i.e. $k_t=0.0001$. The corresponding leakage length changes into:

$$\Lambda = \sqrt{\frac{d_f d_t k_f}{k_t}} = \sqrt{\frac{0.2 \cdot 0.2 \cdot 0.05}{0.0001}} \approx 4.5 \text{ m} \quad (7.5)$$

With the help of Maple the two situations are studied for an "finite" revetment length (figure 7.8). The left graph shows the hydraulic head difference and the right graph displays the resultant load on the revetment. It can be noted that a change in leakage length has a significant influence in the resultant load situation.

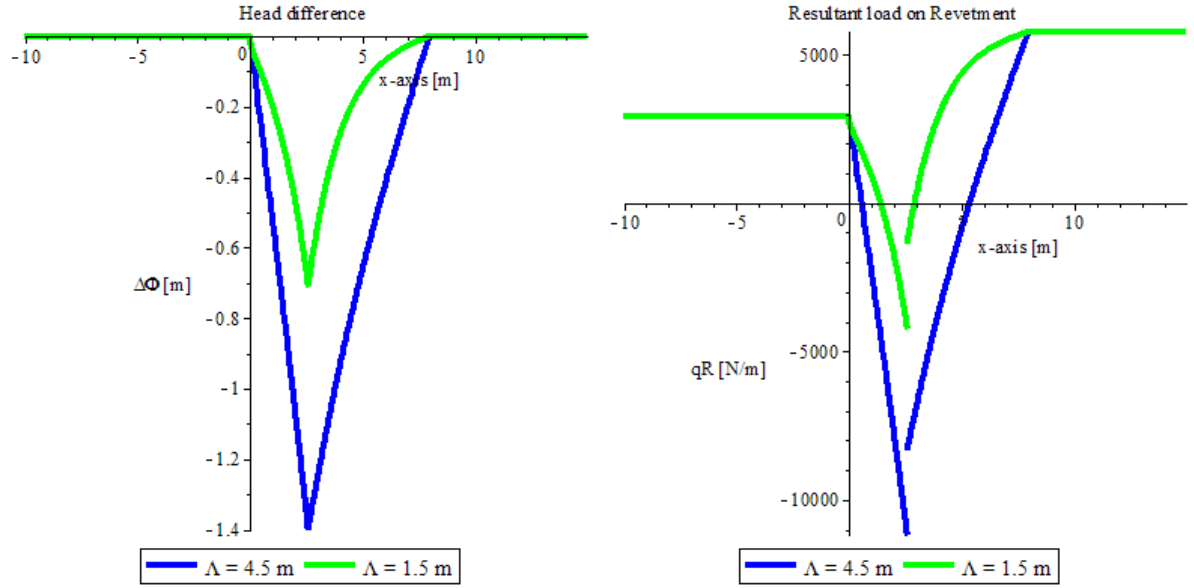


Figure 7.8: The hydraulic head difference (l) and the resultant load (r) over the revetment for both $\Lambda = 4.5$ m and the original Λ of 1.5 m (Waddenzee)

WAVE HEIGHT AND PERIOD

Like in the previous section also the response of the Wolsink model is studied when increasing the hydraulic loads. In chapter 4 it is shown that the (time-dependent) wave load is schematized as a static situation, described with two parameters: the wave steepness β and Φ_b . It is researched what will happen if the wave height is doubled, therefore calculations are performed with very high waves of 2.5 m, it is expected that the loads will increase when applying bigger waves. The calculations are furthermore elaborated with the original leakage length of 1.5 m. The results are depicted in figure 7.9. It can be seen that there is a huge difference between the two situations. If the wave height doubles, the resultant load over the revetment increase considerably. In the first case the maximum upward load is -4 kN, when increasing the wave height to 2.5 m this value is equal to approximately -11 kN.

7.3. FULL FRICTION VERSUS FULL SLIP

So far it is assumed that the PBA layer and the concrete elements are fully bonded together and therefore act as a rigid connection (full friction). It is interesting to study to what extent the structural behaviour is influenced when there is a certain amount of slip present between the two layers. Therefore a simple mechanical model is considered to get a first insight in the structural behaviour when two beams are fully connected or not fully bonded. In figure 7.10 two situations are shown: in the left figure the two beams are fully bonded together (full friction) and in the right figure the two beams can move freely between each other (full slip). In both figures the beams are simply supported and are made from two homogeneous members of equal size. First the situation is studied when there is no rigid connection between the two beams. In this case, it can be assumed that both beams carry half of the point load F because the upper beam cannot deflect more than the lower one. By applying mechanics, the section modulus (per meter) of both parts is equal to:

$$W_{top,beam} = W_{bottom,beam} = \frac{1}{6} \left(\frac{1}{2} h \right)^2 = \frac{1}{24} h^2 \quad (7.6)$$

The maximum bending and compression stresses within both beams is therefore equal to:

$$\sigma_{max} = \pm \frac{M}{W} = \pm \frac{\frac{1}{2} \left(\frac{1}{4} Fl \right)}{\frac{1}{24} h^2} = \pm 3 \frac{Fl}{h^2} \quad (7.7)$$

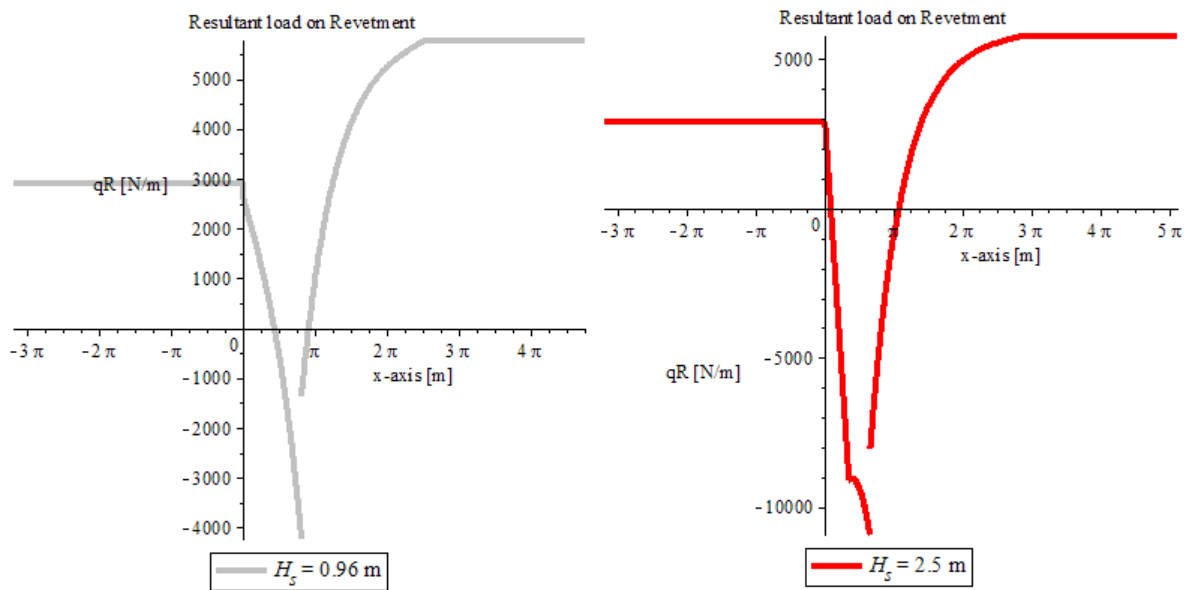


Figure 7.9: The resultant load situations for the initial -Waddenzee dike- wave height of 0.96 m (left) and when applying a wave height of 2.5 m (right)

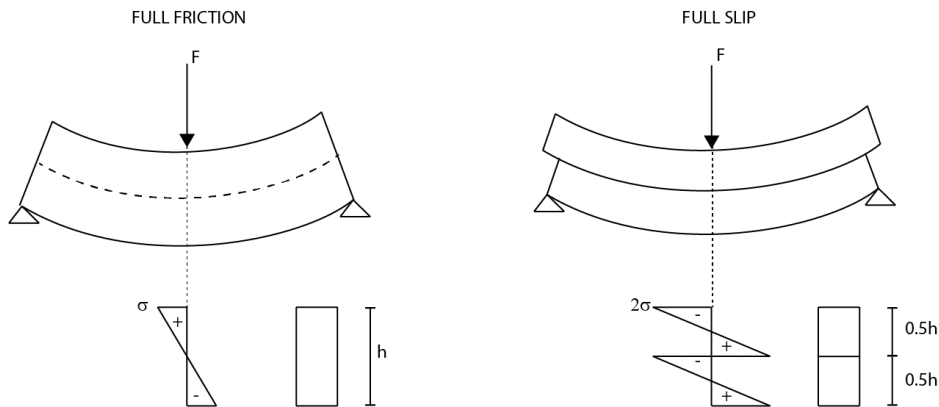


Figure 7.10: Two mechanical situations and their corresponding bending stress diagrams. left figure: two beams fully bonded; right figure: two beams not fully bonded

Subsequently it is now assumed that the two beams are joined together by a stiff connection. The two members then behave as one. This situation is known as full friction or full interaction. The section modulus in this case equal to:

$$W = \frac{1}{6} h^2 \quad (7.8)$$

Which results in the following maximum bending stress:

$$\sigma_{max} = \pm \frac{M}{W} = \pm \frac{\frac{1}{4} Fl}{\frac{1}{6} h^2} = \pm 1.5 \frac{Fl}{h^2} \quad (7.9)$$

It can be concluded that, if both members are fully bonded, the maximum bending stresses are two times lower than when there is fully slip present between the two parts. Therefore it is expected that if the PBA is not fully bonded with the concrete elements, the bending stresses in the outer fibres will increase. FEM calculations are done to check this hypothesis.

In Abaqus an extreme situation is modelled, i.e. a frictionless interaction between the PBA and concrete elements. The calculations are performed with a revetment consisting of individual blocks (thus no bending beam schematization) with a PBA refurbishment layer of 10 cm. The results of this FEM analysis are shown in

figure 7.11. An impression of the Abaqus results are shown in figure 7.12. It can be concluded that due to the

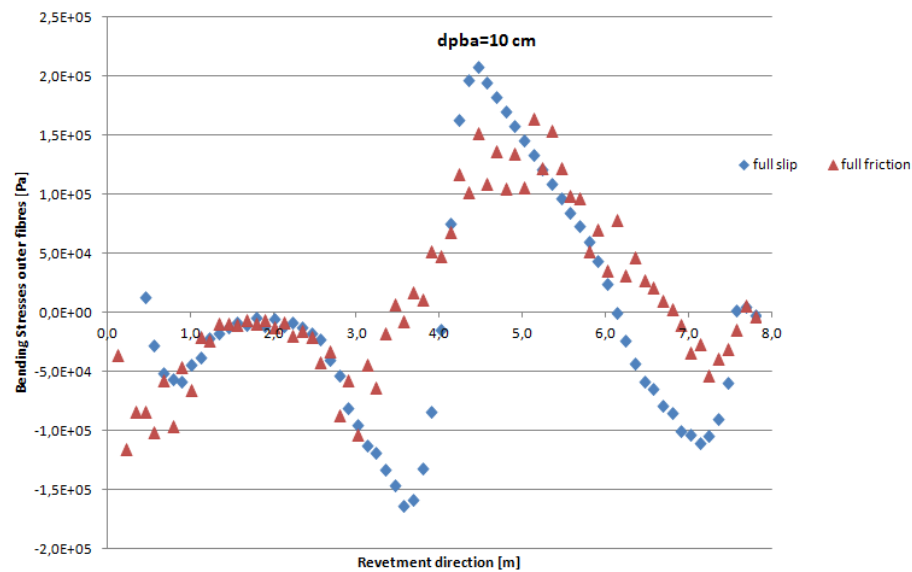


Figure 7.11: Bending stresses in the outer fibres of the PBA layer. Red: full friction between the concrete blocks and the PBA layer; Blue: full slip between the concrete blocks and the PBA layer (Waddenzee situation)

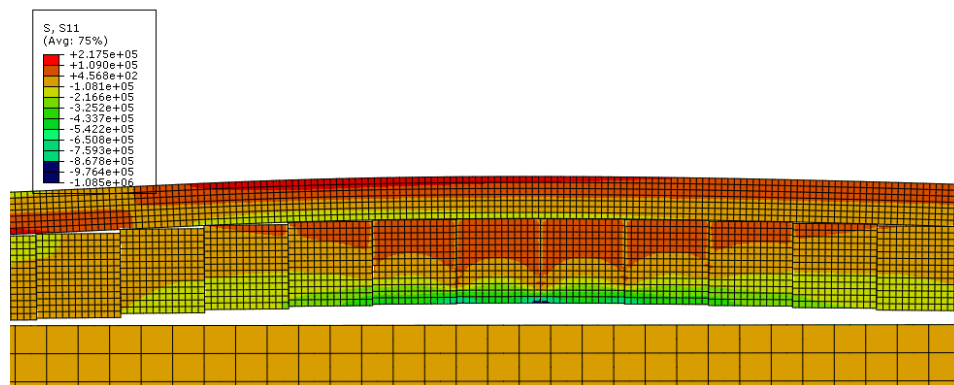


Figure 7.12: Impression of the Abaqus results: bending stresses in the outer fibres of the PBA layer while frictionless connected with the block revetment

slip interaction, the bending stresses will increase in the outer fibres of the PBA layer. Therefore a full bonding is desired. If such a rigid connection is preferred, some surface preparations have to be done before applying Elastocoast. One has to clean the concrete elements, otherwise the polyurethane cannot form a strong bond with the blocks. Any dirt or debris will reduce the strength of the joint by reducing the surface area of the adhesive bond. It is therefore very important that surfaces are made clean and appropriate cleaning procedures are therefore important preconditions for optimum joint strength. However, it is possible that after cleaning procedures the surface of some parts is still not clean enough which could influence the type of bonding and thus the structural behaviour. In this case one has to be aware for higher bending stresses. Besides the increase in stress, also the displacement becomes larger. Although the displacements are relatively small in this case, i.e. 0.5 mm and 1 mm for respectively the full friction and full slip situation, it differs a factor 2. Furthermore the maximum compression stresses increases in the bottom fibres of the concrete elements. When the two layers are fully connected, the maximum compression stress is equal to approximately 0.43 MPa. If there is full slip present between the interaction layers, the maximum compression stress is equal to 1.1 MPa. Although concrete can withstand much higher compression stresses, the difference is significant. Moreover, when designing for bigger hydraulic loads (e.g. bigger waves) this behaviour could become important.

7.4. FRICTION BETWEEN ELEMENTS

The friction between the individual concrete blocks is of great importance when applying no refurbishment layer. Like stated in chapter 6.5, if the upward pressure exceeds the dead weight of the revetment, it is still able to withstand these loads due to the friction between the concrete elements. It is expected that the friction is of minor influence when a PBA layer is fully (rigid) connected to the concrete blocks. In this case the blocks are "glued" to the PBA layer and it already acts as one single structure. On the other hand, if there is (partly) slip interaction, it is expected that it has an influence on the structural behaviour. More friction between the elements will induce a smaller (upward) displacement, therefore the blocks are less "pushed" into the PBA layer, resulting in lower bending stresses. This hypothesis is checked with the help of Abaqus. In the left part of figure 7.13 the results are depicted when the PBA layer is fully (rigid) connected to the concrete elements. The bending stresses are (almost) completely the same like expected. The friction between the elements does not play an important role because the structure already acts as a whole due to the rigid connection between the refurbishment and the blocks. On the other hand, when these two layers are not fully connected the situation changes. In the right part of figure 7.13, it can be seen that there is a significant difference between the two stress graphs. The bending stresses shown in red show the situation when there is more friction between the elements. More friction induces a stiffer structure and therefore lowering the bending stresses in the outer fibres of the PBA layer.

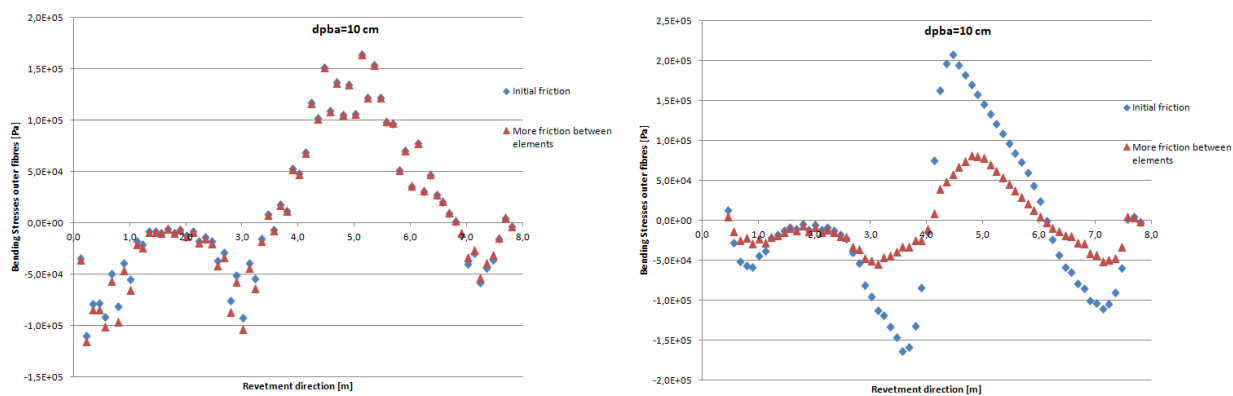


Figure 7.13: The left figure shows the bending stresses when the PBA layer and the pitched stone revetment are rigid connected, in the right figure the two layers are frictionless connected. The red graphs display the stresses when the friction between the elements is increased based on the initial applied friction (blue). The situation at the Waddenzee is considered.

7.5. SOIL VARIABLES

In the analytical model, the soil is represented by a set of linear elastic springs. An important parameter in this case is the spring stiffness or foundation modulus k . A table which points out the range of k -values for various types of soils was shown in figure 5.7 of chapter 5. It was assumed that the filter layer and sand dike core could be described as gravelly soils. In the calculations performed in chapter 5 a modulus of 70 MPa/m is used, based on this table. On the other hand, in the FEM calculations, the soil stiffness is expressed in a Young's modulus. In these calculations the foundation is modelled as a tensionless continuum to model the soil behaviour as realistic as possible. According to Bowles (1997) the soil stiffness greatly varies, therefore it is interesting to study to what extent the foundation modulus k and the soil stiffness E influence the bending stresses. It is expected that the a stiff foundation will reduce the maximum bending stresses in the PBA layer. The stiffness of the subsoil determines the support reaction of the PBA revetment under the hydraulic loads. Subsoil with a high stiffness seems favourable. The stiffer the subsoil is, the larger the part of the load that is directly transferred tot the subsoil, relieving the PBA refurbishment layer. In Abaqus the bending stresses are calculated for different values of the subsoil stiffness. It can be seen that the stiffer the subsoil, the lower the bending stresses in the PBA layer. Furthermore it can be concluded that the stresses are much more sensitive to a variation of the k -value than to changes in stiffness of the filter layer. However, overall it can be concluded that the stiffness does not significantly influence the stress distribution. If the order of magnitude is correct, the bending stresses are more or less of the same order. Especially in the critical areas, i.e. the region of the revetment that is lifted up. For the tensionless foundation/FEM approach, the stresses for both

stiffness situations are even almost the same. Obviously, due to this tensionless character, the stiffness of the subsoil does not influence the structural behaviour in this (uplifting) part of the beam (see figure 7.14). This is in contrast to the analytical model, where the springs also withstand upward displacements and therefore influence the bending stresses in this part of the beam too.

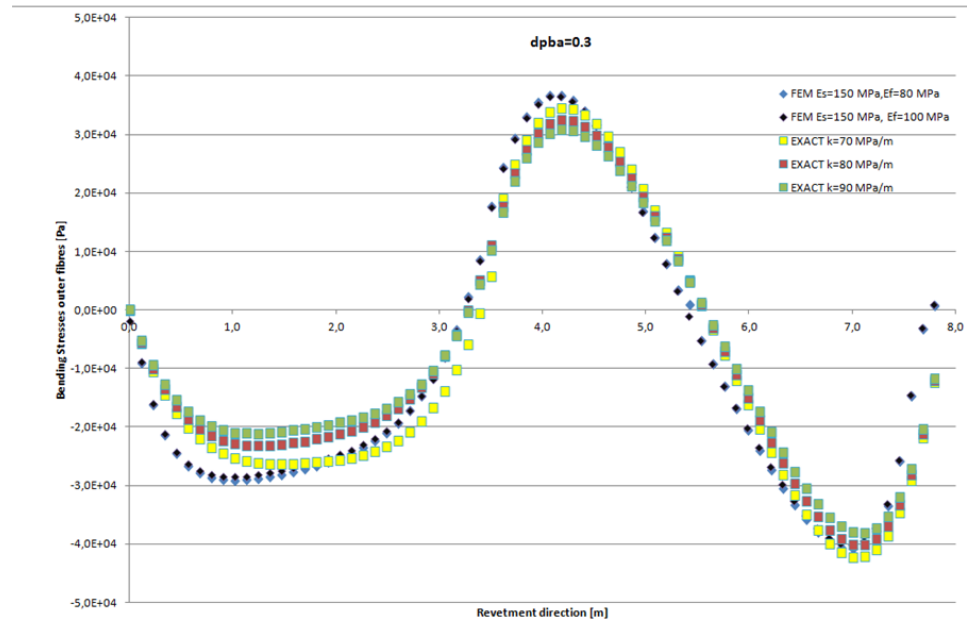


Figure 7.14: The influence of the soil variables; bending stresses in the top fibres of the PBA refurbishment layer (30 cm) both for the analytical and FEM model. The hydraulic conditions at the Waddenzee are used.

7.6. SUPPORTS

In general, structures transfer their loading through a support to the subsoil. The actual behaviour of a support can be quite complicated therefore assumptions were made. In chapter 5 it is explained why the two boundaries of the revetment were modelled as pinned supports based on the assumed rigidity and flexibility. In this section, the support that lie on the other extreme limit is considered, i.e. on both end fixed. Firstly, a simple mechanical model is considered to get a first insight in the structural behaviour like shown in figure 7.15. In the left figure a beam is considered which is on both ends pinned, in the right part the beam is on both

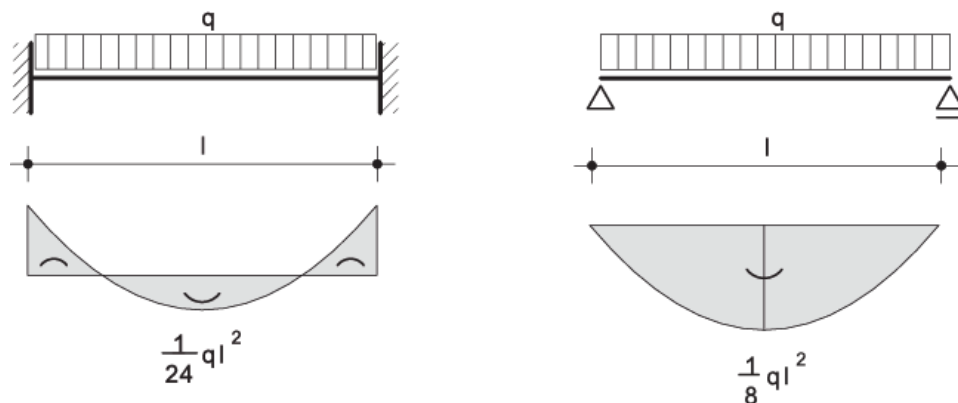


Figure 7.15: Two beams with different supports and their corresponding moment diagram. Left: beam on both ends pinned support; right: fixed beam

ends fixed. Both beams are furthermore loaded with a uniformly distributed q load. Based on mechanics, the

bending moment in the middle is for the left beam equal to:

$$M_{max} = \frac{1}{24} q l^2 \quad (7.10)$$

For the right beam, the maximum bending moment is equal to:

$$M_{max} = \frac{1}{8} q l^2 \quad (7.11)$$

The stiffer -fixed- supports will attract more load and therefore relieve the beam. Therefore it is expected that the bending stresses will be lower when the revetment is assumed to be fixed on both ends. The calculations are performed with individual concrete blocks thus no bending beam schematization for the block revetment. In figure 7.16. It can be concluded that due to the fixed supports the bending stresses in the critical

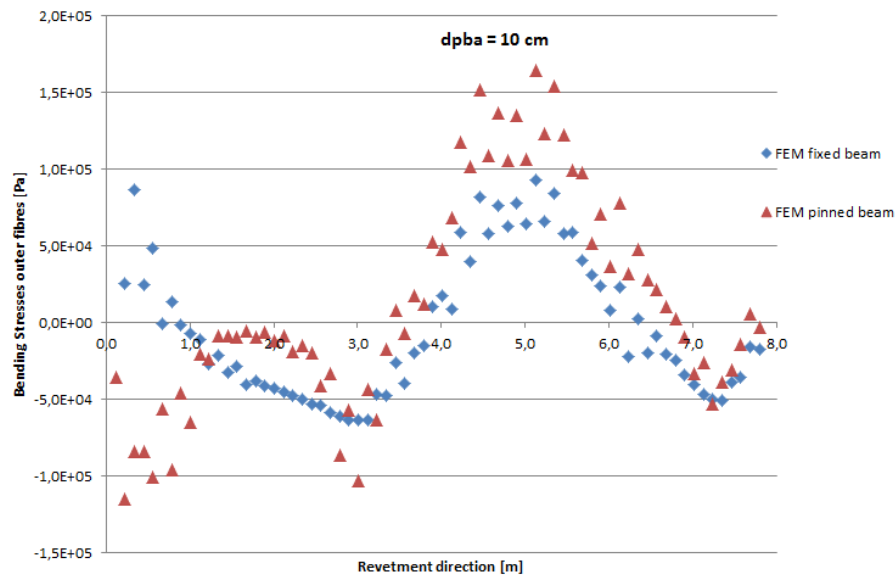


Figure 7.16: FEM results: the red graph shows the bending stresses if the revetment is on both ends pinned, the blue graph shows the results if the revetment is on both ends fixed. The hydraulic conditions at the Waddenzee are used.

(uplift) region are reduced. Furthermore, this graph implies that the assumption of "pinned ends" is a safe estimation.

7.7. SIMPLY SUPPORTED BEAM MODEL

Both the analytical method and the finite element method results show similarities regarding the maximum bending stresses in the PBA layer. However, it is shown that this only holds when the displacement is negative or almost completely zero which requires a relatively thick PBA layer. An advantage of using a PBA refurbishment, in contrast to the conventional method (just adding more weight by replacing the current block with heavier ones), is that a (PBA) refurbishment also adds extra coherence to the structure. Therefore it is still interesting to check whether it is possible to model the structural behaviour of the beam with an analytical method when a certain upward displacement is allowed. The proposed analytical model is less complicated as the elastically supported bending beam mentioned earlier, however, it need to be studied whether it could be a good approximation. This model is already used by ARCADIS for preliminary designs in the PBA design manual (Bijlsma & Voortman, 2009). The method is never proved or researched with FEM software or other measurements. The model is based on the following assumptions. The bending stresses, as a result of the hydrostatic water pressures (static load model), are estimated by considering only the part of the revetment over which the total loading becomes negative in the form of a basic mechanical problem, i.e. a simply supported beam. This approach is shown in figure 7.17.

When applying this model, one assumes that only the PBA layer contributes to the bending capacity, thus the block revetment only contributes to its dead weight and does not contribute to the structure's flexural strength. The results shown in figure 7.18 suggest that this is a conservative approach. The bending stress

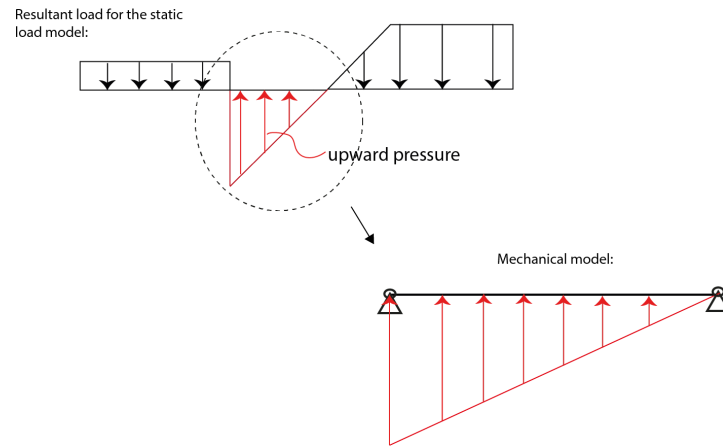


Figure 7.17: Second analytical model: it is assumed that the displacement is zero where the load changes sign. Subsequently the bending stresses in the PBA layer are calculated for a simple mechanical model

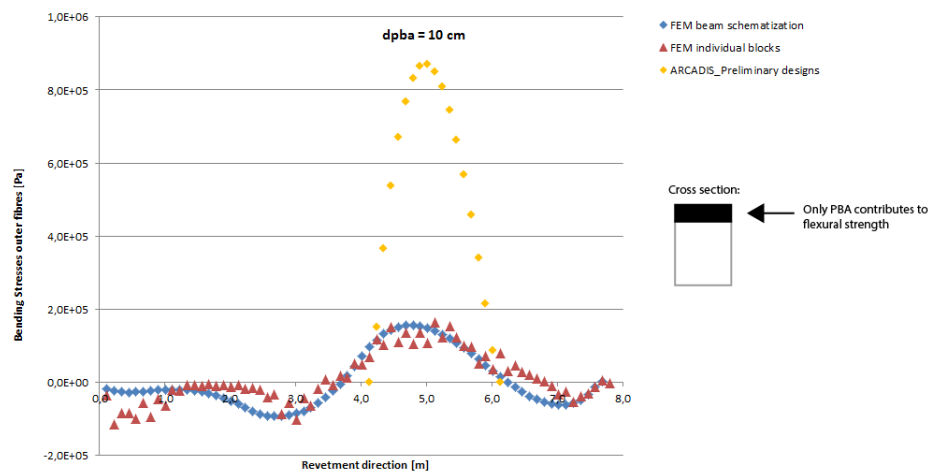


Figure 7.18: The FEM calculations (red and blue) compared with the (analytical) simply supported beam model provided by ARCADIS for preliminary designs

according to the preliminary design method is equal to 0.9 MPa while the FEM calculations show both maximum bending stresses in the order of 0.15 MPa. This implies that one is designing with a maximum bending stress which is six times bigger than the stresses obtained with the FEM analysis. Furthermore one has to choose a finer mixture class (see figure 5.2). In order to improve this model, it is proposed to take the entire cross section of the PBA/block revetment into account, i.e. also the concrete elements contribute to the flexural strength of the structure and therefore lowering the maximum occurring bending stresses. Therefore the same approach is used but is extended for the behaviour of a composite beam. The results are shown in figure 7.19. It can be seen that this new analytical method better follows the stresses of the FEM model but now underestimates the stresses with respect to the FEM results. This problem could be solved by, for instance, applying certain safety factors.

7.8. CONCLUSIONS

A lot of assumptions were made in the previous chapters to perform calculations regarding the structural behaviour of the composite PBA/pitched stone revetment. It is studied to what extent the most important variables influence the outcomes of the FEM and analytical model. The findings suggest that a Young's modulus of 10 percent of the mother material (concrete) can be used for the block revetment (approximately 3000 MPa). There are furthermore some notable advantages. First of all, it is very easy to estimate its stiffness by taking 10 percent of the mother material. Secondly, by coincidence, PBA has a Young's modulus of 3000 MPa too. This is very convenient since one can design with a homogeneous cross-section which reduces the time

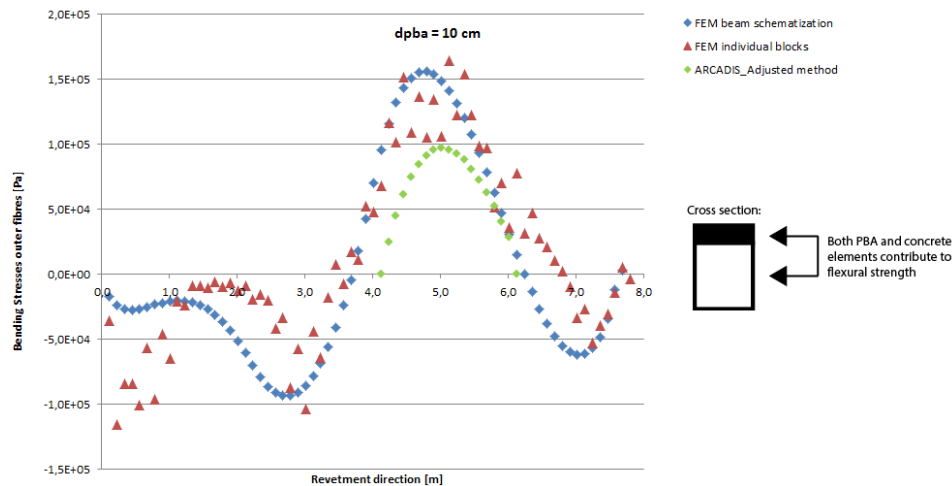


Figure 7.19: Comparing the bending stresses, based on the new analytical approach, with the FEM results (Waddenzee conditions are used).

needed for performing calculations significantly and makes the calculation procedure less complex.

Obviously, the maximum bending stresses will increase when the hydraulic loads will grow. An important parameter of the static load model is the vertical distance Z . Since Z -the vertical distance between the SWL and the dike slope- is dependent of the wave height and period, these variables greatly influence the resultant load over the revetment. These variables are also of importance when applying the Wolsink load model. Another important parameter for this load model is the leakage length. The more permeable the structure, the lower the leakage length will be. If the leakage length increases, the head difference will be higher. On the one hand, if the leakage length goes to zero, the revetment is very leaky and the piezometric level in the filter therefore completely follows the curve of the hydraulic level present at the top layer. On the other hand, when the leakage length goes to infinity, the layer is assumed to be impermeable. This results in a horizontal piezometric level plot. A change of leakage length from 1.5 m to 4.5 m, resulted in a two times bigger (maximum) hydraulic head difference (i.e. from 0.7 m to 1.4 m). In general there are two possibilities to reduce the maximum bending stress in the PBA layer. Firstly, one can apply a thicker layer. This results in a larger section modulus and therefore reducing the maximum occurring stresses. Another possibility is choosing a finer PBA mixture which can withstand higher stresses.

In this chapter also the influence of the type of bonding between the PBA and block revetment was studied. Two situations were considered: a frictionless bonding (full slip) and a rigid bonding (full friction). The results indicate that due to the slip interaction, the bending stresses will increase in the outer fibres of the PBA. Therefore a full bonding is desired. If such a rigid connection is desired, some surface preparations have to be done. The concrete elements have to be cleaned otherwise the PBA cannot strong a form bond with the blocks. Plant remains, sludge or sand have to be removed. Cleaning can be done by using for instance an high pressure washer. However, it is possible that after cleaning procedures the surface of some parts is still not clean enough. In this case one have to be aware for higher bending stresses. Another friction criteria, is the friction between the individual concrete blocks. This is in any case of importance when applying no refurbishment layer since it greatly influence the structural's flexural strength. The findings suggest that this is of minor influence when applying a PBA refurbishment layer on top of the original block revetment. In this case the blocks are "glued" to the PBA layer and it already acts as on single structure. However, if the PBA and block revetment are frictionless connected, the situation changes. More friction induces a stiffer structure and therefore lowering the bending stresses in the outer fibres of the PBA layer.

The stiffness of the subsoil determines the support reaction of the PBA revetment under the hydraulic loads. Subsoil with a high stiffness seems favourable. The stiffer the subsoil, the larger the part of the load which is directly transferred to the subsoil resulting in lower bending stresses in the PBA layer. However, the results indicate that if the order of stiffness magnitude is correct, the bending stresses are more of less the same.

Structural systems transfer their loading through a support to the subsoil. The actual behaviour of a support can be quite complicated therefore assumptions were made. In order to perform calculations these boundary conditions have to be translated into general support conditions/assumptions. In the previous chapters it was assumed that both ends of the dike revetment could be represented as pinned supports. They allow

the structure a small rotation but not to translate in any direction. The results suggest that this assumption is a safe estimation.

Also the current mechanical model, which is used by ARCADIS for preliminary designs, was studied. When applying this model, one assumes that only the PBA layer contributes to the bending capacity. Thus the block revetment only contributes to its dead weight and does not contribute to the structure's flexural capacity. The results suggest that this is a conservative approach. The design stresses with this model were six times bigger than the stresses obtained with the FEM analysis. If this approach is extended with the bending beam schematization of the block revetment -and therefore contributing to the structure's flexural strength- the stresses better "follow" the stresses of the FEM model but now underestimates the stresses with respect to the FEM results.

8

PBA AND ASPHALT

In this chapter two conventional asphalt refurbishment techniques (OSA and hydraulic asphalt concrete) are compared with the new technique (PBA). The pros and cons for the different mixtures are discussed. In chapter 3 the most important PBA properties were already elaborated. These properties are compared with those of the 2 asphalt types. Asphalt products have been used in the Netherlands in hydraulic engineering for a long time on a large scale ([van de Velde, 1984](#)). It could be placed much faster than the materials most commonly used in those days. The two most-used types of asphalt mixtures in the hydraulic engineering field are asphalt concrete and Open Stone Asphalt. Other terms which are typically used for asphalt concrete are: asphaltic concrete, bituminous asphalt concrete or hydraulic asphalt concrete (waterbouwasfaltbeton in Dutch). This chapter is divided into three main parts based on the permeabilities of the applied refurbishment material. The first part contains the study of the impermeable hydraulic asphalt concrete, the second part will elaborate on the permeable OSA and PBA. This chapter ends with a part about structural modelling. It will be shown that it is necessary to adjust the previous applied Wolsink load model in order to make a good comparison between the refurbishment techniques. Similarly as in the previous chapters, the maximum bending stresses of the different refurbishment materials will be calculated for certain hydraulic boundary conditions. For this chapter the "State of the Art Asphalt Dike Revetments" report ([Davidse et al., 2010](#)) has been used which describes the latest developments regarding asphalt in hydraulic engineering.

8.1. HYDRAULIC ASPHALT CONCRETE

8.1.1. MECHANICAL PROPERTIES

The components of asphalt concrete include mineral aggregate bound together by asphalt (bitumen). The bitumen content greatly influences the structural behaviour of asphalt and therefore the asphalt mixtures have the same mechanical properties as bitumen. An important property is the viscoelastic behaviour. This implies that under short duration and at low temperatures it acts as an elastic material while under long duration loads and higher temperatures it appears to be viscous ([van de Velde, 1984](#)). For dike revetments this property is an advantage. It yields under long duration loads so it is possible to follow during settlements. On the other hand, it is stiff under short duration loads like wave impacts. Bitumen, and therefore asphalt mixtures, is sensitive to fatigue. Fatigue is a mechanism whereby cracks grow in the material under fluctuating stresses. The value of the strain at break reduces the more the material is loaded. These important properties have to be taken into account when designing such a revetment. This visco-elasticity behaviour also results in a stiffness modulus which is strongly dependent on temperature and loading duration. Based on laboratory tests and taken into account the aspects mentioned earlier, a stiffness value of 4260 MPa can be used ([Davidse et al., 2010](#)). The strength at failure and the stiffness are correlated. According [Davidse et al. \(2010\)](#) one can design with an ultimate strength of 2.4 MPa which has a 5% exceedance probability during its desired lifetime of 50 years. This holds for a voids content of maximum 6% in the asphalt mixture. These strength properties are applicable for 5 °C and for short duration loads. The mass density of hydraulic asphalt concrete is approximately equal to 2300 kg/m³ ([TAW, 2002](#)).

8.1.2. PERMEABILITY

The voids ratio of a mix and the size and orientation of the voids determine the degree of permeability of the mix as a whole. In figure 8.1 the volume percentages of the mixture are shown. A pitched stone revetment is

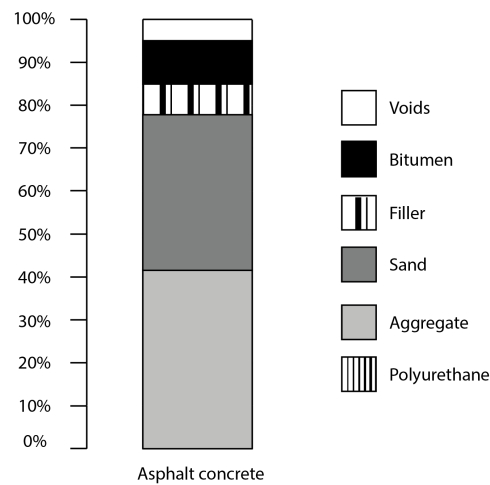


Figure 8.1: Volume percentages of the components in hydraulic asphalt concrete

originally a permeable structure. However, when applying this asphalt mixture as refurbishment material one has to consider the whole structure and not only the original revetment. Asphaltic concrete is impermeable, therefore also the block revetment refurbished by asphaltic concrete will become impermeable.

8.1.3. WAVE IMPACT

In general, an asphalt dike revetment have to be designed on wateroverpressures and wave impacts. After construction hydraulic asphalt concrete is a stiff plate which can withstand high wave impacts. In case of a very stiff foundation, for instance the existing block revetment, the required layer thickness is even no longer determined by wave height (Bijlsma, 2013). Especially when applying porous material like OSA or PBA. Due to the open space the wave energy is (partly) absorbed, resulting in a smaller wave impact. However, it is still interesting to research this hypothesis. In section 8.4 the stresses are calculated for the impermeable asphalt concrete when designing for wave impact.

8.2. OSA AND PBA

In this section the permeable materials, i.e. Open Stone Asphalt (OSA) and polyurethane bonded aggregate (PBA) will be elaborated. Similarly as in the previous section, the mechanical properties and the permeabilities are discussed.

8.2.1. MECHANICAL PROPERTIES

Since OSA contains also bitumen, it is also susceptible to fatigue and shows viscoelastic behaviour. Based on laboratory tests and experiments, a stiffness value of 5700 MPa can be used (Davidse et al., 2010). Furthermore, one can design with an ultimate strength of 3.6 MPa which has a 5% exceedance probability during its desired lifetime of 30 years.

For PBA other properties holds. Based on experiments, it can be assumed that PBA is not susceptible to aging or fatigue during the lifetime of the revetment (Bijlsma, 2013). In other words, the initial design strength is assumed to be irrespective of loading history. In figure 5.2 of chapter 5 the strength values were shown for different PBA mixtures. One can design with a Young's modulus of 3000 MPa. The mass densities for PBA and OSA are respectively 1400 kg/m³ and 1900 kg/m³ (TAW, 2002).

8.2.2. PERMEABILITY

In contrast to asphaltic concrete, PBA and OSA are permeable structures. Especially PBA, which has an open space of approximately 50 %. Therefore, when applying PBA and OSA as refurbishment material, the original block revetment will stay permeable which is a big advantage with respect to hydraulic asphalt concrete.

However, when the open pores of the cover layer are clogged with fine material, the hydraulic conductivity is affected negatively. This could especially be a problem for OSA since it has a twice as low open space volume as PBA. Besides clogging, also leaking of excess polyurethane or bitumen can affect the permeability of the concrete blocks and therefore the composite revetment. In the following calculations these two phenomena will be neglected. It is assumed that the block/PBA or OSA revetment will stay permeable and will have a hydraulic conductivity equal to the original block revetment. In figure 8.2 the volume percentages of OSA and PBA are shown.

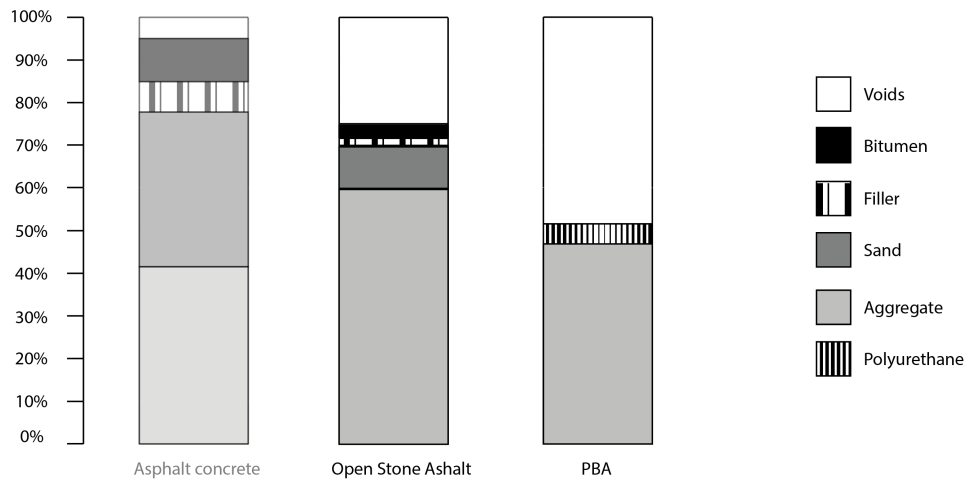


Figure 8.2: Volume percentages of PBA and OSA

8.3. STRUCTURAL MODELLING

The next step is to apply the properties mentioned in the previous sections into the structural models of this thesis. To study the structural behaviour of asphalt cover layers, the same FEM model is used only the material properties are changed. The calculations are performed with a rigid connection between the refurbishment layer and the block revetment, since it is proved that this is most effective in withstanding the hydraulic loads (chapter 7). Furthermore the block revetment is schematized as a bending beam, in chapter 7 it was shown that this assumption was a good approximation with respect to the FEM calculations performed with individual concrete elements. To emphasize the differences between the permeable and the impermeable cover layers, a more extreme situation regarding the hydraulic loads is considered with respect to the Waddenzee dike. The data shown in table 8.1 is used as input. The calculations are performed to research what the most

Hydraulic Boundary Conditions	
significant wave height	1.75 m
wave peak period	6.67 s
still water level	NAP +2.5 m
water density	1025 kg/m ³
revetment length	7.5 m
block thickness	0.2 m
filter thickness	0.2 m
refurbishment thickness	0.1 m
Hydraulic asphalt concrete density	2300 kg/m ³
PBA density	1400 kg/m ³
OSA density	1900 kg/m ³
concrete density	2400 kg/m ³
dike slope	1:3

Table 8.1: Governing data for the modelling calculations

effective approach will be. On the one hand, an impermeable cover layer constructed by asphalt concrete

resulting in higher water overpressures but increasing the revetment's dead weight, or on the other hand, applying a permeable refurbishment layer by PBA or OSA which is less heavier but results in lower (water) overpressures.

8.3.1. LOAD MODEL

In the previous chapters, there has been made a distinction between the static load model and the Wolsink load model. In general, there were two major differences:

1. the static load model assumes an impermeable revetment; the Wolsink model assumes a permeable revetment
2. the static load model assumes a vertical wave front; the Wolsink model assumes a linear wave front

Therefore, if the revetment becomes impermeable by applying hydraulic asphalt concrete, the static load model will be used. Obviously, when using OSA or PBA as refurbishment material, the Wolsink load model will be elaborated. However, when one wants to compare the results after modelling, the assumptions on beforehand have to be similar. Therefore it would be impossible to make a good comparison if in one model a linear wave front is assumed, while in the other model a vertical wave front has been used. The same assumptions have to be applied throughout the analysis. To solve this problem, a vertical wave front will be assumed for both models. This implies that the static model, described in chapter 4, does not have to be changed. On the other hand, the Wolsink load model have to be adjusted. In figure 8.3 an overview of the situation is shown.

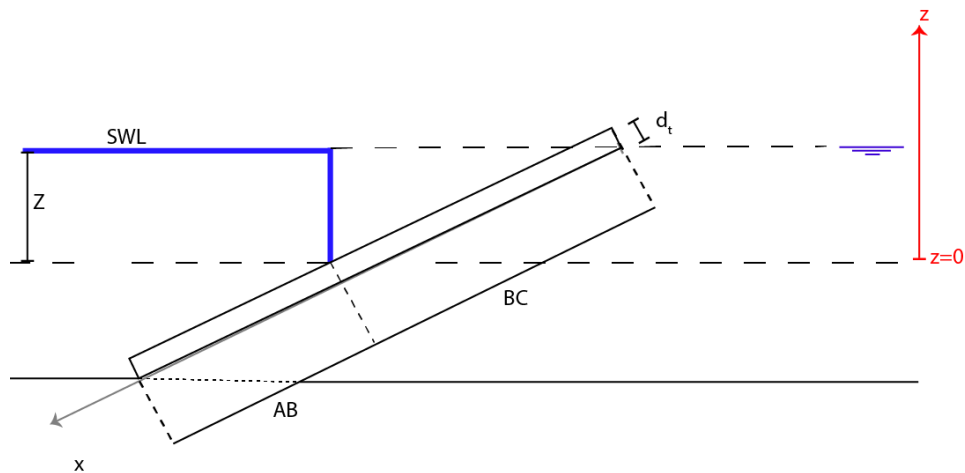


Figure 8.3: Overview of the situation: vertical wave front

In $x = BC + AB$ the hydraulic heads in the filter layer and at the top layer are the same with respect to the reference level $z = 0$. From this point the water particles will try to "follow" the piezometric level at the top layer. An impression of this adjustment, is shown in figure 8.4.

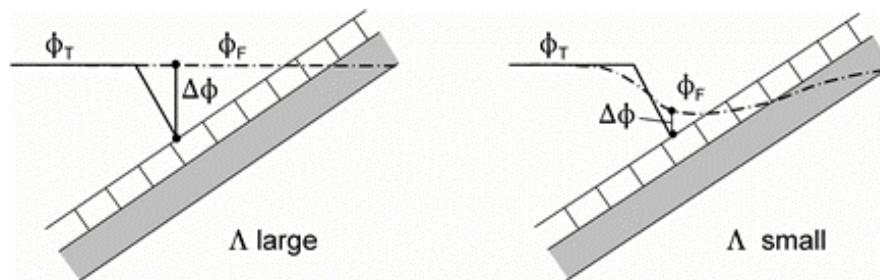


Figure 8.4: Influence of the leakage length: head difference over the block revetment for a large (impermeable) and small (permeable) leakage length (Schierck, 2012)

To calculate the hydraulic head in the filter layer, the Wolsink equation have to be solved. One can distinguish two solution domains (AB and BC), this implies that two boundary conditions and two matching conditions are sufficient to solve the 4 unknown integration constants since it is a second order differential equation. The Wolsink differential equation is defined as follows:

$$\Phi_f - \Phi_t = \Lambda^2 \frac{d^2 \Phi_f}{dx^2} \quad (8.1)$$

By considering the piezometric level at the top layer and the two boundary conditions, the differential equation can subsequently be solved for the two domains. The 4 boundary and matching conditions are:

1. $\Phi_{AB}^f = Z$ for $x = 0$
2. $\Phi_{f1} = \Phi_{f2}$ for $x = BC$
3. $\frac{d\Phi_{f1}}{dx} = \frac{d\Phi_{f2}}{dx}$ for $x = BC$
4. $\Phi_{AB}^f = Z$ for $x = BC + AB$

The hydraulic head at the top layer is known, therefore all the ingredients are available to solve this differential equation. The piezometric level for the 2 domains at the top layer are:

1. $\Phi_{BC}^t = Z - \sin \alpha x$ for $0 < x < BC$
2. $\Phi_{AB}^t = Z$ for $BC < x < BC + AB$

The solution for the hydraulic boundary conditions of table 8.1 can be found in section 8.3.3. The calculation approach of the static load model (impermeable top layer) is elaborated in chapter 4. The results of the static load model corresponding to the new hydraulic boundary conditions of table 8.1 are elaborated in section 8.3.2.

8.3.2. HYDRAULIC ASPHALT CONCRETE

Like stated in section 8.1.2, the block revetment will become impermeable when applying a cover layer of this asphalt mixture. Therefore the static load model, which assumes no flow of water between the top and bottom of the revetment, is used as an input for the structural calculations. More information and explanation about this model can be found in chapter 4. Due to the impermeability, the pressure difference can immediately be calculated by considering the hydraulic heads within the filter and the water level outside. The results are illustrated in figure 8.5.

If subsequently these graphs are subtracted from each other, the resultant head difference over the revetment is obtained. In figure 8.6 this final head difference is shown. Subsequently these hydraulic heads have to be changed into pressures by multiplying it with the specific weight of water. The resisting force is induced by the dead weight of the revetment perpendicular to the slope. The gravity force will reduce the upward pressure and increasing the stability. If a refurbishment of PBA will be applied on top of the block layer, the dead weight will increase. For part BC holds:

$$q_G = \rho_c g d_t \cos \alpha + \rho_{pba} g d_{pba} \cos \alpha \quad (8.2)$$

For part AB this equation does not hold because the revetment is situated below water level. For this part the dead weight is equal to:

$$q_G = (\rho_c - \rho_w) g d_t \cos \alpha + (\rho_{pba} - \rho_w) g d_{pba} \cos \alpha \quad (8.3)$$

Obviously, the same equations hold for a refurbishment layer of asphalt. In this case only the density of the asphalt mixture have to be applied instead the PBA density. Applying these equations result in the final load situation shown in figure 8.7. Since the input is now available, the load model is implemented in the Abaqus model. The results are shown in figure 8.8.

The maximum bending stress is equal to approximately 0.5 MPa. Since the design strength is equal to 2.4 MPa, this stress can be restrained by the asphalt cover layer of 10 cm. However, the purpose of this study is to check whether it is more effective to use an impermeable and heavy material or a permeable but lighter material. In the next section the permeable materials will be elaborated.

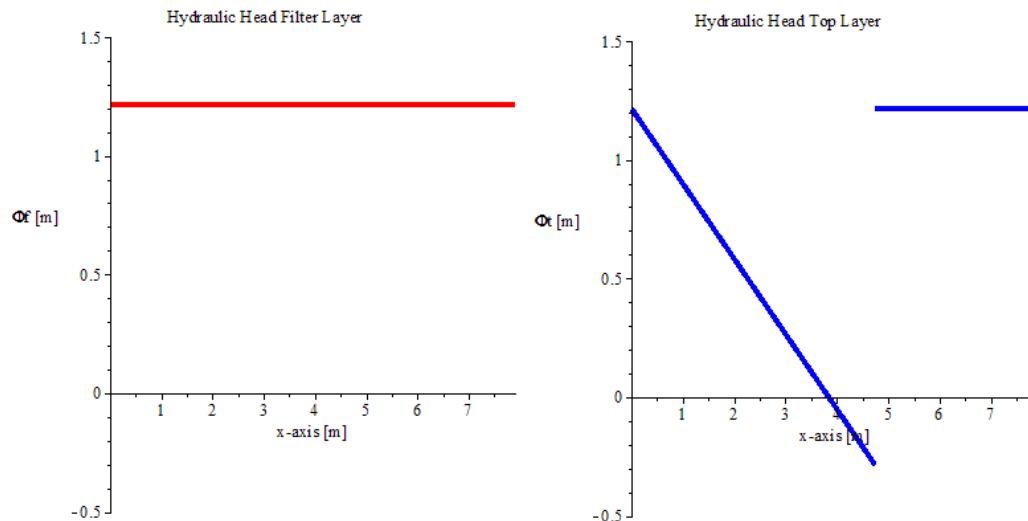


Figure 8.5: Hydraulic heads: blue = hydraulic head top layer, red = hydraulic head in the filter. For both figures an impermeable top layer is assumed

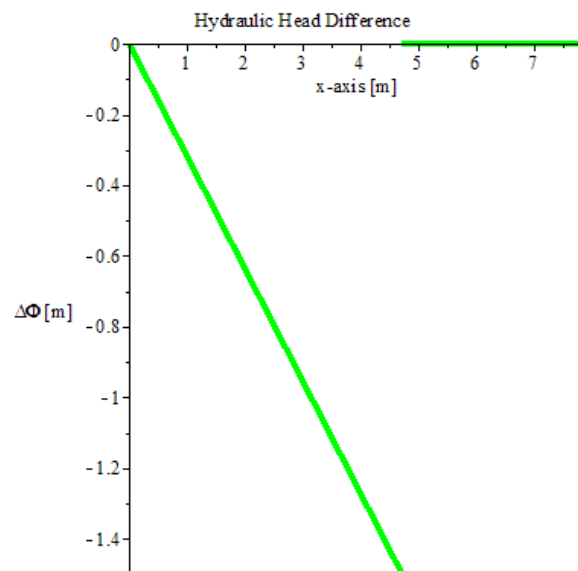


Figure 8.6: Hydraulic head difference over the revetment when applying an impermeable revetment

8.3.3. PBA AND OSA

When applying the hydraulic boundary conditions of table 8.1 the hydraulic heads in the filter can be found by solving Wolsink's equation. The leakage length is an important input variable for this equation. In reality, the revetment could become less permeable or even completely impermeable due to clogging or leakage of the refurbished material in the gaps between the blocks, therefore, also other values of the leakage length have to be studied than the original one. Especially when applying OSA since it has a much less open space percentage than PBA and therefore more sensitive for clogging. If clogging occurs, there is no flow of water from inside to outside. This implies that the revetment becomes impermeable, resulting in larger leakage lengths. In figure 8.9 the hydraulic heads are shown for four different situations:

- $\Lambda = 1.5$ m → leakage length does not change from the original situation
- $\Lambda = 2.0$ m → the initial permeability of the top layer is approximately reduced with a factor 2
- $\Lambda = 4.0$ m → the initial permeability of the top layer is approximately reduced with a factor 5

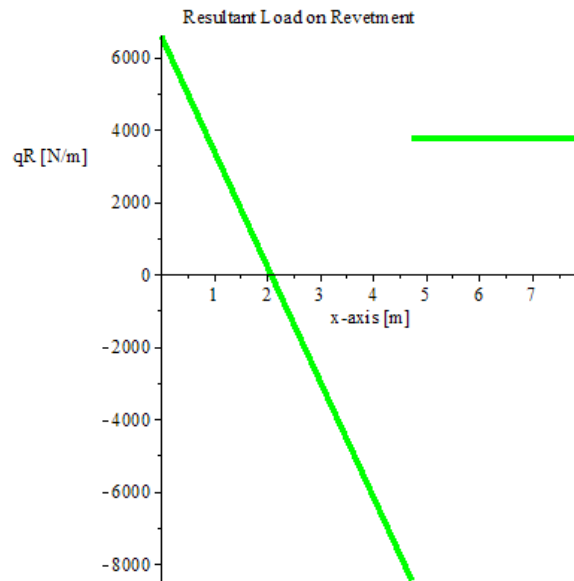


Figure 8.7: The resultant load situation on the revetment when applying hydraulic asphalt concrete

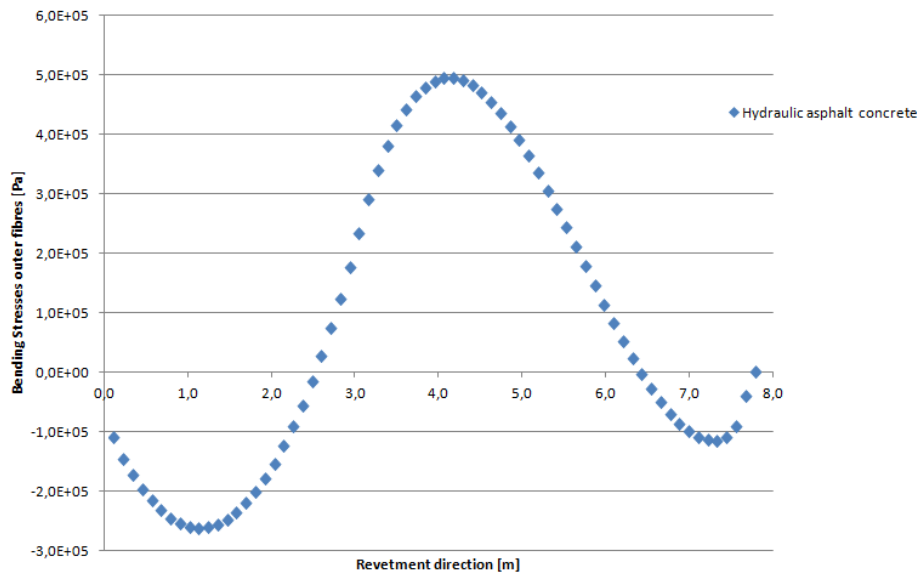


Figure 8.8: Bending stresses in the outer fibres of the asphalt concrete cover layer (10cm)

- $\Lambda = \infty \rightarrow$ the revetment becomes impermeable

In figure 8.9 it can be seen that the static load model is obtained (figure 8.5) if a infinitely large leakage length is applied. An infinity large leakage length corresponds to an impermeable top layer and therefore the outcomes of the Wolsink equation correspond to the results of the static load model. The hydraulic heads at the top layer are the same as for both the Wolsink model and the static load model. These levels are not dependent of the leakage length and are therefore correspond to the right graph of figure 8.5.

Subsequently, if the hydraulic heads in the filter and at top layer are subtracted from each other, the hydraulic head difference is obtained. This is shown in figure 8.10 for the different leakage lengths. Similarly, when $\Lambda \rightarrow \infty$, the hydraulic head difference for both the static load model and Wolsink model are the same.

Like in the previous section, these hydraulic heads have to be changed in pressures by multiplying the values with the specific weight of water. Furthermore the dead weight of the revetment has to be taken into account. The final load distribution over the revetment for both PBA and OSA are shown in figure 8.11. It can be concluded that the (resultant) upward distributed load is higher for PBA. The bigger the dead weight of the

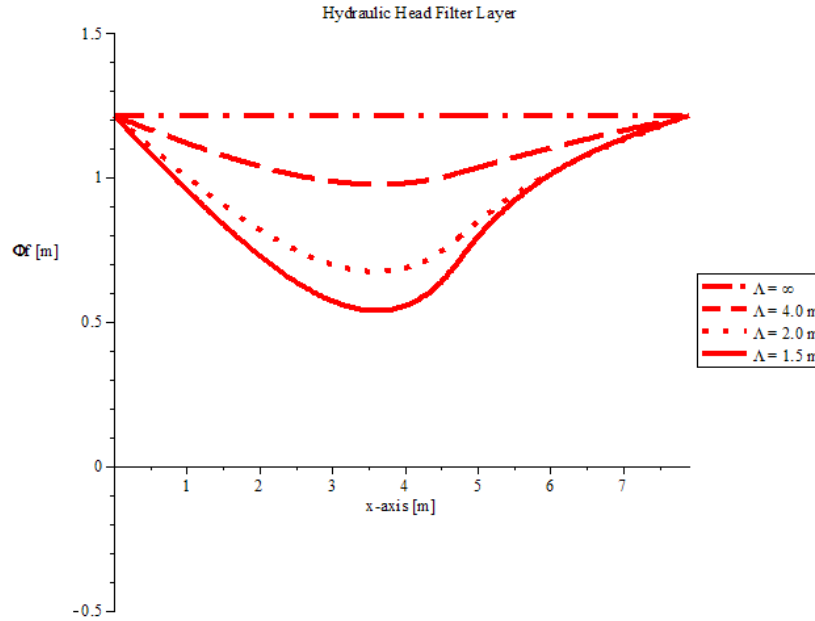


Figure 8.9: Hydraulic heads in the filter layer for different leakage lengths

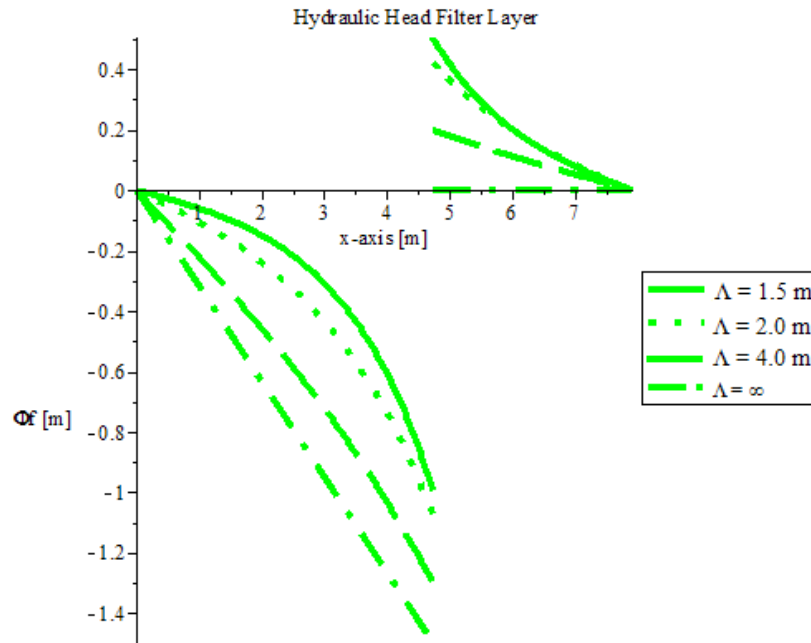


Figure 8.10: Hydraulic head difference over the revetment when applying different values for the leakage length

structure, the better the upward pressures will be reduced. The upward (water) pressures are better reduced when applying OSA due to its bigger dead weight density.

The next step is to implement these resultant loads in Abaqus. Firstly, the stresses in the PBA layer are studied when using a leakage length of the initial 1.5 m, 4 m and infinitely large. Like shown in figure 8.12 the stresses are low in the area of interest (uplift region) when using $\Lambda = 1.5$ m, in the order of 20 kPa, which can easily be restrained by the different PBA mixtures of figure 5.2 in chapter 5. However, when applying larger leakage lengths the bending stresses increase significantly. A leakage length of 4 m, which corresponds to a permeability reduction factor of approximately 5, results in 10 times bigger stress (0.2 MPa versus 0.02 MPa). Moreover, if the revetment becomes impermeable ($\Lambda \rightarrow \infty$), the bending stresses cannot even be withstood any more by the 30/60 or 20/40 mm mixture class.

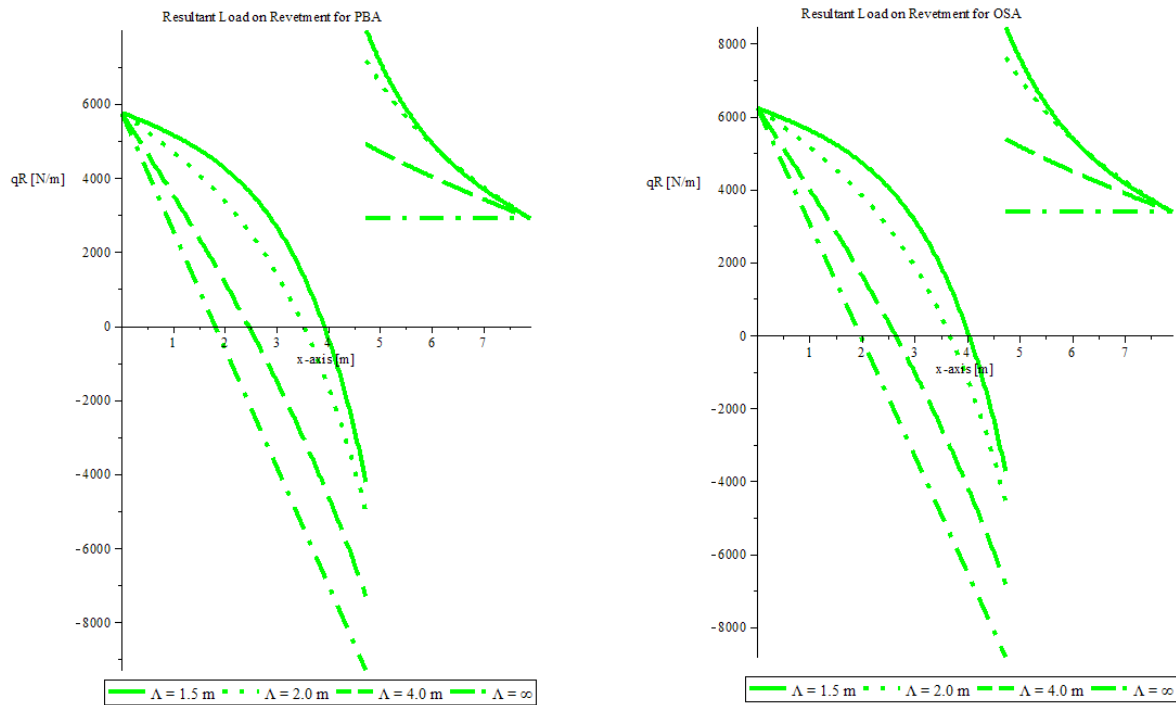


Figure 8.11: The resultant load situation on the revetment when applying PBA (left) and OSA (right)

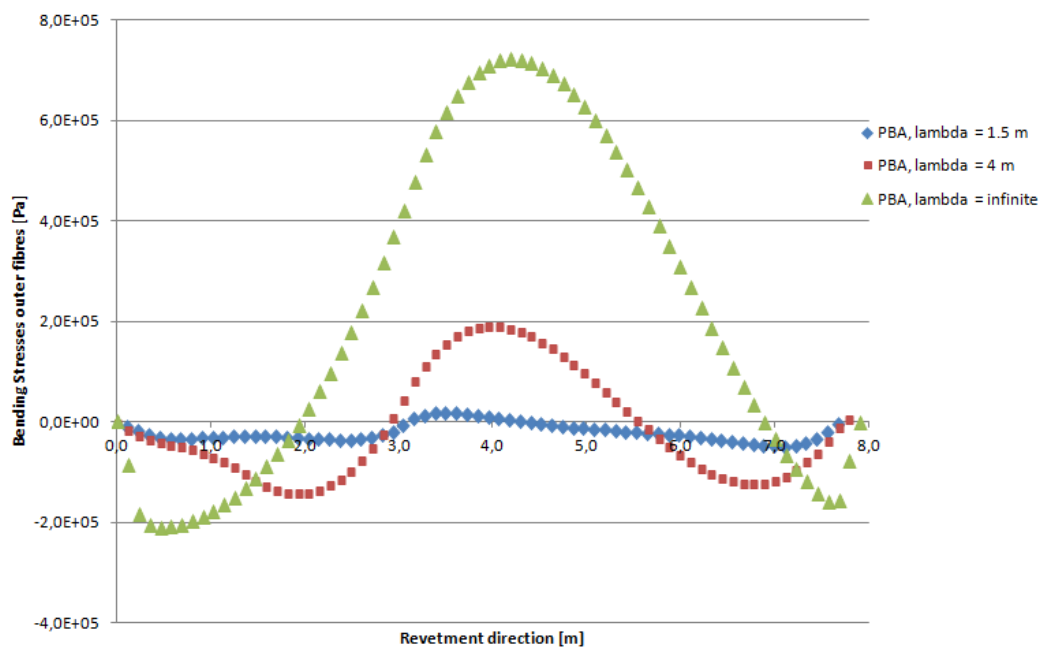


Figure 8.12: The bending stresses in the outer fibres in the PBA cover layer

Subsequently the bending stresses are researched when applying OSA as refurbishment material. The results are depicted in figure 8.13. The stresses are in the same order as the stresses which occur in the PBA cover layer for the leakage length values. On the one hand, PBA is less stiff than OSA (respectively 3000 MPa versus 5700 MPa) and therefore "attract" less load, on the other hand, PBA is less heavier which results in a higher upward loading. However, as can be seen in the figures, the stresses in the uplift region are overall more or less the same.

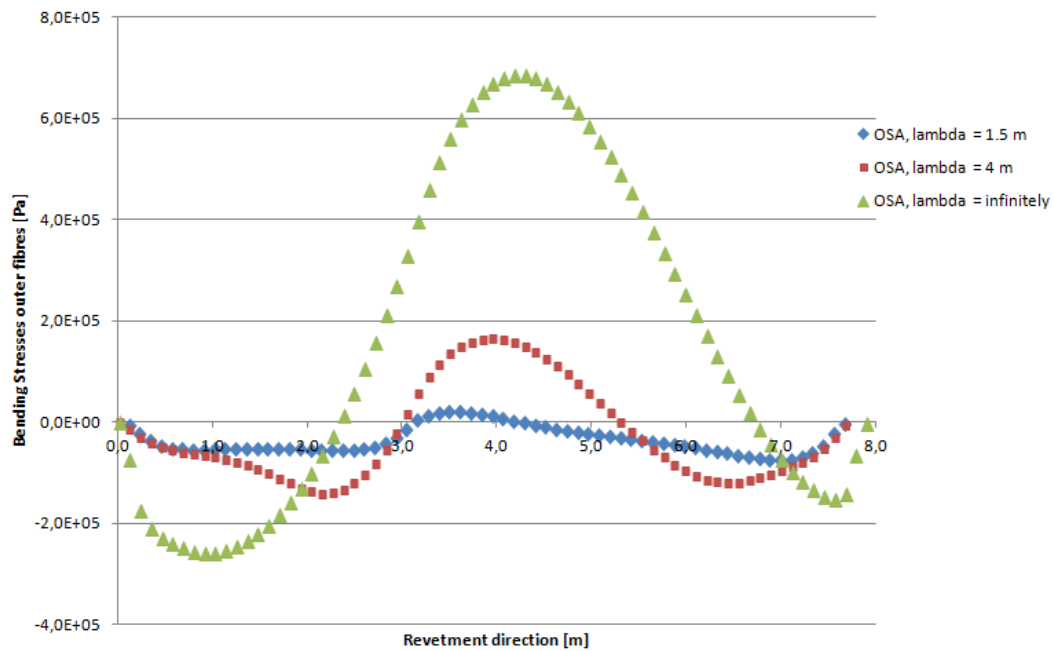


Figure 8.13: The bending stresses in the outer fibres in the OSA cover layer

Some important conclusions can be drawn from the previous calculations. In general, the calculations were performed to study what the most effective approach would be. On the one hand, an impermeable cover layer constructed by asphalt concrete resulting in higher water overpressures but increasing its dead weight, or on the other hand, applying a permeable refurbishment layer by PBA or OSA which is less heavier but results in lower (water) overpressures. This study suggest that the latter is the most effective, i.e. applying a (less) heavier refurbishment layer but with a certain permeability results in lower bending stresses. However, it must be realized that this statement is based on the assumption that the revetment stays permeable when applying OSA or PBA. The maximum occurring bending stresses are very sensitive to a fluctuation in the leakage length. The revetment could become less permeable or even completely impermeable due to clogging or leakage of the refurbished material in the gaps between the blocks. Especially when applying OSA since it has a much less open space percentage than PBA and therefore more sensitive for clogging. Besides clogging due to sand and dirt, dripping of excess unhardened PU or bitumen from the cover layer in the gaps between the concrete blocks is also possible and unwanted. The permeability, and therefore leakage length, can be reduced locally resulting in a significant increase of the bending stress when clogged with PU or bitumen. It must be noted that leakage of the polyurethane into the gaps of the block revetment is not likely since the granular aggregate is mixed together with only 2-3 vol. % of PU (Bijlsma, 2013). This results in a very thin film for each individual rock. When the adhesive is cured, this film fixes the rocks together only on their contact point. Because of the small amount of PU, leakage on a large scale is not very likely. Since the volume percentage of bitumen is larger (approximately 6%), the risk of leakage of excess bitumen in the gaps is higher which results in a higher probability for (local) clogging. If the PBA and/or OSA becomes completely impermeable, the refurbishment technique with hydraulic asphalt becomes more effective. Obviously, an heavier material will reduce the upward pressures better. This was also shown in the different graphs. The maximum bending stress for asphalt concrete was approximately 0.5 MPa, while the maximum stress for PBA and OSA was approximately 0.75 MPa (when $\Lambda \rightarrow \infty$).

8.4. WAVE IMPACT

Due to the high open space percentage of PBA and OSA, the wave energy will be (partly) dissipated. The porosity of such revetments allows the wave impact pressure to partly dissipate within the revetment, and partly to be transferred to the subsoil (see chapter 3.4.1). However, asphalt concrete does have a neglectable open space percentage and is therefore not able to efficiently absorb wave energy resulting in an high wave impact. Until this section, it is assumed that the governing load mechanism happens during run down of the wave. The ground water level within the dike core is larger than the water level outside, which causes water overpressures. Also in several literature (e.g. (Bijlsma, 2013) and (Schierreck, 2012)) it is stated that this load situation is governing. However, it is still interesting to prove this hypothesis. Therefore the wave impact is also elaborated when applying hydraulic engineering asphalt. To study this impact the same approach of Golfklap (Rijkswaterstaat, 2009) is applied. This model is currently used for determining the required asphalt thickness regarding wave impact. The wave impact load is schematized as a triangular distributed load with a maximum of p_{max} and a base width equal to H_s . The maximum wave load occurs in the middle of the wave load and can be estimated with the following equation (Rijkswaterstaat, 2009).

$$p_{max} = \rho_w g q_\alpha H_s \quad (8.4)$$

Wherein:

q_α = wave impact parameter [-]

The wave impact parameter is dependent on the dike slope. It can be estimated by considering the measured impact parameter for a 1:4 slope and applying formula 8.5:

$$q_\alpha = \frac{\tan \alpha}{0.25} q_{tan(0.25)} \quad (8.5)$$

By applying the hydraulic boundary conditions of table 8.1, the bending stresses in the bottom fibres of the asphalt concrete layer can be found. The triangular load is implemented in both FEM models, i.e. when schematizing the block revetment as a Euler Bernoulli bending beam and when considering the concrete blocks as loose elements. The results are shown in figure 8.14. From this graph it can be concluded that the

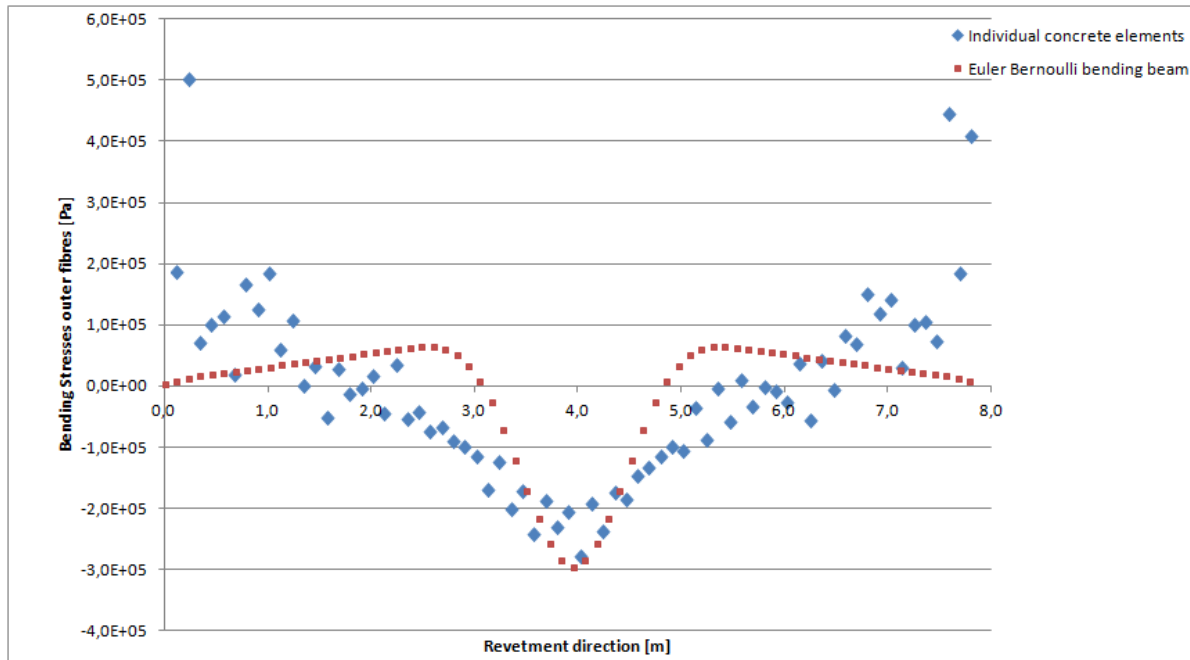


Figure 8.14: The bending stresses in the bottom fibres of the asphalt concrete refurbishment layer when modelling the block revetment as an Euler Bernoulli bending beam (red) and as loose concrete elements (blue)

maximum bending stress is in the order of 0.30 MPa. Comparing this value with the maximum bending stress for the other load situation (0.50 MPa), in case of water overpressures, one can conclude that the wave impact

is not the governing situation. This can be explained by considering the thickness of the structure. When the revetment is lifted up due to the water (over)pressures, only the concrete elements and the refurbishment layer are restraining the loads. On the contrary, in case of wave impact, the concrete elements, refurbishment layer and the stiff subsoil are contributing to the stiffness of the structure. Moreover, also in this case the bending beam schematisation "follows" the curve of the individual concrete elements in FEM pretty good, especially in the region where the biggest stresses occur. However, at the supports of the structure the stresses differ.

8.5. DURABILITY

Besides the strength criteria, also the durability is of great importance. The revetment must, with the course of time, continue to fulfil its function. Construction materials are subject to the impact of weathering when used outdoor (Bijlsma, 2013). Weathering is the response of a material to e.g. climate, ultraviolet radiation, salt water and frost. The characteristic mechanical properties should not deteriorate too much within a reasonable time. The expected lifetime of hydraulic asphalt concrete varies between 50-75 years (TAW, 2002) applied at both river and sea dikes. The expected lifetime of OSA is in practice much lower than hydraulic asphalt concrete. It must be noted that asphalt is 100 % recyclable which has to be taken into account. On the other hand, the expected lifetime of PBA is very high. In table 8.2 the expected lifetime of asphalt concrete, OSA (TAW, 2002) and PBA (Bijlsma, 2013) are shown. The expected lifetime of PBA is based on experiments with UV-light and salt water.

	Asphalt concrete	OSA	PBA
sea dike	50-75	15-30	80-100
river dike	50-75	25-50	80-100

Table 8.2: Expected lifetime of hydraulic asphalt concrete, OSA and PBA in years

Besides the durability also other properties are decisive for selecting the right material. One of them is the wave run-up and wave run-down. Wave run-up is the maximum extent of wave uprush on structure above the still water level, defines as a vertical distance. The porosity of the revetment and the roughness greatly influences the extent of wave run-up. Therefore, the wave run-up is in general higher for impermeable materials than when applying permeable materials. Especially PBA reduces the wave run-up significantly. For highly permeable structures with a rough surface, like PBA, most of the energy is dissipated at the structure face and within the revetment (Bijlsma, 2013). This results in different wave run-up behaviour on PBA than with other, less permeable, revetments hence Bijlsma (2013). The wave run-up can be reduced with 25% and up to 50% with a PBA revetment in comparison to an impermeable slope.

8.6. COSTS

Although a cost-benefit analysis is a completely different study, some general statements about the costs for the different refurbishment techniques are discussed in this section. Obviously, the costs of the possible materials play a very important role in the final selection. The main goal is often to minimize costs while meeting the performance goals. During construction, the majority of the costs will start to occur: cost of materials, man-hours, equipment and construction time. During the service life of the project, cost of maintenance and repair will be added. Important is expected lifetime of a material. In this section the most important aspects regarding the costs for PBA and asphalt refurbishments are briefly discussed. These aspects are the amount of required materials, maintenance costs, recycling, durability and impact on the environment.

In general, one has to use less material when applying PBA in contrast to asphalt refurbishments. Sometimes, like in the previous calculations, the minimum required layer thickness (10 cm) is already sufficient to withstand the hydraulic loads for both options (PBA and asphalt). It is not feasible to achieve layers thinner than 10 cm due to the used equipment. Such a layer thickness is already obtained to ensure complete coverage of the application area. Overall can be concluded that the costs for a square meter PBA is approximately equal to a square meter OSA or asphalt concrete. The components of PBA are a bit more expensive but, on the other hand, one can reduce the amount of material needed. When applying asphalt, it is the other way around. One can reduce the costs when buying the required asphalt components but a thicker layer is often needed.

Another important aspect are the maintenance costs. The PBA revetment is relatively easy to repair when damaged (Bijlsma, 2013). By hand or with light equipment small amounts of PBA can be produced on-site to fill any holes that have been formed. This is a big advantage in contrast to asphalt which is more difficult to repair, especially regarding the required equipment.

Also durability plays an important role. In section 8.5 the different lifetimes were discussed. Although PBA is only 5 years available on the market, its lifetime is estimated to be in the order of 80-100 years. This expectation is based on UV and salt water experiments. Time will tell whether this estimation is correct. The stated lifetimes of asphalt can be assumed to be correct. Asphalt products have been used in the Netherlands in hydraulic engineering for a long time on a large scale. The experience is that the lifetime of asphalt revetments is in the order of 25-50 years and therefore lower than the expected lifetime of PBA.

Although asphalt has a lower lifetime, its ingredients can be fully recycled. The same material can be recycled again and again, it never loses its value. Using recycled asphalt reduces disposal costs and conserves aggregate. It reduces the need of raw materials and reduces the costs of waste transport and disposal. An advantage of PBA is that one can use recycled material to construct PBA. Basically any type of coarse graded aggregate can be used, which creates opportunities to make use of recycled material. Relatively large stone sizes can be used to form PBA mixtures, which are unsuitable for use in conventional revetments like asphalt. However, it can not be fully recycled as asphalt. At the end of its lifetime the PBA have to be handled as non hazardous waste (Bijlsma, 2013).

The last category which is discussed, is the impact on the environment. PBA revetments can provide ecological benefits by acting as novel habitat for biological colonisation (Bijlsma, 2013). Research has shown that PBA seems to be a material which allows ecological recovery to be fast and according to the typical vegetation of that area. Experience in practice show that vegetation has returned within 4 months after construction. Compared to asphalt, PBA revetments has a low impact on the environment (Bijlsma, 2013). Asphalt has a very high impact with respect to energy consumption because of the high consumption of fuels and energy for bitumen production, processing and energy content of bitumen itself. In contrast to bitumen, PU does not have to be heated at all during transport and application (Bijlsma, 2013).

In figure 8.15 the 5 costs aspects are shown. However, a cost-benefit analysis is not in the scope of this research. Further research is required to get more insight into the total costs and benefits for both materials.

	required materials	maintenance	recycling	durability	impact environment
PBA					
ASPHALT					

Figure 8.15: Important cost aspects which are (partly) decisive for selecting the material. A green box implies that this specific material scores better on this aspect than the other one.

8.7. CONCLUSIONS

Two conventional techniques (OSA and hydraulic asphalt concrete) are compared with the new technique (PBA). In general, it was researched what the most effective approach would be: applying an impermeable layer constructed by asphalt concrete resulting in higher water overpressures but increasing the structure's dead weight or, on the other hand, applying a permeable refurbishment layer by PBA or OSA which is less heavier but reducing water overpressures. The results suggest that the latter is the most effective approach. However, it must be noted that the occurring bending stresses are greatly influenced by the permeability of the PBA and OSA. An increase in leakage length results in a significant increase of the maximum appearing bending stress. If the revetment becomes completely impermeable, a refurbishment layer constructed by hydraulic asphalt concrete becomes more effective since its density is higher. Reduction of permeability could be caused by (locally) clogging due to sand or dirt. Especially when applying OSA one has to be aware for an increase of permeability since it has a much less open space percentage than PBA. Besides clogging by sand or dirt, the revetment could become less permeable by dripping of excess unhardened PU or bitumen from the cover layer in the gaps between the concrete blocks. Leakage of PU is not very likely since only a small percentage of PU is used when constructing PBA. Besides the properties of the specific refurbishment materials, also the properties of the block revetment is of importance. It seems only effective to apply PBA or OSA on a relatively permeable block revetment (e.g. Hydroblocks). If one wants to apply a refurbishment layer of PBA or OSA on a block revetment with a relatively large leakage length (e.g. Haringmanblocks), the structure will probably become practically impermeable since it is likely that the cover layer will affect its -already low-permeability (especially when applying OSA). In this case it would be more effective to use hydraulic asphalt concrete due to its bigger self weight.

Besides their permeability properties, also other aspects are important for selecting the desired type of cover material. The characteristic mechanical properties should not deteriorate too much within a reasonable time. The revetment must furthermore, with the course of time, continue to fulfil its function. Both revetments, asphaltic or PBA, are susceptible to the impact of weathering. In contrast to asphalt revetments, PBA provides some notable advantages. The expected lifetime of PBA (80-100 years) is higher than the expected lifetimes of asphalt concrete (50-75 years) or OSA (20-40 years). Another significant difference is the wave run-up reduction. The wave run-up can be reduced by 25% and up to 50% with a PBA revetment in comparison to asphalt revetments (Bijlsma, 2013).

9

CONCLUSIONS AND RECOMMENDATIONS

This research is related to the structural behaviour of a composite PBA/block revetment. A lot of research has been done regarding the behaviour of block revetments or PBA revetments applied individually. However, the behaviour of a block revetment refurbished by PBA has not been researched yet. A dike protected by pitched blocks will fail when the concrete blocks are lifted up out of the revetment and if the waves subsequently induce erosion of the dike body. It is therefore of great importance that the blocks will remain stable under the governing hydraulic loads. The blocks are susceptible for uplifting during wave run-down. The pressure on the blocks is low in front of the wave at maximum downrush, while under the blocks it is still high due to the phreatic level within the dike. This induces uplift forces on the blocks. The hypothesis is that adding a relatively thin layer of PBA effectively increases its stability. This chapter reports the conclusions and recommendations that resulted from this study. The results are furthermore reflected; a final comment and judgement is given on the main areas and topics covered in the writing. These comments also include suggestions for improvement and recommendations for future work. The conclusions will be formulated based on the research questions stated in chapter 1.

- 1. To what extent can the mechanical behaviour of the composite revetment be described in an analytical model and FEM model, and do the results of these models correspond?**

The three most significant findings regarding this question are that the analytical and FEM model show similarities given that the displacements are small (1A), the Euler Bernoulli bending beam showed good similarity with the results when modelling the composite PBA/block revetment with individual blocks (1B) and the current ARCADIS design method seems to be conservative (1C).

1A. To study the stress distribution in the composite revetment, it was modelled both analytically and numerically. In the analytical method, the interaction and stress distribution between the revetment and the subsoil were modelled as an elastically supported beam (Winkler model). The analysis of beams on elastic foundations is widespread in civil engineering. For the numerical calculations the finite element method (FEM) was used. Different FEM software packages are available, in this research the Abaqus package is used. The results of the analytical model and the results obtained with the finite element software were explained, compared and discussed. In general, it is assumed that the FEM model is a better schematization of the real revetment behaviour than the analytical Winkler model. The main reason is that the Winkler model assumes tension forces in the subsoil which do not occur in reality since soil cannot take tension stresses. Furthermore the subsoil, which consists of a filter and a sandy dike core, is modelled as individual layers in the FEM which is more realistic than representing these individual soil layers by one single spring stiffness in the Winkler approach. The finite element method enables the most accurate modelling of the real situation with respect to the loadings, the geometry of the revetment, the material characteristics and the interaction between the various layers of the structure. One can expect more detailed and more realistic data about stresses and displacement from finite element calculations than can be obtained by means of the analytical methods. This study shows that the Winkler foundation greatly influences the bending stresses in the uplift region although

these displacements are very small. On the other hand, it showed that when the upward displacements tend to zero or even become completely negative the proposed analytical model shows similarity with the FEM results. However, as a consequence, a relatively thick refurbishment layer has to be applied, which is not preferred. The advantage of Elastocoast is that it adds extra coherence and that a certain upward displacement is still allowed resulting in thinner layers, in contrast to conventional methods where only dead weight is added to improve its stability. Returning to the sub question posed at the beginning of this study, the results of this study indicate that the analytical model can only be applied when the upward displacement is less than or equal to zero. If a certain upward displacement is allowed, it is advised to use the finite element method.

1B. An important assumption for both analytical and FEM calculations, was the Euler-Bernoulli bending beam schematization for the composite PBA-block revetment in order to study the maximum bending stresses in the outer fibres of the PBA layer. This study provides evidence that modelling an individual block revetment as a bending beam is a rough representation. The moment capacity of a block revetment (thus without a PBA layer) is equal to the developed compression force times its eccentricity. However, when using this representation for a composite PBA-block revetment to study the bending stresses in the PBA layer, it showed good similarity with the results when modelling the block revetment as individual concrete elements. The two approaches differ approximately 5%. An important reason is the extra coherence and the monolithic behaviour induced by the PBA layer. The fictitious Young's modulus of the pitched stone revetment is obviously of great importance for this approach. A Young's modulus of 10 percent of the concrete mother material (approximately 3000 MPa (Peters, 2003)) appeared to be a good approximation. By coincidence, PBA has a Young's modulus of 3000 MPa too, which is very convenient. As a result, one can design with a homogeneous cross-section and it reduces the time needed for performing calculations significantly.

1C. The findings of this study were furthermore compared with the current design method of ARCADIS. In this design method it is assumed that only the PBA cover layer contributes to the flexural strength of the structure. The design stresses with the ARCADIS model were six times bigger than the stresses obtained with the FEM analysis. The results therefore indicate that this design approach is conservative and therefore resulting in thick PBA layers. If this approach is extended with the bending beam schematization of the block revetment -and therefore contributing to the structure's flexural strength- the stresses better "follow" the stresses of the FEM model but now underestimates the stresses with respect to the FEM results.

2. Which type of bonding (full slip or full friction) between the two layers is most effective to withstand the internal and external loads?

The results from this study show that a rigid connection between the two layers is most effective (2A). The friction between the concrete blocks is of minor influence if a rigid connection between the layers is present (2B).

2A. This study has shown that a full friction bonding is more effective to withstand the governing hydraulic loads. In Abaqus an extreme situation was modelled, i.e. a frictionless interaction between the PBA and concrete elements. Subsequently these results were compared with the outcomes when applying a rigid connection between the two layers. Based on the findings it can be concluded that due to the slip interaction, the bending stresses will increase in the outer fibres of the PBA layer. Therefore a full bonding between the PBA layer and the concrete elements is desired. The maximum bending stress in the uplift region (governing area) increases with approximately 33% in the frictionless case. If a rigid connection is preferred, some surface preparations have to be done before applying Elastocoast. One has to clean the concrete elements thoroughly otherwise the polyurethane cannot form a strong bond with the blocks. However, it is possible that after cleaning procedures the surface of some parts is still not clean enough which could influence the type of bonding and thus the structural behaviour. In this case one has to be aware for higher bending stresses.

2.B Friction between the individual concrete blocks is of great importance when applying no refurbishment layer since this greatly determines its flexural strength. The amount of friction is of minor influence when the PBA layer is fully (rigid) connected to the concrete blocks. In this case the blocks are "glued" to the PBA layer and it already acts as one single structure.

3. What are the main similarities and differences between a refurbishment constructed with asphalt and with PBA?

The findings suggest that it is more effective to apply a less heavy but permeable cover layer (PBA and OSA) than, on the other hand, an impermeable but more heavy cover layer (hydraulic asphalt concrete).

In this thesis the two conventional refurbishment techniques (OSA and hydraulic asphalt concrete) were compared with the new technique (PBA). The pros and cons for the different mixtures were discussed. The calculations were performed to study what the most effective approach would be. On the one hand, an impermeable cover layer constructed by asphalt concrete resulting in higher water overpressures but increasing its dead weight, or on the other hand, applying a permeable refurbishment layer by PBA or OSA which is less heavy but results in lower water overpressures. The findings suggest that the latter is the most effective, i.e. applying a less heavy refurbishment layer but with a certain permeability results in lower bending stresses. However, it must be noted that the bending stresses are greatly influenced by the permeability -and therefore leakage length- of the revetment. An increase in leakage length results in a significant increase of the maximum occurring bending stress. The revetment could become (locally) less permeable or even completely permeable due to clogging or leakage of the refurbished material in the gaps between the blocks. When the revetment becomes completely impermeable, the refurbishment technique with asphalt concrete becomes more effective since it is heavier and therefore more effective in reducing the upward water pressures. Furthermore it seems only effective to apply PBA or OSA on a relatively permeable block revetment (e.g. Hydroblocks). If one wants to apply a refurbishment layer of PBA or OSA on a block revetment with a relatively large leakage length (e.g. Haringmanblocks), the structure will probably become practically impermeable since it is likely that the cover layer will affect its -already low- permeability. In this case it would be more effective to use hydraulic asphalt concrete due to its bigger self weight.

9.1. RECOMMENDATIONS AND REFLECTION

In this thesis the bending stresses in the PBA layer have been studied. When the PBA layer deforms during uplifting, bending stresses will develop in the PBA layer. The biggest bending stresses will occur in the outer fibres of the PBA layer. Structural failure will eventually happen when the bending stresses induced by the hydraulic loads cannot be withstood by the PBA. Besides its flexural capacity also other criteria and properties are decisive for selecting the right material and thickness. Firstly, like stated in the introduction, dikes can be breached by many failure mechanisms. The designer has to proof that the designed revetment and dike is able to meet the safety norms during the given lifetime of the structure. Besides these "macro" dike failure mechanisms and failure by bending criteria, also other design principles for the composite PBA/block have to be taken into account. Other design criteria are for instance: currents, traffic loads, ice loads, uneven settlements, liquefaction and shear failure. Future work needs to be done to research these categories and possible failure mechanisms for this composite system.

In this thesis only a rectangular block is considered. Obviously, there are several types of elements available like stated in chapter 2. The different types all have different properties which influence their structural behaviour and stability, e.g. different shapes, dimensions, permeabilities (leakage length), friction and densities. Furthermore only one hydraulic situation is considered; a dike situated at the Waddenzee. It would be therefore impossible and incorrect to formulate design rules and make big statements about every refurbished pitched stone revetment in general, based on this report. This would not be correct. Future research is therefore required. However, it is possible to formulate a few qualitative statements which resulted from this study and could hold in general. Although the current study is based on one single situation, the findings suggest that the PBA layer has to be as rigid as possible be connected with the current block revetment. This is most effective in reducing the bending stresses in the PBA layer. The results of this research support furthermore the idea that the composite PBA/block revetment could be schematized as an Euler Bernoulli

bending beam. The findings also indicate that the current design method of ARCADIS is conservative. Lastly, the results suggest that it is more effective to use a less heavier but more permeable material as a refurbishment than the other way around.

Besides the assumed block shape, the findings of this study are also limited by the use of multiple other assumptions for both the analytical and numerical approach. Solving complex real life engineering problems with an analytical or FEM analysis, involves many explicit and implicit assumptions. The finite element method is very useful but only gives an approximate numerical solution to an already idealized problem. The results are only as good as the many assumptions and modelling steps involved throughout the analysis. It is wrong to assume that the outputs or results of the FEM analysis are *the* reflection of reality. This study is based on dozens of assumptions, e.g. load models, block shape, stiffness values, 2D situation, beam type failure, soil and foundation characteristics, permeability values and assumed boundary conditions. Therefore, a reasonable approach to tackle this issue could be by validating the results -and therefore the assumptions- with real experiments. If the numerical and experimental results show similarity, one can use the FEM results and the qualitative statements for designing PBA layers on pitched stone revetments. A large scale model test is already performed in the Large Wave Flume (GWK) of the Forschungszentrum Küste (FZK) in Hannover to study the behaviour of PBA under wave loading. To improve the understanding of the wave-structure-foundation interaction and to develop prediction formulae for the hydraulic performance, more than 75 large-scale model tests were performed in 2010. However, experiments for a composite PBA/block revetment have not been done yet. In order to improve the understanding of all the relevant processes and to study its composite structural behaviour additional large scale experiments have to be performed. Large model tests in a flume with these dimensions allows for physical models on a scale which is close to prototype. The waves can be artificially created by a wave generator. Pressure gauges can be installed to measure the impact load on the revetment, the pressure underneath the PBA layer, at the bottom of the filter layer and the fluctuation of the internal water level. Furthermore one can measure the wave run-up and run-down which are important to study the pressure difference over the structure. To give an impression; the PBA scale model which was used in Hannover is shown in figure 9.1. Further analysis and careful study of an additional scale PBA/block revetment model tests is needed.



Figure 9.1: Large Wave Flume (GWK) of the Forschungszentrum Küste (FZK) in Hannover; artificial waves are breaking at the PBA revetment (photo: Elastogran GmbH)

Since the leakage length of the refurbished revetment is of great importance, it is recommended to get more insight in the effect of the refurbished material on the permeability of the composite structure. It is advised to study to what extent leakage of the refurbished material (PU or bitumen) in the gaps between the blocks will occur and therefore influence its permeability. Furthermore it is recommended to study the bonding behaviour in different environmental circumstances and practical situations. Like stated in the conclusion, one has to clean the concrete elements thoroughly otherwise the PU or bitumen cannot form a strong bond with the blocks. However, it is still possible that the surface of some parts is still not clean enough after cleaning procedures. It is important to investigate the influence of dirt, sand and vegetation on the strength of the

bonding. Besides dirty elements, they could also be wet when applying the refurbishment. It is recommend to study to what extent this will influence the bonding and therefore the structure's strength.



APPENDIX

To reduce the overall report size, the Maple and Abaqus scripts are not attached in the appendix to this report. Because of the amount of used files, the files are provided as a downloadable zip file. Both Maple and Abaqus files are compressed in the *PBA_PSR_MCKRUIS.zip* file. The files that correspond to the equations and figures shown in the different chapters are depicted in the enumeration below. Lots of files have been used, therefore, to make a clear overview, first the specific section is mentioned followed by the corresponding file name. In almost every section, only one file has been used, therefore it is possible to make this distinction. However, if two files were used in one section, an additional description has been made between brackets. The files with a *.mw* extension correspond to a Maple sheet, the files with a *.cae* extension can be opened with Abaqus. In the file names some abbreviations have been used:

- CE = Concrete Elements
- CF = Continuous Foundation
- ES = Elastically Supported
- FLS = Final Load Situation
- LA = Loads Analysis
- MOE = Modulus of Elasticity
- NFA = Normal Force Analysis
- SA = Structural Analysis
- SEA = Sensitivity Analysis
- SLM = Static Load Model
- WLM = Wolsink Load Model

A.1. LOADS ANALYSIS

- Section 4.3 → *SLM_LA.mw*
- Section 4.4.2 → *WLM_LA_S1.mw*
- Section 4.4.3 → *WLM_LA_S2.mw*
- Section 4.6.1 → *SLM_LA_FLS.mw*
- Section 4.6.2 → *WLM_LA_FLS.mw*

A.2. STRUCTURAL ANALYSIS

- Section 5.8 → *NFA.mw*
- Section 5.9 → *SLM_SA.mw*
- Section 5.10 → *WLM_SA.mw*

A.3. FINITE ELEMENT METHOD ANALYSIS

- Section 6.2 → *SLM_ES_0cm.cae*
- Section 6.2 → *WLM_ES_0cm.cae*
- Section 6.3.1 → *CF_10cm.cae* (10 cm PBA)
- Section 6.3.1 → *CF_20cm.cae* (20 cm PBA)
- Section 6.3.1 → *CF_30cm.cae* (30 cm PBA)
- Section 6.5 → *CE_Beam_0cm.cae*
- Section 7.7 → *AM_10cm_S1.mw*
- Section 7.7 → *AM_10cm_S2.mw*

A.4. SENSITIVITY ANALYSIS

- Section 7.1 → *MOE_1360.cae*
- Section 7.2.1 → *RLS.mw*
- Section 7.2.1 → *SEA_Hs_150.cae* ($H_s = 1.5\text{m}$)
- Section 7.2.1 → *SEA_Hs_200.cae* ($H_s = 2.0\text{m}$)
- Section 7.2.2 → *SEA_HD_WLM.mw* (Head difference)
- Section 7.2.2 → *SEA_RLS_WLM.mw* (Resultant load)
- Section 7.3 → *FF_FS.cae*
- Section 7.6 → *FB_CE.cae*

A.5. PBA AND ASPHALT

- Section 8.3.3 → *LLV_PBA_OSA.mw*
- Section 8.3.3 → *WAB_SM_10cm.cae* (WAB)
- Section 8.3.3 → *OSA_WM_10cm.cae* (OSA, $\lambda = 1.5\text{ m}$)
- Section 8.3.3 → *OSA_WM_10cm_4.cae* (OSA, $\lambda = 4\text{ m}$)
- Section 8.3.3 → *PBA_WM_10cm.cae* (PBA, $\lambda = 1.5\text{ m}$)
- Section 8.3.3 → *PBA_WM_10cm_4.cae* (PBA, $\lambda = 4\text{ m}$)
- Section 8.3.3 → *PBA_WM_10cm_infinite.cae* (PBA, $\lambda = \text{infinitely large}$)
- Section 8.4 → *BB_WAB_0.1_WI.cae* (Bending beam)
- Section 8.4 → *CE_WAB_0.1_WI.cae* (Concrete elements)

LIST OF FIGURES

1.1	Left: Dutch safety norms of the primary flood defences according the "Waterwet", the required standards vary between 1:250 along river the Maas and 1:10000 for Southern and Northern Holland provinces. Right: the primary flood defences are indicated in red (Ministerie van Infrastructuur & Milieu, 2014)	1
1.2	Failure mechanisms of a dike (Ministerie van Verkeer en Waterstaat, 2007)	2
1.3	Cross section of a dike protected by a pitched stone revetment (<i>Projectbureau Zeekeringen</i> , 2010)	3
1.4	Overview of the chapters with respect to the research questions	4
1.5	Flow chart of the different chapters	6
2.1	Block types and filters in revetments (Schiereck, 2012)	8
2.2	Impression of elements currently on the market, varying from (l) basic pitching stone elements ("checkerboard" placing) to alternative (less rectangular) shapes	8
2.3	Placement of the blocks (Schiereck, 2012)	9
2.4	Influence Leakage Length (Schiereck, 2012)	10
2.5	Overview Failure Mechanisms; the focus of this thesis will be on the subjects shown in the red boxes	10
2.6	Loading mechanisms in block revetments (Burger et al., 1990)	11
2.7	top: model beam type failure (photo: Verhagen)	11
2.8	Failure of interlocking blocks in New York (photo: Kruis)	12
2.9	The original elements are reused: by rotating the blocks, the dead weight per area increases (<i>Projectbureau Zeekeringen</i> , 2010)	12
2.10	Riprap refurbishment of an existing block revetment (photo: Hoogheemraadschap Hollands Noorderkwartier)	13
3.1	Mixing of the components in situ: polyol and the isocyanate (photo: Bijlsma)	16
3.2	The polyurethane and the aggregate are inserted and subsequently mixed (photo: Bijlsma)	16
3.3	Before curing takes place, the unhardened mixture can be processed for approximately 20 minutes (photo: Bijlsma)	17
3.4	Example for a quality defect caused by residual moisture on the granular material during the mixing process (photo: IMS)	17
3.5	Wave energy dissipating when applying a conventional concrete revetment (left) and PBA (right) (BASF, 2010). Due to the open structure of PBA, the wave energy can be better absorbed.	18
3.6	PBA ensures rapid new growth of algae and provides habitats (photo: Bijlsma)	19
3.7	PBA measurements related to temperature (Bijlsma, 2013)	20
3.8	Flexural strength of PBA related to stone size (Bijlsma, 2013)	20
4.1	For calculation purposes the properties of a dike at the Waddenzee are used	23
4.2	Static Load Model	25
4.3	Static Load Situation	26
4.4	Hydraulic heads: blue = hydraulic head top layer, red = hydraulic head in the filter	26
4.5	Hydraulic head difference between top and filter layer	27
4.6	Wolsink Load Model	27
4.7	Small Element for Derivation Wolsink Differential Equation	28
4.8	Situation Wolsink Load Model	29
4.9	Definition sketch assumed wave front and steepness (Burger et al., 1990)	30
4.10	Results of solving Wolsink's DE for the Waddenzee dike; blue: hydraulic head top layer, red: hydraulic head in filter layer	31
4.11	The resultant head difference, a minus height results in an upward water pressure	31

4.12 Situation Wolsink Load Model of Waddenzee dike; layers with a black line pattern are assumed to be impermeable	32
4.13 Maple results when applying the hydraulic parameters of the Waddenzee dike; blue is the hydraulic head of the top layer, red the hydraulic head in the filter layer	33
4.14 The resultant head difference (a minus height results in an upward water pressure)	33
4.15 Resultant (distributed) loads on the revetment	34
4.16 Wolsink load model: Infinite long slope, with the x-axis in the slope direction	35
4.17 Head difference over the revetment with the x-axis in the slope direction	36
4.18 Resultant revetment load when using the Wolsink load model on an infinite slope	36
4.19 Wolsink load model: Waddenzee dike situation, with the x-axis in the slope direction	37
4.20 Head difference over the revetment with the x-axis in the slope direction for the Waddenzee case	37
4.21 Resultant revetment load when using the Wolsink load model on an finite revetment for the Waddenzee case	37
5.1 Flowchart Structural Analysis	39
5.2 Design values of the flexural strength of PBA (Bijlsma, 2013)	40
5.3 Non homogeneous elastically supported Euler Bernoulli bending beam	41
5.4 Equilibrium of an Euler Bernoulli beam element elastically supported (Simone, 2011)	41
5.5 To perform calculations a representation of the boundary conditions is made. At the left side the revetment is bounded by a dike toe, at the right side the structure is bounded by a refurbishment of asphalt.	43
5.6 Three different support types	44
5.7 Approximate range of CBR and k-values for soil groups of the soils classification as used by the Corps of Engineers (Eres Consultants, 1994)	44
5.8 The block revetment is a sandwich beam consisting of concrete blocks and gap filling material	45
5.9 Determining the centre of gravity of an inhomogeneous cross section, taking into account the different MOE	46
5.10 Illustration of the stress and strain distribution over the cross section	47
5.11 Normal force as a function of the beam length, a normal force can only be developed over the length where the waterpressure is negative	48
5.12 Displacements [m] of the revetment based on the static load model for the three situations	49
5.13 Moment (left) and Shear force (right) diagram of the block revetment	49
5.14 Displacements [m] of the revetment based on the Wolsink load model for the three situations	50
5.15 Moment diagrams for different PBA thicknesses based on the Wolsink load model	51
6.1 Flowchart FEM Analysis	53
6.2 A beam resting on a Winkler foundation on which a part is loaded and unloaded. The arrows illustrate the amount of support; the bigger the deflection the higher the supporting force	54
6.3 Schematization of the different calculations done in this research	54
6.4 Displacements of the revetment when loaded with the two load models, calculated analytically and with FEM software. In this case there is no PBA refurbishment layer present. A fictitious stiffness is used for the block revetment like explained in chapter 5. Left: static load Model; right: Wolsink load model	55
6.5 Bending stresses in the top fibres of the PBA refurbishment layer (10 cm) both for the analytical and FEM model (Waddenzee data is used)	56
6.6 Bending stresses in the outer fibres of the PBA refurbishment layer (20 cm) both for the analytical and FEM model (Waddenzee data is used)	56
6.7 Bending stresses in the top fibres of the PBA refurbishment layer (30 cm) both for the analytical and FEM model	57
6.8 Bending stresses in the top fibres of the PBA layer (10 cm) both for the analytical and FEM model	57
6.9 Bending stresses in the top fibres of the PBA layer (15 cm) both for the analytical and FEM model	58
6.10 Pitched stone revetment (without refurbishment layer) modelled as individual concrete blocks, i.e. no bending beam schematisation. The blocks are lifted up and rotated. The hydraulic conditions of the Waddenzee are used.	58
6.11 An eccentric (e) compressive force develops in the bottom of the concrete blocks. As a result the structure is able to withstand the bending moments caused by the external loads ($M = F \cdot e$)	59

6.12 The block revetment/PBA structure modelled both as a bending beam (blue) and modelled as individual concrete blocks	59
6.13 An impression of the FEM results of the block/PBA revetment modelled as individual concrete blocks (region of upward displacements)	60
7.1 Flowchart Sensitivity Analysis	61
7.2 The blue line displays the original FEM results, i.e. the calculations performed with a block revetment (modelled as a bending beam) with a Young's modulus of 3000 MPa. The red line shows the results when applying a Young's modulus of 1360 MPa.	62
7.3 Different load scenarios (static load model) when applying a PBA layer of 0.2 m (green), 0.1 m (blue) and no layer (red)	63
7.4 Increasing the wave height results in a different load diagram; q_2 is the initial situation, q'_2 is the adjusted situation	63
7.5 FEM results: bending stresses in the outer fibres of the PBA layer when loading with a significant wave height of 1.5 m (left) and 2.0 m (right)	64
7.6 FEM results: bending stresses for varying PBA layer thickness, a wave height of 1.5 m is applied	64
7.7 Piezometric levels in filter (red) and at top layer (blue); left: very large leakage length, right: very small leakage length	65
7.8 The hydraulic head difference (l) and the resultant load (r) over the revetment for both $\Lambda = 4.5$ m and the original Λ of 1.5 m (Waddenzee)	66
7.9 The resultant load situations for the initial -Waddenzee dike- wave height of 0.96 m (left) and when applying a wave height of 2.5 m (right)	67
7.10 Two mechanical situations and their corresponding bending stress diagrams. left figure: two beams fully bonded; right figure: two beams not fully bonded	67
7.11 Bending stresses in the outer fibres of the PBA layer. Red: full friction between the concrete blocks and the PBA layer; Blue: full slip between the concrete blocks and the PBA layer (Waddenzee situation)	68
7.12 Impression of the Abaqus results: bending stresses in the outer fibres of the PBA layer while frictionless connected with the block revetment	68
7.13 The left figure shows the bending stresses when the PBA layer and the pitched stone revetment are rigid connected, in the right figure the two layers are frictionless connected. The red graphs display the stresses when the friction between the elements is increased based on the initial applied friction (blue). The situation at the Waddenzee is considered.	69
7.14 The influence of the soil variables; bending stresses in the top fibres of the PBA refurbishment layer (30 cm) both for the analytical and FEM model. The hydraulic conditions at the Waddenzee are used.	70
7.15 Two beams with different supports and their corresponding moment diagram. Left: beam on both ends pinned support; right: fixed beam	70
7.16 FEM results: the red graph shows the bending stresses if the revetment is on both ends pinned, the blue graph shows the results if the revetment is on both ends fixed. The hydraulic conditions at the Waddenzee are used.	71
7.17 Second analytical model: it is assumed that the displacement is zero where the load changes sign. Subsequently the bending stresses in the PBA layer are calculated for a simple mechanical model	72
7.18 The FEM calculations (red and blue) compared with the (analytical) simply supported beam model provided by ARCADIS for preliminary designs	72
7.19 Comparing the bending stresses, based on the new analytical approach, with the FEM results (Waddenzee conditions are used).	73
8.1 Volume percentages of the components in hydraulic asphalt concrete	76
8.2 Volume percentages of PBA and OSA	77
8.3 Overview of the situation: vertical wave front	78
8.4 Influence of the leakage length: head difference over the block revetment for a large (impermeable) and small (permeable) leakage length (Schiereck, 2012)	78
8.5 Hydraulic heads: blue = hydraulic head top layer, red = hydraulic head in the filter. For both figures an impermeable top layer is assumed	80

8.6	Hydraulic head difference over the revetment when applying an impermeable revetment	80
8.7	The resultant load situation on the revetment when applying hydraulic asphalt concrete	81
8.8	Bending stresses in the outer fibres of the asphalt concrete cover layer (10cm)	81
8.9	Hydraulic heads in the filter layer for different leakage lengths	82
8.10	Hydraulic head difference over the revetment when applying different values for the leakage length	82
8.11	The resultant load situation on the revetment when applying PBA (left) and OSA (right)	83
8.12	The bending stresses in the outer fibres in the PBA cover layer	83
8.13	The bending stresses in the outer fibres in the OSA cover layer	84
8.14	The bending stresses in the bottom fibres of the asphalt concrete refurbishment layer when modelling the block revetment as an Euler Bernoulli bending beam (red) and as loose concrete elements (blue)	85
8.15	Important cost aspects which are (partly) decisive for selecting the material. A green box implies that this specific material scores better on this aspect than the other one.	87
9.1	Large Wave Flume (GWK) of the Forschungszentrum Küste (FZK) in Hannover; artificial waves are breaking at the PBA revetment (photo: Elastogran GmbH)	92

LIST OF TABLES

2.1	Revetment types with their characteristics (Schiereck, 2012)	7
3.1	Examples of materials and grading that have been used for PBA, (Bijlsma, 2013)	15
3.2	Structural Properties	19
4.1	Governing data for the Waddenzee dike	24
5.1	Governing positive and negative moments based on the static load model for the three situations	50
5.2	Bending stresses over the cross section for different PBA layers	50
5.3	Governing positive and negative moments based on the static load model for the three situations	51
5.4	Bending stresses over the cross section for different PBA layers	51
8.1	Governing data for the modelling calculations	77
8.2	Expected lifetime of hydraulic asphalt concrete, OSA and PBA in years	86

REFERENCES

- BASE. (2010). *All you need to know about modern coastal protection*. (PU Solutions Elastogran)
- Bijlsma, E. (2013). *Polyurethane bonded revetments design manual* (C ed.) [ARCADIS Nederland B.V.].
- Bijlsma, E., & Voortman, H. (2009). Polyurethane bonded aggregate (pba) revetments in coastal engineering.
- Bowles, J. (1997). *Foundation analysis and design* (5th ed.) (No. ISBN: 0071188444). McGraw-Hill.
- Burger, A., Klein Breteler, M., Banach, L., Bezuijen, A., & Pilarczyk, K. (1990). Analytical design method for relatively closed block revetments. *Journal of waterway, port, coastal and ocean engineering*, vol. 116, p. 525-544.
- Davidse, M., 't Hart, R., de Looft, A., Montauban, C., van de Ven, M., & Wichman, B. (2010). *State of the art asfaltdijkbekledingen* (Tech. Rep. No. 2010-W06). Rijkswaterstaat.
- Dorst, K., Provoost, Y., & Verhagen, H. (2012). Stability of pattern placed revetment elements. *PIANC-COPEDEC VIII, Proceedings of the eight international conference on coastal and port engineering in developing countries: Meeting the challenges of the coastal environment*, p. 978-987.
- Eres Consultants. (1994). *Aashto design procedures for new pavements* (Tech. Rep. No. FHWA-HI-94-xxx). Federal Highway Administration.
- Escameia, M. (1998). *River and channel revetments: a design manual* (Vol. 1st) (No. ISBN: 0727726919). Thomas Telford publications.
- Frissen, C. (1996). *Numerieke modellering van steenzettingen* (Tech. Rep. No. 96-NM-R-0994). TNO.
- Gu, D. (2007). *Some important mechanical properties of elastocoast for safety investigation of dikes* (Master's thesis, Delft University of Technology). Retrieved from <http://repository.tudelft.nl/view/ir/uuid%3A793f469e-129c-4778-a0b7-2efb6a1f0d89/>
- Hartsuijker, C., & Welleman, H. (2012). *Module: Non-symmetrical and inhomogeneous cross sections* (Tech. Rep.). Delft University of Technology.
- Infram B.V. (2008). *Factual report, golfoverslagproeven zeeuwse dijken* (Tech. Rep. No. 08i011).
- Isopa. (2009). *Eco-profiles of the european plastics industry polyurethane precursor* (Tech. Rep.). Association of Plastics Manufacturers in Europe.
- Klein Breteler, M. (1991). *Taludbekleding van gezette steen* (Tech. Rep. No. TAW-A2). Rijkswaterstaat Dienst Weg- en Waterbouwkunde.
- Ministerie van Infrastructuur & Milieu. (2014). *Waterwet*. Retrieved from http://wetten.overheid.nl/BWBR0025458/geldigheidsdatum_10-06-2014
- Ministerie van Verkeer en Waterstaat. (2007). *Voorschrift toetsen op veiligheid primaire waterkeringen* (Tech. Rep. No. 9789036957625).
- Peters, D. (2003). *Gezette steenbekleding onder golfaanval* (Tech. Rep. No. 9M8621/R001). Royal Haskoning.
- Pilarczyk, K. (1998). *Dikes and revetments: Design, maintenance and safety assessment* (No. ISBN: 9054104554). Balkema.
- Projectbureau zeekeringen. (2010). Website. Retrieved from www.zeekeringen.nl

- Rijkswaterstaat. (2009). *Golfklap gebruikershandleiding bij versie 1.3* (Tech. Rep.). Ministerie van Verkeer en Waterstaat. Retrieved from <http://repository.tudelft.nl/view/hydro/uuid:84652b94-ab6b-440d-86c8-1e72186c0a6f/>
- Schierreck, G. (2012). *Introduction to bed, bank and shore protection* (2nd ed.; H. Verhagen, Ed.) (No. ISBN: 9789065623065). VSSD.
- Simone, A. (2011). *An introduction to the analysis of slender structures* (Tech. Rep.). Delft University of Technology. Retrieved from <http://cm.strumech.citg.tudelft.nl/simone/>
- TAW. (2002). *Technisch rapport asfalt voor waterkeren* (Tech. Rep. No. 903695519X). Technische Adviescommissie voor de Waterkeringen.
- Tsudik, E. (2013). *Analysis of structures on elastic foundations* (No. ISBN: 1412079500). J.Ross Publishing.
- van de Velde, P. (1984). *The use of asphalt in hydraulic engineering* (Tech. Rep.). Rijkswaterstaat. Retrieved from <http://repository.tudelft.nl/view/ir/uuid%3A50536170-22d2-4084-8b2a-c945c6e250fe/>
- Verhagen, H. (2009). Elastomeric revetments - a new way of coastal protection. *Aquaterra conference, Amsterdam*. Retrieved from <http://repository.tudelft.nl/view/ir/uuid:7222834a-bdd3-404a-afb7-5551b5419eb0/>
- Vrijling, J., van der Horst, C., van Hoof, P., & van Gelder, P. (2001). The structural analysis of the block revetment on the dutch dikes. *Coastal Engineering 2000*, p. 1991-2003.